

# Cluster-based Analysis of Airline Adherence to Flight Plans

## The European Case

MSc. Thesis  
V. Ciulei



# Cluster-based Analysis of Airline Adherence to Flight Plans

## The European Case

by

Victor Ciulei

to obtain the degree of Master of Science  
at the Delft University of Technology,  
to be defended publicly on Monday June 29, 2020 at 09:30 AM.

Student number: 4622413  
Project duration: April 15, 2019 – June 29, 2020  
Thesis committee: Dr. ir. B. F. Santos, TU Delft, AE ATO, chair  
Dr. M. A. Mitici, TU Delft, AE ATO, supervisor  
Dr. ir. D. M. Pool, TU Delft, AE C&S, external examiner

An electronic version of this thesis is available at <http://repository.tudelft.nl/>.



# Contents

<b>List of Figures</b>	<b>ix</b>
<b>List of Tables</b>	<b>xi</b>
<b>I Introduction</b>	<b>1</b>
<b>II Scientific Article</b>	<b>5</b>
<b>III Literature Review</b>	<b>37</b>
<b>1 Introduction</b>	<b>41</b>
<b>2 Data Description</b>	<b>43</b>
2.1 Flight Trajectory data . . . . .	43
2.2 Weather data . . . . .	43
<b>3 Complex Network Theory</b>	<b>45</b>
3.1 Graph Theory . . . . .	46
3.2 Random subgraphs and random graph evolution. . . . .	46
3.3 Complex Network properties. . . . .	47
3.3.1 Degrees and degree distributions . . . . .	47
3.3.2 Node strength. . . . .	48
3.3.3 Clustering Coefficient. . . . .	49
3.3.4 Average path length . . . . .	49
3.3.5 Connectedness and diameter . . . . .	49
3.3.6 Centrality measures . . . . .	50
3.3.7 Graph spectra . . . . .	51
3.4 Generating function . . . . .	51
3.5 Small-world networks. . . . .	51
3.6 Scale-free networks . . . . .	52
3.7 Percolation Theory . . . . .	52
3.8 Complexity Science in Air Transport. . . . .	53
3.9 Agent-Based Modelling in ATM . . . . .	55
<b>4 Trajectory Deviations</b>	<b>59</b>
4.1 Flight Deviations . . . . .	59
4.2 Weather in ATM . . . . .	61
4.2.1 Convective events analysis and modelling . . . . .	61
4.2.2 Alpine Weather Operations . . . . .	62
4.3 Airline Types . . . . .	62
4.4 Deviation KPIs . . . . .	63
<b>5 Research Questions</b>	<b>67</b>
<b>Bibliography</b>	<b>69</b>
<b>IV Annexes to the Scientific Article</b>	<b>75</b>
<b>A Airline Clustering</b>	<b>79</b>
<b>B Efficiency</b>	<b>83</b>

---

<b>C FAIR</b>	<b>91</b>
<b>D Additional trajectory analysis results</b>	<b>93</b>
<b>E Mutual Information</b>	<b>95</b>
<b>F Metric Altitude Reference</b>	<b>97</b>

# List of Figures

1	The Clustering Ensemble workflow . . . . .	4
1.1	Network Performance: traffic and en-route ATFM delays. EUROCONTROL [27] . . . . .	41
3.1	Supercluster example of airports delay causality. Cook et al. [21] . . . . .	46
3.2	Example Power law distribution and Gaussian distribution. Barabási [6] . . . . .	48
3.3	Betweenness-centrality increase from red to dark blue hue. Author: Claudio Rocchini . . . . .	50
3.4	Example of regular lattice randomization with small-world instances. Watts and Strogatz [67] . . . . .	52
3.5	Percolation example of a 2d lattice network. Chen et al. [18] . . . . .	53
3.6	Shortest path trees for Atlanta airport and Shanghai harbour. Woolley-Meza et al. [69] . . . . .	54
4.1	En-route weather ATFM delay statistics EUROCONTROL [27] . . . . .	59
4.2	En-route weather avoidance strategies EUROCONTROL [26] . . . . .	60
4.3	Point-to-point Network (left) and Hub-and-spoke network model (right). AE4423 TU Delft . . . . .	62
A.1	Left: Clustering dendrogram of the final result with average linkage and a cut at 0.5. Right: Clustering dendrogram with Ward Linkage and a cut at 1.05. . . . .	82
B.1	M3 efficiency comparison between groups. . . . .	84
B.2	Efficiency T-tests between all operators. Left (M1) and right (M3). . . . .	84
B.3	M1 and M3 efficiency comparison per groups of airlines per hour. All eight groups are presented here. . . . .	85
C.1	M3 hourly FAIR comparison between groups. Note the slightly different axes. . . . .	91
D.1	Daily (first row) and monthly (second row) flights exhibit a peak during Fridays, Sundays and Mondays, and during summer months. Besides showing weekly and monthly trends, the images in the left and right columns show that, although most airline groups (6/8) fly similar number of flights, the average airline within each group behaves differently. . . . .	93



# List of Tables

2.1	DDR2 ALLFT+ Planned Trajectory (M1) data sample. . . . .	43
2.2	M1 point profile detailed . . . . .	43
3.1	Random Graph evolution with increase of $Z = \frac{-k}{l}$ Erdős and R�nyi [25]. . . . .	47
3.2	Most encountered degree distributions in Complex Network Theory. Clauset et al. [20] . . . . .	47
3.3	Table with main topology aspects of various papers. Columns 2 and 3 explain the meaning of nodes and links. In column 4, starred * elements represent a value, not a distribution. Column 5 refers to different coefficients used to characterize the correlations. . . . .	57
3.4	Table containing quantitative aspects of surveyed literature. All networks assume airports as nodes and direct flights as existing links, except those with an additional(f) in Column 3 who refer to number of flights in the network (traffic). Columns 5 and 6 show the Clustering Coefficient at entire network level, with the randomized counter parts. Columns 7,8 and 9,10 do the same for average path length and network diameter . . . . .	58
4.1	Different weather severity thresholds Gelhardt et al. [29] . . . . .	61
4.2	Deviation metrics derived from the original table in Gurtner et al. [35]. The respective table provides a summary from the metrics found by the authors in literature, mainly from Chatterji and Sridhar [17], Laudeman et al. [44], Gurtner et al. [34], C11 Di-fork is an original metric developed by the authors in Bongiorno et al. [14]. . . . .	63
4.3	Possible novel deviation metrics. . . . .	64
4.4	Complexity Network metrics, surveyed from Albert* and Barab�si [3] and Erdős and R�nyi [24] . . . . .	65
4.5	Deviation metrics for the initial characterization of Airlines. Columns 3,4,5 mention if they will have a Probability Distribution Function attributed over various time scales. Column 3 will show the PDF for 24h to distinguish day and night variation, column 4 will present the probabilities every day of the week to show weekend variations and finally the last column will integrate season variability. . . . .	66
A.1	All airline features. Intercontinental flights and weekends included. . . . .	81
A.2	PC features correlation. ECAC flights, weekends included. An example of the amount of correlation between each of the 10 features and the resulting 5 principal components. . . . .	81
B.1	Variance and average planned (M1)efficiency for every hour per airline group. . . . .	83
B.2	Variance and average of planned (M1) efficiency for every day per airline group . . . . .	83
B.3	Variance and average of realized (M3) efficiency for every day per airline group . . . . .	84
B.4	Individual airline efficiency and FAIR values. Both 'flights' columns refer to the total flights in 2017 used in each analysis. . . . .	90
F.1	Metric Altitude Reference table. Source: Skybrary. This table shows the function by which the unit transformation of vertical deviation has been transformed from Flight Levels (FL) which are measured in feet, to meters. . . . .	97



---

# I

## Introduction

The European Air Transport Network and its underlying Air Traffic Management system are a jewel of modern engineering and the epitome of European collaboration: they are vast, complex, and they never stop. One of their key resources is always in plain sight, yet it is barely thought of as a resource: air is free and, seemingly, plentiful. However, a closer look reveals that the intense demand for airspace makes it a scarce and increasingly important public good.

European airspace is a shared resource and, as such, is vulnerable to excessive or unfair use, either through free-riding by participants or subtle methods to capture disproportionately large allotments [60]. Starting from this observation, this research is in part rooted in my deep commitment to a future, better society in which resources are equitably used, and those who benefit from them do so in a transparent manner. The first point I explored was whether European airspace is utilized in a fair way, by defining a precise and representative trajectory deviation measure. The second task was to define a method to categorize airline types, and compare flight path deviations between these types. The categorization exercise was necessary given that the current mainstream labels defining business models (flag carrier, low-cost operator, etc.) were in fact coined decades ago and may no longer be representative. To classify airline types, first I defined the features to extract from the available data. Besides the obvious operational ones, some more recent papers introduced Complex Network metrics in the airline environment, which I also integrated. Then, to translate these metrics into a classification, I employed Unsupervised Machine Learning. In hindsight, the airline clustering played into my personal curiosity and inclination towards understanding economics and behaviour stemming from economic decisions, making this research particularly exciting for me. To summarize, this research addresses the following questions:

1. How can deviations between the planned and actual flight trajectories be measured in a precise manner?
2. Do some airline types deviate more than others? By how much?
3. How can airline types be categorized in groups based on objective indicators?

This report answers the questions mainly through the scientific article in part II: Sections 1 and 2 introduce the three topics (airline clustering, horizontal and vertical deviations) and provide background for trajectory deviations, airline business models and airline features, both operational and stemming from Complex Network Theory.

Next, Section 3 describes the trajectory data that was used, and provides some context: the number of flights and the requirements for each analysis, and the airspace limits of the European Civil Aviation Conference Airspace that defined the area of the study.

Section 4 presents the Unsupervised Machine Learning method by which the airline groups have been defined. It is an ensemble method, meaning that the same data was clustered several times, either by different algorithms, or by the same algorithms with different parameters. Having defined 10 features for each airline, and with the final number of clusters identified and imposed in the objective function, two preliminary representative sets of clusters are identified. The tiebreak is decided by a number of internal clustering indices that assess data compactness and cohesiveness of the data points within each group. An outline of the clustering methodology which answers the third research question is shown in Figure 1.

Section 5 defines the two deviation metrics and answers the first two research questions, along with a part of the literature survey: the horizontal efficiency ( $E_h$ ) and the novel Flight Level Adherence Index for Realized trajectories (FAIR). The FAIR is a novel index, that provides a precise measure of the amount of vertical deviations during the cruise phase of a flight.  $E_h$  being a known index, the focus is mainly on the different analyses, while for the FAIR, both the method to calculate it and the results are presented.

Section 6 concludes the scientific article with ideas about the potential use of the new index, that promote the equitable use of airspace. Following the scientific article, the Literature Review is presented in III. Here, a

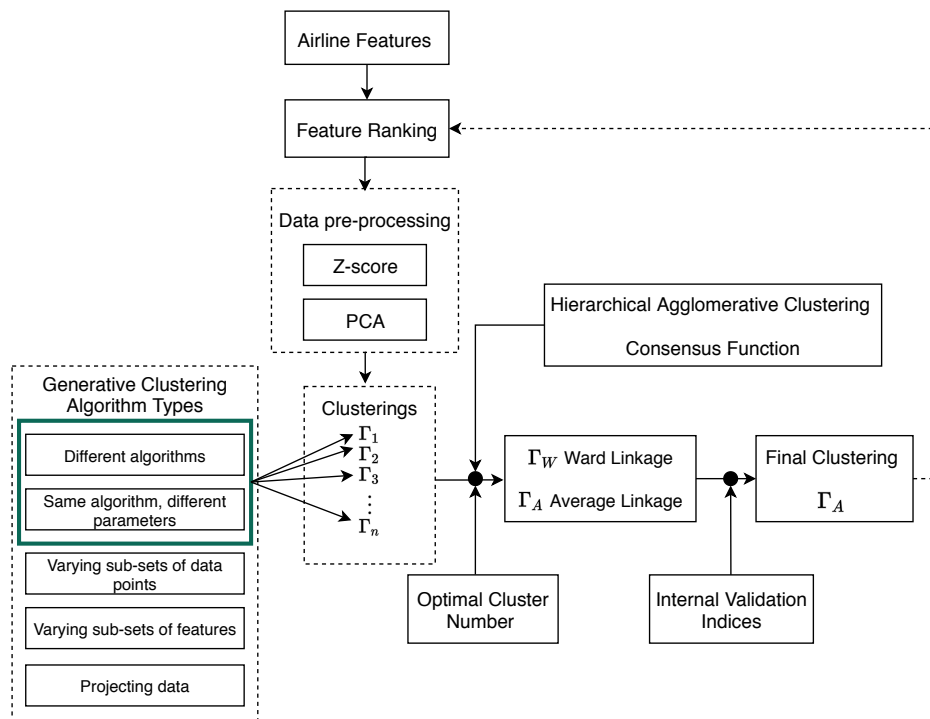


Figure 1: The Clustering Ensemble workflow

slightly more in-depth approach with regards to Complex Network Theory was taken, in order to understand how much of it is useful to define airline features.

Finally, the annexes in Part IV contain additional results from all three analyses done in the first part. The average efficiency and FAIR for each airline, along with the individual features are presented, providing a closer look at the behaviour of individual airlines.



# II

## Scientific Article

to be graded for AE5310 Final Thesis



# Cluster-based Analysis of Airline Adherence to Flight Plans The European Case

Author: MSc. V. Ciulei

Supervisor: Dr. M. A. Mitici

Air Transport Operation Section, Faculty of Aerospace Engineering  
Delft University of Technology, Delft, The Netherlands

---

## Abstract

Airlines plan the trajectory of their flights in advance. However, this plan is not always followed since, during the actual flight, aircraft deviate either horizontally by rerouting, or vertically by choosing a different Flight Level (FL). The issue arises when some airlines frequently deviate from their flight plans frequently, to the disadvantage of other airspace users. In this paper we analyse aircraft en-route trajectory deviations for clusters of European airlines. We focus on two metrics: vertical flight level deviation, and horizontal deviation. We analyze these deviations for clusters of airlines operating in the European Civil Aviation Conference (ECAC) airspace in 2017. The airline clusters are obtained using unsupervised machine learning algorithms with operational and Complex Network features. The results show that major Low-Cost Carriers (LCCs) deviate on average, per flight, 34% more vertically than major Network Carriers, while Network Carriers (NC) have on average, more efficient horizontal trajectories. However, NCs show a larger fraction of flights with equally planned and realized efficiency, which points to less horizontal deviations overall. The findings reflect a general, network-wide horizontal inefficiency in trajectory planning, and that LCCs deviate horizontally a larger percentage of their flights. Moreover, they manage to use the available Flight Levels consistently to their advantage. This research could be used for future policy-making on a fair and equitable routes and slot allocation.

*Keywords:* flight plan deviations, flight efficiency, airline clustering, unsupervised Machine Learning

---

## 1. Introduction

To accommodate the increasing demand of flights in the ECAC airspace Unit [1], flights are planned several days before the actual day of flight execution [2]. Due to prediction inaccuracies and delays, the situation is different on the day of operations than planned, prompting some aircraft operators to request and fly different routes and/or cruise Flight Levels on the day of operations. The issue arises when some aircraft operators frequently request direct routes or do not adhere to their planned FL [3][4]. The downstream effects are potentially disruptive, causing other delays, capacity issues and network-wide inefficiencies. Thus it is important to investigate whether some airlines deviate from their planned trajectories. To uncover the potential differences between airlines, this research clusters airlines, with a focus on major European Low-Cost and Network Carriers.

The goal of this paper is twofold: first, we cluster airlines based on operational and network features using unsupervised machine learning algorithms. Second, we compare the en-route horizontal and vertical trajectory deviations between these established groups. The horizontal deviations are compared by means of horizontal efficiency, and the vertical deviations by means of a novel index: the Flight Level Adherence Index for Realized trajectory (FAIR) during cruise. Finally, we provide a spatio-temporal analysis of deviations by these two metrics, i.e. hourly and daily flight plan deviations in the ECAC airspace.

The remainder of this paper is structured as follows: Section 2 presents the literature review on deviations and airline classifications, Section 3 describes the trajectory data that was used, Section 4 presents the detailed clustering methodology and the resulting groups of airlines, Section 5 presents the horizontal and vertical trajectory deviation analyses, and Section 6 concludes the research paper.

## 2. Literature review

The performance of a trajectory is quantified by a number of horizontal and vertical trajectory efficiency metrics [5]. They measure the performance with respect to the time and fuel used, and have been the subject of plethora of research: at network level [6][7] or flight-centric, and during specific phases of flight [8][9]. Deviations, however, have received considerably less attention, especially during the en-route phase of flight. One study assesses the horizontal deviations from planned trajectories during the entire flight from the perspective of the German network of navigation points. The authors emphasize the relationship between the day-night cycle and patterns of deviation, and find that aircraft deviate at a larger angle-to-destination when they are closer to the departing airport [10]. Another similar study analyses the network of Italian navigation points and studies the statistical regularities of spatio-temporal deviations from the planned flight-plan [11]. EUROCONTROL’s Performance Review Unit [12] proposes a number of vertical efficiency indicators. However, the en-route deviation metric has several drawbacks [13]: it is applicable per Origin-Destination (OD) pair instead of individual flight, under-estimates deviations and uses an aggregated reference trajectory from other OD pairs instead of the planned trajectory. To the best of our knowledge, there are no vertical deviation metrics geared specifically to the cruise phase, and no other research has compared en-route deviations between groups of different airline types.

The second focus of this paper is classification of airlines in groups, based on their business models. Throughout this paper, the focus converges towards Low-Cost Carriers and Network Carriers, due to their inherent differences in strategy. Starting with the pioneering Southwest Airlines[14], the LCC business model has disrupted the air transportation market [15]. But as the market has changed over time, so have the airlines: 33 of the 43 airlines commencing operations between 1992 and 2002 had filed for bankruptcy by 2013 [16], leaving the rest to adapt in order to survive. This hybridization process has been increasing, with LCCs adopting some features of full-service network airlines [17] and network carriers adopting similar behaviour as LCCs.

Perhaps the most coherent and well-explained airline characterization can be extrapolated from the work of Belobaba et al. [18], that details to the level of fleet and route network development strategy. Other studies have looked at the airports served [19][20], or specifically at the LLC competition strategy [21][22]. Our study classifies 99 European airlines in 8 groups by considering their operational and complex network (CN) metrics. A complex network is a network that has non-trivial topological characteristics, i.e. do not occur in random graphs. These can be, among others, specific degree, clustering and betweenness distributions, and the presence of communities or small-world properties.

The CN paradigm has been widely used to model real-world systems [23], such as the internet [24] or terrestrial transportation systems [25][26], the spread of infectious diseases [27], or social networks [28]. In ATM it is particularly useful as it sheds light on passenger mobility and reflects the characteristics typical to the airline business model [29] or market segment [30]. Many scientific articles have also characterized different networks within the ATM system: the network of navigation points and air routes [31] or the networks of airports [32][33][34][35]. For an overview on the Complex Network metrics in ATM, the reader is invited to consult [36].

## 3. Data Description

For our analysis, we consider the approximately 10.6 million flights managed by the EUROCONTROL Network Manager in 2017 in the ECAC airspace [1]. The data was obtained from the Demand Data Repository (DDR2) [37].

We consider 2 types of commercial trajectories: the last Filed Tactical Flight Model (FTFM), referred to as the M1 trajectory, and the Current Tactical Flight Model (CTFM), referred to as M3 trajectory. The FTFM contains points and airspace volume profiles [38], generated when the flight is planned. The CTFM has a similar structure, but contains the actual flown flight profile. Both contain actual points defined in 3 dimensions with an associated time-stamp and speed. The geographical limits considered for this paper are presented in Figure 1. The parts of trajectories outside the perimeter have been discarded, such that the analysis will reflect only ECAC-wide behaviour. Moreover, each analysis (airline clustering, horizontal and vertical trajectory), presented different data requirements. The resulting datasets and their associated requirements can be consulted in Table 1.



Figure 1: ECAC upper airspace under consideration in this paper.

	Nr. of flights	Requirements
ECAC flights	10.600.000	Approximate number of total flights in 2017
Clustering Methodology	3.129.561	5 months data: January, March, May, August, October 2017
Horizontal efficiency	6.206.277	Flights reaching $\geq$ FL245 with $\geq$ 5 data points
Vertical (FAIR)	5.721.123	An FTFM with $\geq$ 3 data points in level flight at a primary FL

Table 1: Total number of flights considered for each analysis and the filtering used.

#### 4. Airline Clustering Methodology

In this section, airlines are clustered in groups by an Unsupervised Machine Learning (UML) process by 10 airline features: four operational and six Complex Network features. The UML approach is used in many applications, such as classifying unstructured text and images i.e. online reviews, reports [39]; classifying indoor objects [40] or identifying cars from a moving target [41]. To the best of our knowledge, it has not been used to classify airlines until now. The UML approach has two main advantages over qualitative methods, or methods that only looks at one aspect (geographical location of destinations, ticket price a.o): first, it is based on objective features, eliminating the bias of qualitative methods. Second, it does not need a training data set, i.e. there is no reference set of groups that the algorithm strives to replicate. Finally, it incorporates information from multiple aspects (operations, fleet compositions and network metrics).

Airline business models are heavily influenced by the geographic location of their destinations and by their schedules. To show how context influences the clustering results, Section 4.1 presents an example in which the features of two known Low-Cost Carriers are compared with those of two major European Network Carriers for the two cases presented in Table 2. Case 2 is used only to underline the effect of context, while

	Description
Case 1	Intercontinental flights, weekends included
Case 2	ECAC flights, weekends included

Table 2: The two cases and their associated descriptions, considered in the analysis

Case 1 is used alone for the remainder of this paper as it includes intercontinental flights and without them, Network Carriers results would be skewed.

This section is organized as follows: airline features are defined in Section 4.1 followed by a case study on the feature differences between two LCCs and two NCs in Section 4.2. Section 4.3 presents the data pre-processing steps: the unsupervised feature ranking, dimensionality reduction and Z-scoring. The unsupervised feature ranking is complemented by a supervised feature ranking in an attempt to further reduce the dimension of the dataset. Section 4.4 presents the methodology to determine the optimal number of airline clusters. The clustering ensemble together with its generative algorithms and consensus function are briefly

described in Section 4.5. The two preliminary clustering results are compared by internal indices to decide on the final one in Section 4.6. The final airline clusters are presented in Section 4.7.

#### 4.1. Airline Features

Airline features are quantified indicators of airline business models and relate to their network of destinations and to their operations. To compute the features, a model for a generic airline is proposed. We model the global Air Traffic Network (ATN) as an undirected graph  $\mathcal{G}(\mathcal{WA}, \mathcal{E})$ , where the nodes represent the global airports ( $\mathcal{WA}$ ) and the edges ( $\mathcal{E}$ ) represent the flights between OD pairs. The graph is mapped with a binary adjacency matrix  $\mathcal{X}_{|\mathcal{N}| \times |\mathcal{N}|}$ , where  $x_{jr} = 1$  if there is an edge connecting node  $j$  with node  $r$ , i.e. if a flight connects the two airports. It is undirected as the direction of flights is not taken into consideration, and unweighted as all edges are assigned unit weight, irrespective of the number of flights flown on that particular OD pair.

##### Complex network metrics

The first complex network metric is the number of airport nodes  $n_A$ . An airport belongs to the set of an airline's airports  $\mathcal{A}$ , if and only if at least one flight  $f_i \in \mathcal{F}$  belonging to the airline that departs to or arrives from the airport in question:

$$a_j^i \in \mathcal{A} \iff \sum_{r=1}^n a_{jr} \geq 1, \forall f_i \in \mathcal{F}. \quad (1)$$

where  $\mathcal{F}$  is the set of flights. The second metric is the total number of links in  $n_L$ . From the adjacency matrix  $\mathcal{X}$ , we conclude that:

$$n_L = \sum_{j=1}^{n_A} \sum_{r=1}^{n_A} \frac{x_{jr}}{2}, j \neq r, \forall j, r \in \mathcal{A} \quad (2)$$

The third network metric is the average degree  $k$  of a network, defined by the number of nodes each node is connected to. The average degree for a network is simply  $\bar{k} = \frac{n_L}{n_A}$ . The fourth network metric is the average clustering coefficient  $\bar{C} \in [0, 1]$ , which provides a measure of how well-connected the neighbours of a node are between themselves. Full graphs have  $\bar{C} = 1$ . For an entire network, it is defined as:

$$\bar{C} = \sum_{j=1}^{n_A} \frac{2E_j}{k_j(k_j - 1)(n_A)}, \forall j \in \mathcal{A} \quad (3)$$

where  $E_j$  is the number of connections between the neighbours of airport node  $j$ , and  $k_j$  is the number of nodes connected to node  $j$ , or its degree. The fifth complex network metric is the average strength  $\bar{S}$  of an airline network. It is the weighted version of the degree:

$$\bar{S} = \sum_{j=1}^{n_A} \sum_{r=1}^{n_A} \frac{x_{jr} w_{jr}}{n_A}, \forall j, r \in \mathcal{A}, j \neq r \quad (4)$$

where  $w_{jr}$  is the weight or the number of flights between airport  $j$  and airport  $r$ . In this paper we consider the out-strength i.e. only the departures from an airport. Finally, the average path length  $\bar{L}$  of a network indicates how easily reachable a node is, starting from any other node in the same network. Considering all links of unit length in a graph, we define  $d_{jr}$  as the shortest path between airport  $j$  and airport  $r$ . Thus the average path length for a network is:

$$\bar{L} = \sum_{j=1}^{n_A} \sum_{r=1}^{n_A} \frac{d_{jr}}{n_A(n_A - 1)}, \forall j, r \in \mathcal{A}, j \neq r \quad (5)$$

### Operational metrics

The first operational metric is the total number of commercial flights that take off from any given airport and arrive at any given airport:

$$\overline{n_F} = \sum_{j=1}^{n_A} \sum_{r=1}^{n_A} x_{jr} w_{jr}, \forall j, r \in \mathcal{A}, j \neq r \quad (6)$$

The second operational feature is the total number of aircraft types  $n_K$  in a fleet, defined simply as  $n_K = |K|, \forall ac^k \in \mathcal{AC}$ . Similarly, the fleet size  $n_{AC}$  is the sum of all aircraft in an airline's fleet:

$$n_{AC} = |\mathcal{AC}| = \sum_{k=1}^{n_K} ac^k, ac^k, \forall k \in \mathcal{K} \quad (7)$$

The final operational feature is the average daily aircraft utilization for an airline  $\overline{U}$ , calculated in block time units  $\overline{BT}$ . Block time refers to the total operating time since brakes are released, i.e. Actual Off-Block Time (AOBT) at the departing airport, until the aircraft is fully parked again at the destination, with brakes active:

$$BT_{c,d} = t_{taxi_{arr}} + t_{flight} + t_{taxi_{dep}}, \forall c \in \mathcal{AC}, \forall d \in \mathcal{Z}_c \quad (8)$$

wher  $\mathcal{Z}_c$  is the set of days aircraft  $c$  has flown.  $BT_{c,d}$  is defined for a particular aircraft  $c$  in a particular day  $d$  and includes the total flight time, taxiing in and taxiing out. Due to data limitations, a modified  $BT$  is used which does not take into account the taxi on arrival:

$$BT' = BT - t_{taxi_{arr}} = t_{taxi_{dep}} + t_{Flight} \quad (9)$$

Let  $\mathcal{F}_{d,c}$  be the set of flights during day  $d$  for aircraft  $c$ ,  $\mathcal{F}_{d,c} \subset \mathcal{F}$  and  $n_{\mathcal{F}_{d,j}} = |\mathcal{F}_{d,c}|$  the number of the flights during day  $d \in \mathcal{Z}_c$  for any aircraft  $c \in \mathcal{AC}$ . The average daily utilization per one aircraft becomes:

$$\overline{BT'}_{d,c} = \sum_{i=1}^{n_{\mathcal{F}_{d,c}}} \frac{BT'_i}{n_{\mathcal{F}_{d,c}}}, \forall d \in \mathcal{Z}_c, \forall f_i \in \mathcal{F}_{d,c}, \quad (10)$$

Thus the average utilization for an entire fleet is:

$$\overline{U} = \sum_{c=1}^{n_{AC}} \sum_{d=1}^{n_{days}} \frac{\overline{BT'}_{c,d}}{n_d \cdot n_{AC}}, \forall d \in \mathcal{Z}_c, \forall c \in \mathcal{AC} \quad (11)$$

#### 4.2. Case study: airline characterization by network and operational features

We present a comparison between two traditionally-known LCCs and two NCs by their complex network and operational features. This comparison underlines why the specific airline features have been chosen, and how they differentiate between the two airline types. To emphasize the importance of context, the features are compared with a variant of features obtained from a reduced dataset, that considers flights departing and arriving within the ECAC airspace only.

### Complex Network metrics

We start with the CN metrics in Table 3. The first major difference is in the size of the airline networks: LCCs operate a large point-to-point (P2P) network and consider each pair of Origin-Destination (OD) as a separate market, while NCs operate an overall smaller Network of interrelated OD pairs, with one or more hubs, commonly referred to as 'Hub&spoke' (H&S) [18].

The second major difference is in the average degree, which is evident from the difference in topology in Figures 2.a and 2.b: Ryanair's network is spread across multiple destinations which are connected by a higher number flights, while KLM's flights are focused on its hub, EHAM.

Feature	Case 1				Case 2			
	KLM	Lufhansa	EasyJet	Ryanair	KLM	Lufhansa	EasyJet	Ryanair
$n_L$	215	450	1.120	1.982	139	322	1.086	1.898
$n_A$	188	249	172	222	113	163	166	213
$\bar{k}$	2,29	3,61	13,02	17,86	2,46	3,95	13,08	17,82
$\bar{L}$	2,19	2,26	2,17	2,15	2,3	2,3	2,17	2,15
$\bar{C}$	0,16	0,49	0,51	0,51	0,24	0,55	0,51	0,52
$\bar{S}$	586,68	875,23	1.318,11	1.394,11	747,27	1.097,39	1.340,45	1.419,08

Table 3: CN metrics comparison between two 'traditional' LCCs and two NCs. The evident differences in  $\bar{S}, n_L, n_A$  for NCs stem from the lack of transcontinental flights which have been filtered in Case 2.

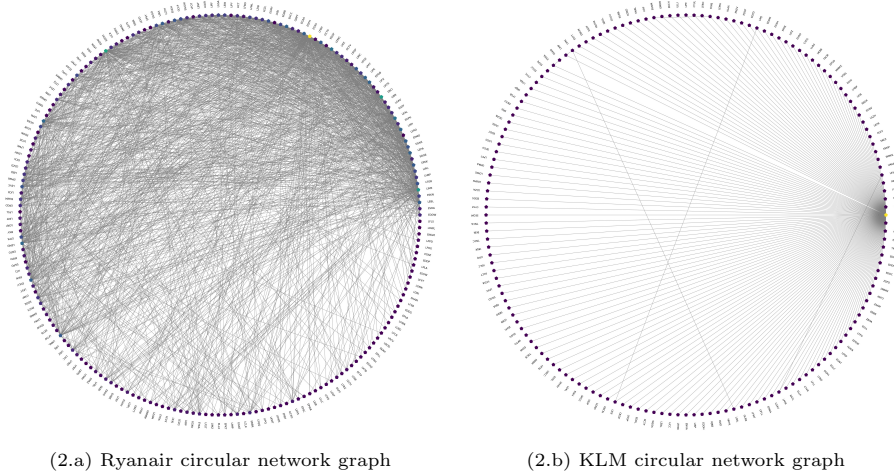


Figure 2: Airline network displayed as a circular graph for flights in August 2017: the airports are nodes and are linked if at least one flight connected the OD pair.

The difference in clustering coefficient is easily deduced from the same graphs: there are few triangles formed in KLM's network, as most flights happen between the hub and another airport. Ryanair's P2P network on the other hand, has a much higher clustering coefficient as two neighbours of a node are connected by more flights. The high value for Lufthansa's  $\bar{C}$  compared to KLM's is given by the existence of its 2 hubs, EDDM and EDDF, and the connections resulting thereof.

Finally, the average strength provides insight into the average frequency of departures at an airport. Although the averages themselves provide some information, it is also worthwhile to compare the strength survival function  $Surv = 1 - CDF$  where CDF is the Cumulative Distribution Function. The survival function shows the probability to find an airport with a specific strength, among the airports of each airline's network.

First we observe that roughly 80% of the distributions follow an exponential curve, indicated by the straight line on the semilog plot. Starting from the upper left corner of Figure 3, a few remarks are in order: Ryanair and EasyJet have different strategies for low-strength airports: 18% of EasyJet's airports exhibit 10 or less departures, while the same low frequencies represent only 5% for Ryanair. Both CDFs exhibit similar shapes, although EasyJet's distribution is consistently lower than Ryanair's, except for the high-strength airports (top 20%), where they overlap. On the NCs side, the german carrier spreads its strength more, while the dutch one focuses most of its strength between airports with  $[10^2; 10^3]$  departures. The LCCs on the other hand spread 80% of their strength over two orders of magnitude.

The comparison above clearly shows major differences in network features between traditionally-known Low-Cost and Flag Carriers and confirm the validity of the chosen features. However, these differences may be obvious only in the cases where airlines exhibit all characteristics of a certain business model, and not when they have a hybrid business model. Therefore, operational metrics are included to complete the picture.

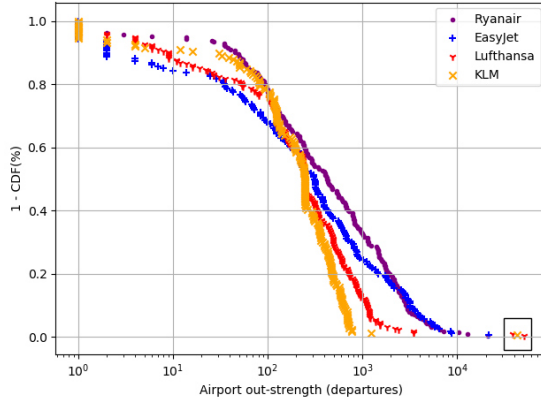


Figure 3: Airline strength survival plot. Each point represents the number of departures at one airport: the ordinate indicates the chances of finding an airport with an equal or greater (or smaller) frequency of departures, while the abscissa gives an indication on the magnitude of the number of movements. Major hubs with departures and arrivals with an order of magnitude higher are highlighted by the box in lower right corner (EHAM, EDDF, EDDM). Their position in the survival function is expected, as 99% of the rest of airports have a lower number of departures.

### Operational metrics

Table 4 shows the average values of operational features used in the clustering in Section 4.5. The average utilisation shows that when considering long-haul operations, Network Carriers have an edge over the LCCs; however when focusing on European operations only, Ryanair and EasyJet maintain their initial utilisation, while both KLM and Lufthansa drop by 40%. It is worth noticing that in Case 1, long-haul flights make up 15 – 20% of total flights for NCs. Finally, the fleet composition and size confirm that Ryanair has the biggest and most homogeneous fleet in Europe, while both Lufthansa and KLM have 4 – 5 times more aircraft types in their fleets.

Feature	Case 1				Case 2			
	KLM	Lufthansa	EasyJet	Ryanair	KLM	Lufthansa	EasyJet	Ryanair
$\bar{U}$	12,6	11,48	10,36	10,57	7,15	6,95	10,10	10,36
$n_F$	107.351	217.932	225.396	306.676	84.442	178.874	221.174	299.425
$n_{AC}$	190	355	288	413	133	286	288	413
$n_K$	19	20	5	3	16	18	5	3

Table 4: Operational airline features for operations considering intercontinental flights, weekends included (Case 1) and European flights, weekends included (Case 2).

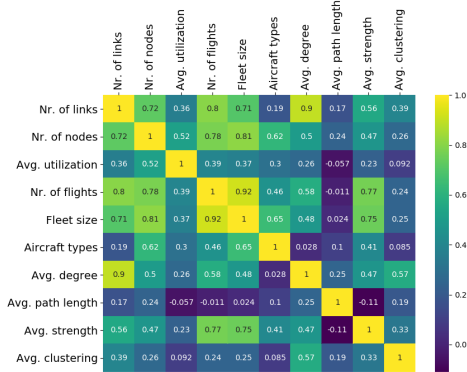
### 4.3. Data pre-processing

In this section we present the two steps of data pre-processing: reducing the data set dimensionality and z-scoring. The first step reduces computational time and permits visualisation, while the latter scales the data distribution to unit norm and renders it comparable. The size of data sets can be reduced by two methods: by discarding features that are irrelevant or already represented by others, or by merging features with the Principal Component Analysis (PCA) into a smaller number of components.

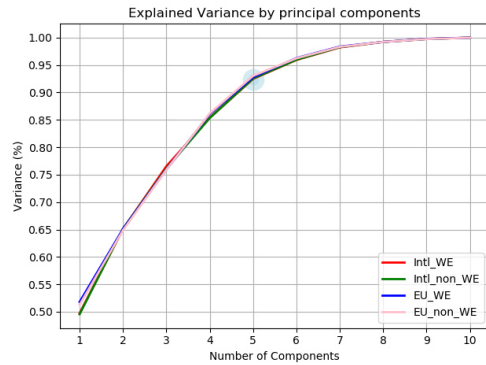
We first attempt to reduce the data set by identifying the features that are overly represented. We do this by first assessing the feature correlation: the values in the correlation heatmap shown in Figure 4.a which are close to 0 indicate a feature that brings variance in the data, while values close to  $\pm 1$  point to features that do not add much variance.

The resulting correlations are to be expected: the number of links, number of airport nodes, number of flights and fleet size are interrelated. Next, we rank the features in the order of their importance. Two approaches are proposed: supervised (SFR) and unsupervised feature ranking (UFR). The three UFR

methods used are: the Laplacian Score (LS) [42], a filtering method based on Laplacian Eigenmaps [43] and Locality Preserving Projection [44] and two Spectral Analysis (SPEC) [45] methods. Despite the lack of consistent results, they are included in this paper to be compared with the SFR rankings, as the latter makes use of the existing labels and provides trustworthy results. SFR employs the Mutual Information (MI), on which we will detail later on in (Eq. 16 and Eq. D.1). In feature ranking, MI values indicate how much each feature is influencing the resulting clustering. MI’s main advantage is that it is normalized and that it captures non-linear relationships.



(4.a) Feature Correlation heatmap. Lighter correlations indicate a higher correlation. The matrix is almost a positive manifold.



(4.b) Percentage of variance explained by PCA. 93% variance retained with 5 components.

Rank	Unsupervised Feature Ranking			Supervised Feature Ranking	
	Spectral -1	Spectral 0	Laplace	Mutual Information	Score
1	Average strength	Nr. of links	Aircraft types	Fleet size	0,77
2	Nr. of nodes	Average path	Fleet size	Nr. of links	0,67
3	Average clustering	Nr. of nodes	Average path	Total flights	0,63
4	Average path	Fleet size	Average clustering	Average degree	0,57
5	Aircraft types	Average clustering	Average utilization	Nr. of nodes	0,56
6	Average utilization	Aircraft types	Total flights	Average utilization	0,5
7	Nr. of links	Average strength	Nr. of links	Aircraft types	0,46
8	Average degree	Average utilization	Nr. of nodes	Average strength	0,40
9	Fleet size	Total flights	Average strength	Average path	0,39
10	Total flights	Average degree	Average degree	Average clustering	0,36

Table 5: UFR and SFR feature ranking results. Different rankings for all UFR methods indicate that none of them would have been close to the correct ranking. The Mutual Information (MI) score in the last column indicates how much each SFR result influenced the final clustering in Table 10. MI values are normalized  $\in [0, 1]$ .

Table 5 shows all 4 feature ranking results. The last column shows the mutual information score for the supervised feature ranking. Since the  $MI \in [0.36, 0.77]$ , it has been deemed that all features influence the final clustering a considerable amount. Thus none were discarded and the Principal Component Analysis (PCA) was used to reduce the data dimension. Noteworthy are the lower scores of the network features, except the average degree. This might occur due to the inherent lower values compared to other operational features, such as the number of flights.

### Z-score. Principal Component Analysis

Z-scoring is a common practice in Machine learning workflows and it is particularly useful when clustering by features with different scales. It is always the preliminary step, before reducing the data set dimensionality and in essence, makes features comparable:

$$Z = \frac{x - \mu}{\sigma} \quad (12)$$

where  $x$  is the feature value.

The second method used is the PCA. It reduces the dimensions (number of features) by choosing features with higher variance and combining them in a smaller number of components, while retaining as much relative variance as possible. A cumulative variance between 80 and 95% ensures a minimum fidelity with the original dataset. In this case, 5 components retain roughly 93% variance, as shown in Figure 4.b. Grouping airlines in different clusters was done on the resulting five Principal Components.

#### 4.4. Determining the number of clusters

A common issue in unsupervised ML is determining the 'right' number of clusters. As there are no existing class labels to train the algorithm on, the actual number of classes is unknown. To circumvent this issue, three solutions are proposed: K-means majority voting scheme [46], Gap Statistics (GS) [47] and Consensus Index (CI) [48][49].

Out of all, only the Consensus Index methodology has provided consistent and relevant results. The Majority Voting method performed the worst, with no relevant results all-together i.e. the optimal number of clusters increased with the increase of clusters considered. The second method was the GS. It was implemented by editing an existing application [50]. GS works by comparing 'the change of within-cluster dispersion with that expected under an appropriate reference null distribution'. According to the GS method and the maximum values in Figure 5, the optimum number of clusters is two. This was deemed to small for the amount of airlines present in the data set, however the smaller peaks for  $K = 7, 8$  point to a potentially robust clustering sub-structure.

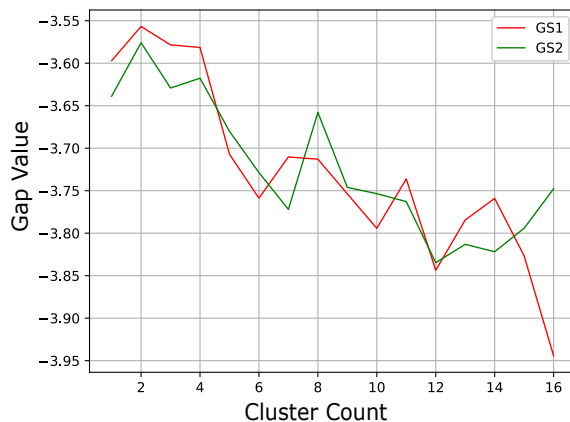


Figure 5: Gap Statistic results corresponding to two random uniform reference distribution. The maximum values point to the 'optimal' number of clusters.

##### 4.4.1. Consensus Index methodology

The Consensus Index (CI) method draws its utility from two popular measures: the Adjusted Rand Index (ARI)[51] and the Adjusted Mutual Information (AMI)[52]. The main idea behind the Consensus Index (CI) is that a robust data structure is uncovered in the data set by comparing the clusterings<sup>1</sup> generated from multiple, random data (sub)sets. The underlying hypothesis is that with the correct number of clusters  $K_{\text{true}}$  imposed on the data, 'the discrepancy between the clusterings obtained [...] should be minimized, meaning that the cluster structure discovered is robust.'[48]. Given a value of  $K$  and a set of  $B$  clustering solutions  $\mathcal{U}_K = \{\mathbf{U}_1, \mathbf{U}_2, \dots, \mathbf{U}_B\}$ , each with  $K$  clusters, the Consensus Index (CI) of  $\mathcal{U}_K$  is:

<sup>1</sup>A clustering refers to a solution to the cluster problem and is composed of a number of clusters, or groups.

$$CI(\mathcal{U}_K) = \sum_{i < j} AM(\mathbf{U}_i, \mathbf{U}_j) \quad (13)$$

with AM being any suitable 'Adjusted Measure'. The optimal clustering number  $K^*$  is chosen as the one that maximizes the CI:

$$\begin{aligned} K^* &= \max CI(\mathcal{U}_K) \\ K &= 2 \dots K_{\max} \end{aligned} \quad (14)$$

meaning that, similar to the GS method, a peak in the CI plot points to the optimal number of clusters.

The first AM is the Adjusted Rand Index (ARI) [49]: it is a pair-counting method that quantifies the agreement level between clustering results of different clusters, i.e. if data points in the clusterings belong to the same group or not. The ARI is the adjusted-for-chance form of the Rand Index [53], and is defined as:

$$ARI(\mathbf{U}, \mathbf{V}) = \frac{2(N_{00}N_{11} - N_{01}N_{10})}{(N_{00} + N_{01})(N_{01} + N_{11}) + (N_{00} + N_{10})(N_{10} + N_{11})} \quad (15)$$

where each element in Eq. 15 refers to the number of events of that type. The four types of events are described in the right side of Table 6). The relationship between two clusters is described by a contingency table, shown in the left side of Table 6.

$\mathbf{U} \setminus \mathbf{V}$	$V_1$	$V_2$	...	$V_C$	Sums	Event	Definition
$U_1$	$n_{11}$	$n_{12}$	...	$n_{1C}$	$a_1$	$N_{11}$	same clustering U and V
$U_2$	$n_{21}$	$n_{22}$	...	$n_{2C}$	$a_2$	$N_{10}$	same clustering U but not V
$\vdots$	$\vdots$	$\ddots$	$\vdots$	$\vdots$	$\vdots$	$N_{01}$	same clustering V but not U
$U_R$	$n_{R1}$	$n_{R2}$	...	$n_{RC}$	$a_R$	$N_{00}$	different clustering U and V
Sums	$b_1$	$b_2$	...	$b_C$	$\sum_{ij} n_{ij} = N$		

Table 6: Left: Contingency Table  $n_{ij} = |U \cap V|$ . Right: Event types considered for pair counting.

The second measure is the Adjusted Mutual Information (AMI) [49], an Information Theoretic based measure. In essence,  $MI(\mathbf{U}, \mathbf{V})$  indicates how much can be deduced of cluster  $\mathbf{U}$  by looking at cluster  $\mathbf{V}$ . AMI is mathematically defined by joint, conditional and simple entropy  $\mathbf{H}$ , which are derived from the marginal distributions from the left side of Table 6:

$$AMI(\mathbf{U}, \mathbf{V}) = \frac{MI(\mathbf{U}, \mathbf{V}) - E\{MI(T)|a, b\}}{\sqrt{H(\mathbf{U})H(\mathbf{V}) - E\{MI(T)|a, b\}}} \quad (16)$$

where entropy is defined as :

$$H(\mathbf{U}) = - \sum_{i=1}^R \frac{a_i}{N} \log \frac{a_i}{N} \quad (17)$$

#### 4.4.2. Consensus Index methodology steps

The applied CI methodology is summarized below ( $K$  is the resulting cluster numbers):

1. **Pre-processing:** airlines with fewer than 10 flights each month or a fleet consisting of four aircraft or less are discarded.
2. **Standardization:** Z-scoring each feature.
3. **Cluster generation:** for each cluster number  $K \in [2, 14]$ , we randomly sub-sample 90% of the original data set. With this new data set, we perform a (KMeans++)-type clustering, 200 times. This results in a set of 200 solutions (group labels).
4. **Consensus Index:** for each  $K$ , we assess the agreement between all 200 clusterings defined previously, by computing the AMI and ARI values.

5. **Stability Assessment:** due to the stochastic nature of the sub-sampling approach, the process is repeated.  $200 \cdot 199 = 39,800$  values for both indices per  $K$  are calculated and averaged, leading to  $39,800 \cdot 13 = 517,400$  iterations for each round of sampling for each measure. There are two measures and the process has been repeated twice, thus:  $517,000 \cdot 4 = 2,068 \cdot 10^6$  iterations were done in total.
6. **The maximum value** of the CI in Figure 6 indicates the 'optimal' number of clusters.

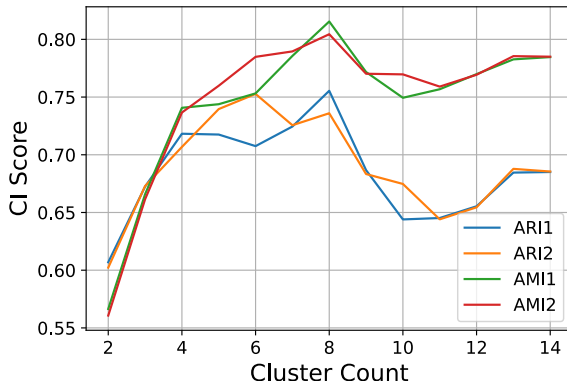


Figure 6: Consensus Index results. Due to the stochastic nature of the sub-sampling, both measures have been calculated twice. The maximum peaks represent the number of clusters for which the clustering is deemed more robust and thus, optimal. 3/4 measures point to  $K^* = 8$

Figure 6 shows 3/4 measures with maximum values at  $K = 8$  and one with  $K = 6$ . Thus the final number of clusters is  $K^* = 8$ . This result is also in line with what was hinted by the first round of the Gap Statistics results in Figure 5.

#### 4.5. Clustering Ensembles

This section presents the clustering ensembles, which are a better alternative to individual clustering algorithms, because of their improved stability, robustness and accuracy. The strength of this method lies in the multiple algorithms that generate individual partitions, which are then integrated in one final, representative clustering. This last step is commonly referred to as a consensus or objective function. In total, 17 individual partitions have been obtained by six different algorithms, each with varying parameters<sup>2</sup>. Except HDBSCAN, all runs have been performed with  $K^* = 8$  imposed on the data. The Clustering Ensemble was built by editing the OpenEnsemble library [54], which integrates most of scikit-learn [55] algorithms and independent algorithms, such as HDBSCAN. [56]. The ensemble consists of: one run with K-means ++ [57] with  $n\_jobs=1$ , one run of Gaussian Mixture Models (GMMs) [58], one run of Birch [59], two runs of Spectral Clustering, one with Euclidian (l2) and one with Manhattan (l1) distance; four HDBSCAN runs, each with one of the following pairs of `min_sample` and `min_cluster_size`: (2, 2), (3, 2), (5, 2), (2, 3); and finally eight runs of Hierarchical Agglomerative Clustering (HAC): a combination of the two distances (l1 and l2) and four linkage types: Ward's, average, complete and single. The linkage defines how the distance between clusters is computed. The last three linkages are presented in Figure 7. One other type, Ward's linkage [60] is used, which merges groups at each step while minimizing a cost index, defined as:  $C = SS_{12} - (SS_1 + SS_2)$ , where  $SS_{12}$  is the error sum of squares of the newly-formed cluster, and the other terms are the error sums of squares of the previous, separate clusters.

##### 4.5.1. Consensus Function

The main challenge posed by clustering ensembles is to find the objective function that uncovers the 'best' or representative partition [61]. A suitable option is the HAC algorithm. The HAC algorithm has two main parameters: the 'cut' and the linkage type. The 'cut' parameter is particularly useful because we can freeze the solution tree at a given number of clusters. More on this in the next section. Regarding the linkage type,

<sup>2</sup>Where no parameters are mentioned, the default settings were used

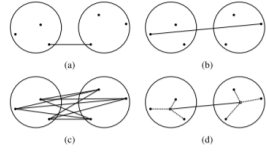


Figure 7: Linkage types a)single, b)complete, c)average, d) centroid [62].

Clustering	Linkage	Cut
$\Gamma_A$	Average	0.5
$\Gamma_W$	Ward	1.05

Table 7: Preliminary Clustering results and the associated parameters.

the average and Ward linkage types are suitable because they use information from all the points within a cluster, and not just an extremity. This leads to an overall more robust and cohesive cluster.

#### 4.6. Initial clustering results.

This section presents the two initial clusterings obtained with the clustering ensemble and the process of selecting the final clustering, based on a number of internal clustering indices. Internal indices are used to assess the clustering structure without external information and assess the cluster cohesiveness, compactness, density and separation. [63].

At this point in the workflow, the desired final number of clusters is known (8) and a total of 17 individual clusterings have been obtained. We reverse engineer the HAC algorithm by looking which combination of 'cut' and linkage parameter yield results with  $K = 8$ . To generate the representative cluster, the HAC is iteratively employed with cuts ranging from 0 to 4 in 0.01 increments. 800 possible results are obtained, out of which only two have  $K = 8$  clusters:  $\Gamma_W$  and  $\Gamma_A$ . The two results are compared by internal indices in Table 8. The final clustering is  $\Gamma_A$ , as it scores better on 10/13 indices.

Aspect	Minimum						Maximum							
	Compactness, separation, density			Cohesion, dispersion						Mean dispersion	Separation	See description		
Validation Indices	$S_{dbw1}$	$S_{dbw2}$	$S_{dbw3}$	DB	XB		P. Bis	CH	$D_1$	$D_2$	$D_3$	BH	modif. H	Coph. corr.*
$\Gamma_A$	0,59	0,56	0,49	1,04	0,63	0,26	-1,04	35,36	0,02	0,09	0,59	2,44	14,58	0,85
$\Gamma_W$	0,64	0,63	0,55	1,6	3,57	0,17	-0,8	22,14	0,025	0,14	0,34	2,5	13,4	0,62

Table 8: Internal validation indices. The first row points to the desirable value. In green are the best values for the given index<sup>a</sup>.

<sup>a</sup>**DB**:Davies-Bouldin; **XB**: Xie-Beni; **P.Bis**: Point Biserial; **CH**: Calinski-Harabasz; **D**-Dunn Family Indices; **BH**: Ball-Hall; **modif.H**: modified Hubert statistic. **Coph. corr**: Cophenetic Correlation

Two indices are briefly analysed: the cophenetic correlation coefficient provides a normalized measure on the similarity between the initial, unclustered points' pairwise distances, and the distance between the groups in which they end up in.  $\Gamma_A$  has a cophenetic correlation of 85%, which indicates a strong resemblance to the initial data. The second index is the average silhouette score, which assesses cluster cohesiveness. In addition, each cluster silhouette profile in Figure 8 shows an individual coefficient: if data points in the cluster are cohesive with the rest of the cluster, they have a positive score.  $\Gamma_A$  displays only one large part of cluster 7 with a negative score, while others groups have few points in the negative area. On the other hand,  $\Gamma_W$  provides more evenly distributed clusters, but its average silhouette score is lower. Three out of seven clusters have a considerable number of points with a negative score, suggesting that these points would fit better in a different cluster.

#### 4.7. Final Clustering results

This section presents the final clustering results. i.e. the airline groups as used in the second part of the paper. Figure 9 shows the process: the HAC algorithm is employed as the consensus function on the ensemble's co-occurrence matrix. The co-occurrence matrix is a square matrix whose entries  $a_{ij}$  are the fraction of each airline  $i$  co-occurring in the same group as airline  $j$ :  $a_{ij} = \frac{x}{17}$ . The resulting groups can be observed in different colours on the dendrogram on the left, which also shows the internal structure of the dataset.

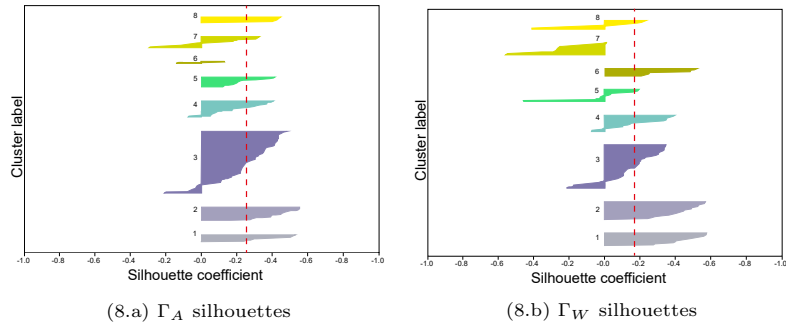


Figure 8: Average silhouette per clustering and silhouettes for each cluster (airline group).  $-1$  is the worst score,  $1$  is the best. Values of or close to  $0$  indicate overlapping clusters.

The dendrogram reflects the co-occurrence matrix and vice-versa. The groups in the dendrogram (same colour) are mirrored by the light areas along the matrix’s main diagonal, while the different hues in the matrix correspond to each airlines’ similarity to the other airlines. The similarity is also reflected by the length of the horizontal lines in the dendrogram. The vertical lines, or plateaus, indicate a newly formed group. The ‘cut’ is the distance above which clusters are no longer merged and thus, dictates the final clusters. The same dendrogram with airline names can be better visualised in full in Appendix A. Its colours correspond to the final airline groups in Table 10.

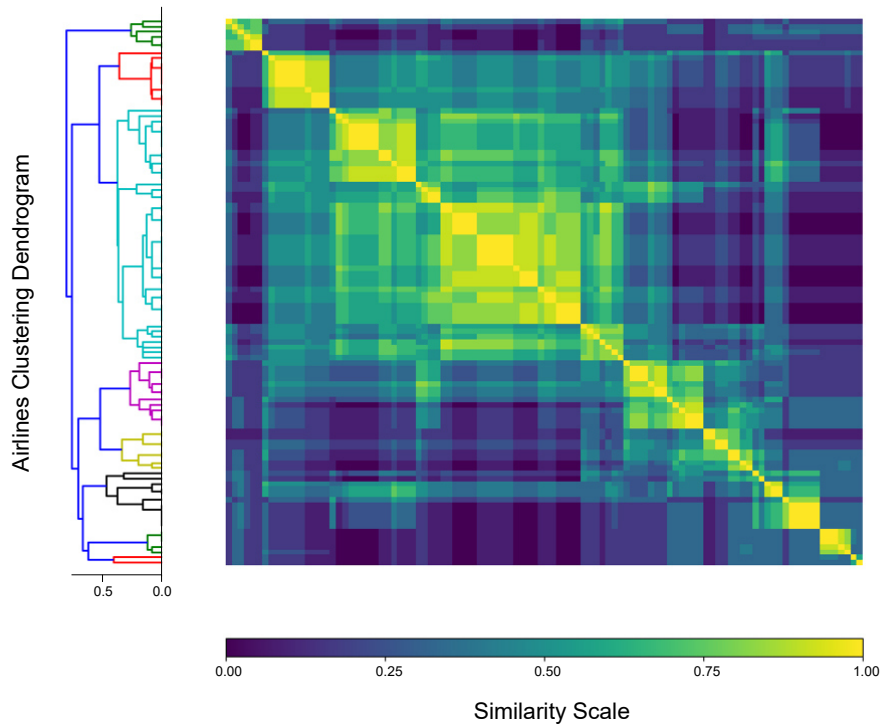


Figure 9: The clustering ensemble co-occurrence matrix with a similarity band below, and the associated dendrogram on the left. Each unit square in the matrix represents the fraction of times airlines  $i$  and  $j$  were in the same group. The lighter an area, the higher the number of times two airlines co-occurred in the clustering ensemble. The co-occurrence matrix also confirms the hints from the Gap Statistics results in Figure 5:  $2 - 3$  initial groups can be identified, one of them rather large, with a vague contour.

Next, we reflect on the results by cross-comparing Table 9 and the airline groups’ feature values. Individual airline features can be found in Annex Appendix A Group 1 components seem to fit together: they show a medium-small network with a low  $\bar{C}$  and a rather low average utilization, typical for small regional or feeder

airline types. Group 2 has also coherent components and consists mostly of traditionally-known flag carriers (except Air Europa). We notice a much larger network and average number of flights compared to the previous group and a heterogeneous fleet. Group 3 is the largest group and contains almost half of the airlines in the dataset, which account for less than 10% of the total flights. Perhaps due to low feature values, it is a mixed group of airlines with smaller fleet, fewer and less connected destinations. Some traditionally-known flag carriers appear here, too: Czech, Croatia, Moldova, Air Serbia, Tarom, Luxair, Bulgaria, Aegean, a.o., most likely because of considerably less flights than those in Group 2, but three to four times more than those in Group 1. Laudamotion, Transavia FR appear here, due to a much lower average aircraft utilization and half the average degree compared to other LCCs in the Groups 5 and 7. Group 4 is a 'clean' group, with no surprise members among the medium LCCs and holiday charters. Group 5 is a mixed group: Alitalia and SAS show similar features as some larger LCCs and regional airlines such as Air Berlin and Hop!: a large, highly clustered network flown by a hundreds of aircraft and double-digits aircraft types. Group 6 is also a mix of long-haul carriers, regional airlines and subsidiaries that operate the smallest networks in the data set. Finally, Groups 7 and 8 represent the major European Flag and Low-Cost Carriers. and account for over 40% of all flights in the dataset, thus are the main focus of the trajectory deviations in Section 5.

Airline Groups	$n_L$	$n_A$	$\bar{U}$	$n_F$	$n_{AC}$	$n_K$	$\bar{k}$	$\bar{L}$	$\bar{S}$	$\bar{C}$
1	144	74	3	3766	24	6	3,61	2,84	67	0,28
2	142	105	10	41134	84	13	2,73	2,1	396	0,25
3	94	54	7	8737	27	5	3,3	2,18	178	0,35
4	394	116	10	29371	57	6	6,65	2,25	283	0,5
5	400	135	8	70802	163	13	5,89	2,22	548	0,5
6	18	16	7	4074	25	3	2,25	1,9	283	0,2
7	373	227	12	149510	303	21	3,18	2,17	678	0,32
8	1551	197	10	266020	350	4	15,44	2,16	1356	0,51

Table 9: Average group airline feature values for the clustering methodology. These are the average features that are included in the five Principal Components on which the clustering has been done.

Group	Airlines	Count
1	CityJet, Adria Airline, Eastern Airways, Sun Air of Scandinavia, Twin Jet	5
2	Air Europa, Austrian Airlines, Ukraine International Airlines, Brussels Airlines, Air Baltic, Aer Lingus, Finnair, Iberia Airlines, LOT Polish Airlines, Swiss Air Lines, TAP Portugal	11
3	Aigle Azur, Adria Airways, Aegean Airlines, Air Malta, Air Nostrum, Air Serbia, Aurigny Air Services, Astra Airlines Regional, Blue Islands, Belair Airlines, Blue Air, Blue Panorama Airlines, Braathens, Regional Airlines, Air Corsica, BA CityFlyer, Czech Airlines, Croatia Airlines, Edelweiss Air, Ellinair, Cobalt, Fly One, Atlantic Airways, Sky Wings Airlines, Iberia Express, Icelandair, Meridiana, AlbaStar, Luxair, Loganair, Bulgaria Air, Montenegro Airlines, Air Moldova, Laudamotion, NextJet, Olympic Air, Helvetic Airways, People's Vienna, Primera Air Scandinavia, Tarom, Malmö Aviation, Sky Express, Stobart Air, Sunexpress DE, Sunexpress TK, Tunisair, Thomas Cook, Transavia NL, Transavia FR	48
4	Condor Flugdienst, Jet2.com, Germania, Germanwings, TUIFly, Monarch Airlines, Neos, Pegasus, TUI Airways, Volotea, Widerøe, Wizz Air	12
5	Alitalia, Flybe, Air Berlin, Eurowings, Hop!, Norwegian Air Shuttle, Scandinavian Airlines, Vueling Airlines	7
6	Albawings, Bergen Air Transport, Dreamjet, Air Dolomiti, Air VIP, British Airways Shuttle, Siavia, Virgin Atlantic Airways, XL Airways	9
7	Air France, British Airways, Lufthansa, KLM, Turkish Airlines	5
8	EasyJet, Ryanair	2

Table 10: The final list of airline groups resulting from the unsupervised clustering ensemble.

## 5. Horizontal and vertical trajectory deviations

In this section we present the en-route trajectory analysis results. First, we present the horizontal efficiency results per groups and a spatio-temporal analysis in Section 5.1. Then, the vertical deviations are characterized by the novel Flight Level Adherence Index for Realized trajectories (FAIR) in Section 5.2. Each section presents first a high-level overview of all groups, followed by a comparison between the Low-Cost and Network Carriers in Groups 7 and 8. More results per individual airline are presented in Appendix B.

### 5.1. Horizontal trajectory efficiency

The horizontal efficiency ( $E_i$ ) is defined for a flight  $i$  and is the ratio between the Great Circle distance (GC) i.e. the shortest path between two points along an ellipsoid, and the actual length of the trajectory:

$$E_i = \frac{d_{GC}(w_{i,1}, w_{i,n})}{\sum_{j=1}^{n-1} d(w_{i,j}, w_{i,j+1})}, \forall f_i \in \mathcal{F}, \forall w_{i,j} \in \mathcal{W}_i \quad (18)$$

Efficiency is derived for the en-route phase considering only navigation points above FL 245, to reduce the variations in trajectories which normally occur due to vectoring or busy traffic at lower flight levels. First, groups are compared by means of efficiency difference  $\delta_{E,i}$ , followed by an hourly and daily analysis. Finally, the trajectories corresponding to a set of efficiency outliers are presented.

The efficiency difference  $\delta_{E,i}$  is the difference between the planned and realized efficiency of the same flight  $i$ :

$$\delta_{E,i} = \begin{cases} \delta_{E,i}^+, & \text{if } \mathcal{E}(M3) > \mathcal{E}(M1) \\ \delta_{E,i}^-, & \text{if } \mathcal{E}(M3) < \mathcal{E}(M1) \\ \delta_{E,i}^0, & \text{if } \mathcal{E}(M3) = \mathcal{E}(M1) \end{cases}, \forall f_i \in \mathcal{F} \quad (19)$$

Table 11 presents the numbers and percentages of flights for each group. Group 8 (LCCs) stands out as the group with the highest fraction of flights whose realized efficiency is higher than its planned efficiency. By contrast, Network Carriers in Group 7 exhibit approximately 10% less flights with positive  $\delta_E$ .

Airline group	1	2	3	4	5	6	7	8
Total	20.773	846.670	699.247	690.387	1.084.764	78.011	1.612.942	1.173.483
$\delta_E^-$	97.73	339.589	270.214	271.599	501.368	42.641	664.754	462.283
$\delta_E^+$	109.39	494.525	419.221	368.660	578.569	31.611	801.646	710.762
$\delta_E^0$	61	12.556	9.812	50.128	4.827	3.759	146.542	438
$\delta_E^- \%$	47	40	39	39	46	55	41	39
$\delta_E^+ \%$	53	58	60	53	53	41	50	61
$\delta_E^0 \%$	0	2	1	8	1	4	9	0

Table 11: Number and percentage of flights per group by efficiency difference  $\mathcal{E}(M1) - \mathcal{E}(M3)$ . Percentage values have been rounded up to the nearest integer.

Next, we show the average hourly and daily efficiency for all groups in Figures 10.a and 10.b. The overall weekly and hourly trends can be easily observed and have been determined by means of averaging all efficiency values:

$$E_{\mu,x} = \sum_{i=1}^n \frac{E_i}{n}, x = \{hour, day\}, \quad (20)$$

where  $n$  is the total number of flights during either the day or hour in question. Daily efficiency averages for groups show the planned and realized efficiency almost constant throughout the week, with the planned trajectory efficiency consistently higher relative to the realized efficiency. This is expected, as each flight is planned on the best available planned route, while the actual trajectory gets deviated and takes on average, 1% longer. The hourly planned efficiency show an additional trend: flights departing during early morning or late night have a higher efficiency (both planned and realized) than the flights departing at other hours

during the day. The trend can be attributable to the increase in traffic during those hours, and is similar to other results, [10], although the horizontal efficiency was computed along the entire trajectory, and not only for the en-route phase, as in the current study. For detailed hourly M3 efficiency values, the reader is invited

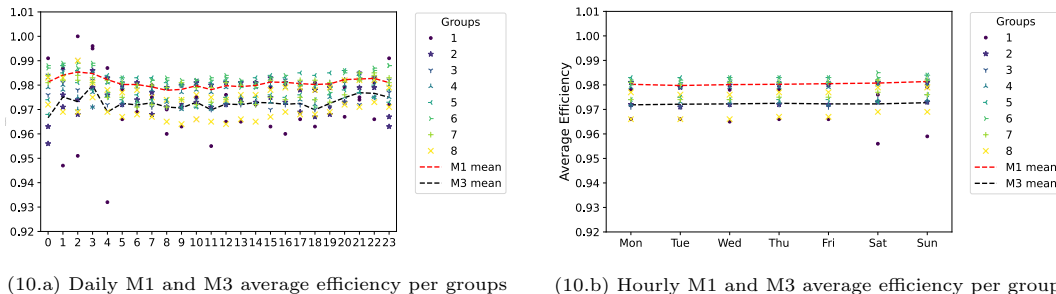


Figure 10: Hourly and daily average efficiency values for the en-route phase of flights throughout the entire year of 2017. The dotted lines represent the daily and hourly overall trends, obtained by averaging the groups averages.

to consult Table 12. The other hourly M3 and daily M1 and M3 efficiency averages and standard deviations are presented in Appendix B.

Group	1		2		3		4		5		6		7		8	
Hour	$\mu$	$\sigma$														
0	0,991	0,008	0,963	0,06	0,984	0,015	0,983	0,024	0,974	0,039	0,988	0,01	0,984	0,017	0,983	0,028
1	0,987	0,012	0,976	0,044	0,986	0,013	0,98	0,024	0,988	0,011	0,989	0,01	0,984	0,013	0,983	0,015
2	1		0,974	0,054	0,985	0,014	0,975	0,03	0,986	0,02	0,989	0,009	0,984	0,024	0,99	0,008
3	0,995	0,006	0,986	0,024	0,982	0,019	0,977	0,027	0,985	0,021	0,989	0,008	0,983	0,02	0,981	0,016
4	0,987	0,014	0,983	0,02	0,982	0,022	0,981	0,023	0,984	0,021	0,981	0,023	0,982	0,02	0,978	0,02
5	0,978	0,024	0,98	0,027	0,981	0,02	0,979	0,024	0,983	0,022	0,983	0,019	0,981	0,021	0,977	0,021
6	0,981	0,02	0,981	0,019	0,98	0,022	0,979	0,024	0,983	0,021	0,98	0,025	0,98	0,02	0,978	0,021
7	0,98	0,025	0,977	0,028	0,979	0,021	0,978	0,023	0,983	0,022	0,982	0,019	0,98	0,021	0,975	0,022
8	0,97	0,033	0,979	0,024	0,979	0,02	0,979	0,024	0,981	0,021	0,982	0,016	0,979	0,025	0,974	0,024
9	0,972	0,032	0,98	0,024	0,98	0,021	0,977	0,027	0,98	0,022	0,982	0,017	0,981	0,019	0,974	0,022
10	0,98	0,025	0,981	0,022	0,982	0,018	0,978	0,021	0,98	0,022	0,982	0,019	0,979	0,021	0,976	0,022
11	0,971	0,029	0,98	0,022	0,98	0,022	0,977	0,025	0,981	0,022	0,982	0,019	0,979	0,023	0,975	0,022
12	0,976	0,027	0,981	0,026	0,981	0,02	0,979	0,023	0,982	0,021	0,984	0,015	0,981	0,019	0,974	0,023
13	0,974	0,032	0,981	0,024	0,981	0,018	0,98	0,022	0,981	0,023	0,982	0,018	0,98	0,02	0,976	0,021
14	0,981	0,023	0,981	0,021	0,98	0,02	0,979	0,022	0,983	0,022	0,979	0,023	0,98	0,02	0,976	0,022
15	0,979	0,021	0,983	0,021	0,981	0,022	0,98	0,022	0,984	0,021	0,983	0,02	0,982	0,019	0,978	0,021
16	0,98	0,022	0,981	0,026	0,982	0,02	0,979	0,023	0,983	0,023	0,984	0,019	0,981	0,022	0,979	0,02
17	0,98	0,021	0,978	0,031	0,981	0,02	0,98	0,021	0,985	0,02	0,98	0,02	0,982	0,02	0,979	0,022
18	0,981	0,019	0,978	0,034	0,98	0,021	0,979	0,025	0,984	0,02	0,98	0,021	0,982	0,019	0,978	0,023
19	0,98	0,021	0,979	0,028	0,98	0,02	0,981	0,02	0,985	0,019	0,979	0,02	0,981	0,02	0,979	0,019
20	0,979	0,021	0,982	0,028	0,981	0,019	0,98	0,024	0,986	0,016	0,986	0,013	0,982	0,019	0,982	0,017
21	0,975	0,023	0,985	0,02	0,982	0,017	0,982	0,018	0,984	0,017	0,985	0,012	0,985	0,015	0,982	0,017
22	0,981	0,014	0,983	0,035	0,982	0,016	0,982	0,019	0,98	0,021	0,987	0,013	0,985	0,013	0,982	0,017
23	0,991	0,011	0,967	0,063	0,982	0,015	0,98	0,025	0,978	0,019	0,988	0,012	0,983	0,018	0,979	0,025

Table 12: Variance and average realized (M3) efficiency for every hour per airline group.

We now turn our focus on groups 7 and 8. In Figure 10.a we observe that Groups 7 and 8 have slightly higher average efficiency during the weekends, even though the overall trend is constant during the week when taking into account all groups. Moreover, NCs have consistently higher daily and hourly average realized and planned efficiency. Figure 11 compares the realized efficiency more in-depth: per hour between Groups 7 and 8. The generic trend seen in Figure 10.b is visible here, too, with flights deviating more during daytime and less in the night and early morning. On average, Group 8 shows a lower efficiency than group 7, except during a few hours during the night and early morning. One reason for this might be the more straight

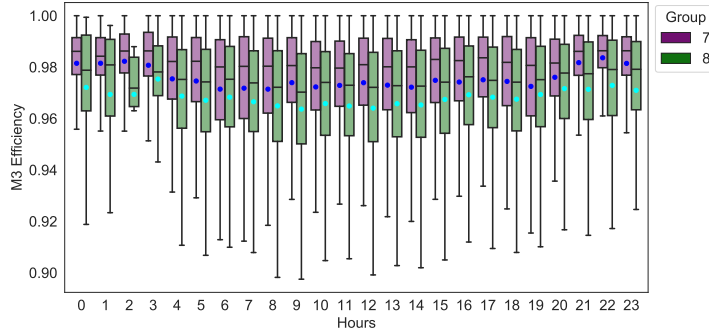


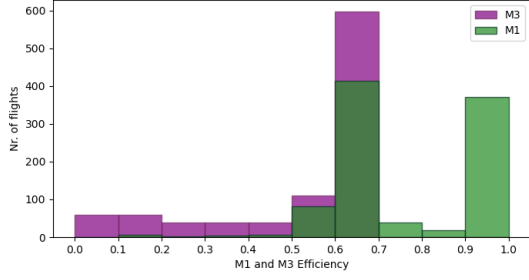
Figure 11: Hourly M3 efficiency comparison between groups 7 and 8. The horizontal edges of the boxes represent the interquartile range and the median values, and the dots represent the average values.

parts of oceanic trajectories included in the analysis, which mostly NCs fly. Next, we use the independent t-test [64] to compare the underlying distribution that yields the averages in Table 12. The t-test is a hypothesis testing method that aims at testing the null hypothesis that two distributions are similar, and the independent version allows testing samples with different number of components. Table 13 shows that only groups 3, 5 and 7 exhibit similar efficiency distributions. This is a reasonable conclusion, as both Groups 3 and 5 consist of a number of traditionally-known Flag Carriers, but with a smaller fleet than the Network Carriers in group 7. Figures B.20.b and B.20.a show the pairwise t-test values between all airlines, ordered by the group they belong to. No conclusion can be drawn directly from the individual airline t-tests.

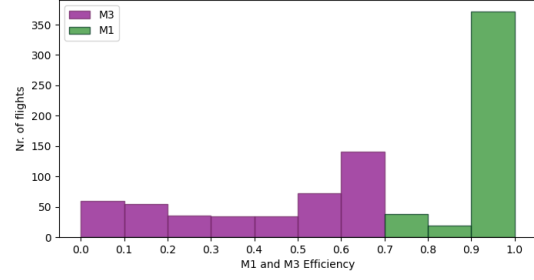
Group	1	2	3	4	5	6	7	8
1	1	0	0	0	0	0,01	0	0
2	0	1	0,01	0	0	0	0	0
3	0	0,01	1	0	0,11	0	0,3	0
4	0	0	0	1	0	0	0	0
5	0	0	0,11	0	1	0	0,44	0
6	0,01	0	0	0	0	1	0	0
7	0	0	0,3	0	0,44	0	1	0
8	0	0	0	0	0	0	0	1

Table 13: T-tests for M3 efficiency per airline groups.

Finally, a number of realized efficiency outliers have been observed and are given additional consideration. In this case, outliers are realized efficiency values  $E^r \in (0, 0.7]$ . First, we identify the flights with realized efficiency in said interval. Out of that particular dataset, we discard those flights that have also planned efficiency  $E^p = (0, 0.7]$ . Therefore only flights that were planned to have an increased efficiency, but failed to do so, are analysed. The process is easily visualised by the histograms in Figure 12.a and Figure 12.b. An example of trajectories with the lowest efficiency bracket are displayed in Figure 13. The U-shaped trajectories reflect flights that were forced to deviate from their planned flight plan, and possibly causing further deviations to other airspace users.



(12.a) Histogram with flights  $E^r < 0.7$



(12.b) Histogram with flights  $E^r < 0.7$  and  $E^p > 0.7$

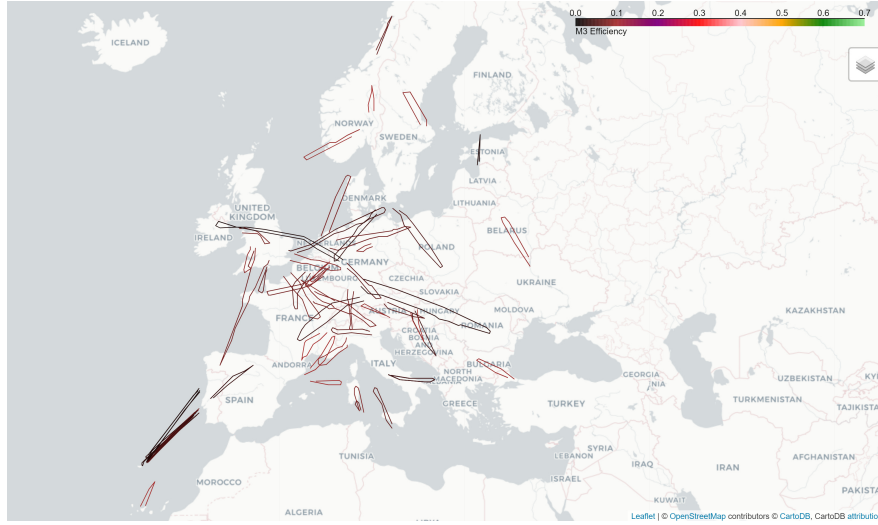


Figure 13: Flights in the realized efficiency bracket (0,0.1]. All trajectories are above FL 245

Table 14 shows the number of flights with unplanned low efficiency per group and for each efficiency bracket. Interesting to observe that, although NCs in group 7 have an overall higher average realized efficiency, they have roughly 3 times more flights with outlier efficiency. Some of the trajectories may be linked to adverse weather over the Alps, which has prompted the neighbouring FABEC ANSPs to implement new ATC procedures [65]. Finally, Figure 13 provides an overview of all deviated trajectories in the ECAC area, in the lowest efficiency bracket. For the rest of efficiency brackets, the reader is invited to consult Appendix B.

Group	(0.0,0.1]	(0.1,0.2]	(0.2,0.3]	(0.3,0.4]	(0.4,0.5]	(0.5,0.6]	(0.6,0.7]	Total
1	0	0	1	0	0	0	0	1
2	14	6	3	3	6	29	367	428
3	6	8	8	5	5	7	30	69
4	7	10	2	4	4	17	33	77
5	11	14	6	12	10	23	29	105
6	1	0	0	0	1	0	0	2
7	11	17	14	13	10	18	107	190
8	9	4	4	2	2	14	30	65

Table 14: Number of flights per M3 efficiency bracket for each group. Only those flights with a planned efficiency higher than 0.7 are included.

In this section we have confirmed the hourly efficiency patterns of efficiency increase during early morning and late night due to the lower flight counts; that Network Carriers are overall more efficient than LCCs, and that both groups see an increase of efficiency in the weekends. Finally, although only a small fraction of the total flights in 2017, unplanned U-shaped trajectories above FL 250 have to a possible network-wide planning

inefficiency and a sub-optimal trajectory management. These findings pave the way towards understanding whether problematic departure slots exist or could be used as a measure of assessing the effectiveness of new ATC procedures.

### 5.2. Vertical trajectory deviations

In this section we present the method by which the novel Flight Level Adherence Index for Realized trajectories (FAIR) has been obtained and a comparative analysis between two groups of airlines obtained in Section 4: Low-Cost Carriers and Network Carriers. The Flight Level Adherence Index for Realized trajectory (FAIR) indicates, on average, how much the true flight trajectory has deviated from its planned flight level during the cruise phase. In essence, it is the average vertical deviation  $\Delta z$  at all waypoints  $w_{ij}^r(x, y, z)$ , along the entire cruise phase  $\forall f_i \in \mathcal{F}$ . The realized cruise flight phase is defined relative to the planned cruise, which begins at the planned Top of Climb ( $TOC^p$ ) and ends at the planned Top of Descent ( $TOD^p$ ). By considering the entire length of the trajectory in defining the metric, we renounce the need of a proxy measure to characterize deviations i.e. 100 ft x 10 minutes. The method is summarized next, followed by a detailed step-wise approach.

### 5.3. FAIR Methodology

Let  $w_{ij}(x, y, z)$  be the  $j$ th waypoint of the  $i$ th flight  $f_i \in \mathcal{F}$ . We denote  $w_{ij}^p$  the waypoints belonging to the planned trajectory  $f_i^p$  of flight  $i$ , and  $w_{ik}^r \in f_i^r$  the navigation points in the realized trajectory  $f_i^r$  of the same flight  $i$ :

$$w_{i,j}^p \in f_i^p, \forall w_j^p \in W_i^p, \forall f_i^p \in F \quad (21)$$

$$w_{i,k}^r \in f_i^r, \forall w_k^r \in W_i^r, \forall f_i^r \in F \quad (22)$$

A point  $w_{ik}^r(x, y, z)$  has a corresponding, closest point  $w_{ik}^{r'}(x', y', z')$  with  $w_{ik}^{r'} \in f_i^p$ . The spatial coordinates of each point  $w_{ij}^r$  are defined as  $x_{ik}^r, y_{ik}^r, z_{ik}^r$ , and for their associated, projected points  $w_{ij}^{r'}$ , in a similar manner. Once the points are synchronized, i.e. each point on the M3 trajectory has a corresponding, closest point on the M1 trajectory, the area  $a_{ij}$  under the vertical differences of each  $j$ th vertical component is defined, and then integrated by trapezoid rule:

$$\int_a^b f(x)dx \approx (b - a) \cdot \frac{f(a) + f(b)}{2} \quad (23)$$

Thus we replace  $x$  with the absolute difference between the vertical components between the M3 trajectory waypoints and their 'pairs',  $\Delta(z) = |z_{ik}^r - z_{ik}^{r'}|$ . The intervals to integrate over are equivalent to the distance along the trajectory for each point,  $da_k^r$ :

$$a_{i,k} = \int_{da_k^r}^{da_{k+1}^r} f[\Delta(z)]dx \approx (da_k^r - da_{k+1}^r) \cdot \frac{f(da_{k+1}^r) + f(da_k^r)}{2} \quad (24)$$

Thus, the  $FAIR_i$  becomes the sum of all such segments, divided by the total length of the trajectory:

$$FAIR_i = \sum_{k=1}^{n-1} \frac{a_{i,k}}{da_{i,n}^r} \quad (25)$$

Note that  $z_{ik}^r$  is the vertical component of the  $k$ th actual vertical point, while  $z_{ik}^{r'}$  is the vertical component of its pair, 'projected' on the planned trajectory. All vertical components have been transformed in meters and corrected for altitude, as explained in Table F.22. Figure 14 shows a visual representation of the FAIR methodology.

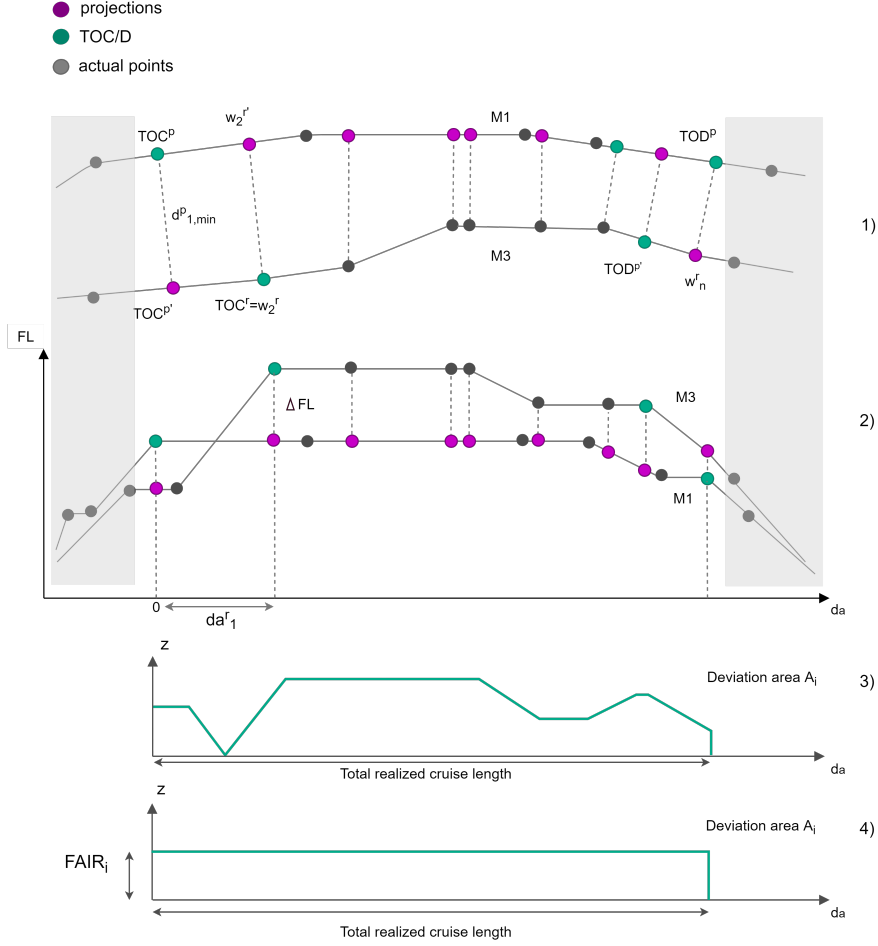


Figure 14: The FAIR method. Step 1 shows the horizontal point projections, step 2 the corresponding absolute vertical differences, step 3 the deviation area and step 4 the final step to obtain the FAIR.

#### 5.4. The FAIR steps

1. **Identification of  $TOC/D^p$**  by determining the first and last segments of level flight. A level segment  $s$  is defined by at least 3 consecutive waypoints with identical altitude ( $z$ ). Each starting level segment  $s_{i,j}^p$  and final level segment  $l_{i,j}^p$  corresponds to a waypoint  $w_{i,j}^p$  that is taken as its reference:

$$\exists s_{i,j}^p \iff z_{i,j}^p = z_{i,j+1}^p = z_{i,j+2}^p \quad (26)$$

$$\exists l_{i,j}^p \iff z_{i,j}^p = z_{i,j-1}^p = z_{i,j-2}^p \quad (27)$$

where  $s_{i,j}^p \in \mathcal{S}_i$  and  $l_{i,j}^p \in \mathcal{L}_i$ .  $\mathcal{L}_i$  and  $\mathcal{S}_i$  are the sets of levelled segments of flight  $f_i$ . The first and last waypoint of the cruise phase are identified:  $w_{i,1}^p = \arg \min_j \{s_{i,j}^p\}$  and  $w_{i,n}^p = \arg \max_j \{l_{i,j}^p\}$ . The rest of the planned waypoints, before and after the identified  $TOC/D^p$ , are discarded, to limit the index to the planned cruise phase. If no level segments in the planned trajectories are identified, the entire trajectory is discarded.

2. **Identification of realized ( $TOC/D^r$ )** by finding the closest points to the  $TOC/D^p$ . After trimming the M1 trajectory in the previous step, we denote  $TOC^p = w_{i,1}^p$  and  $TOD^p = w_{i,n}^p$ . The corresponding  $w_{i,1}^{p'}$  and  $w_{i,n}^{p'}$  are identified by projecting the initial planned points on the actual trajectory. The closest M3 point is not necessarily an already existing point  $w_{i,k}^r$ , but can be any point on the trajectory line. Put differently, the points are found at the intersection between the M3 trajectory and a segment whose length is the minimum length  $d_{k,min}$  between a point  $w_k^r$  and the planned trajectory:

$$d_1^p = \sqrt{(x_{i,k}^p - x_{i,k}^{p'})^2 + (y_{i,k}^p - y_{i,k}^{p'})^2} \quad (28)$$

If more than one closest point is identified, only the first point in the direction of flight is retained.

3. **Identification of realized points on the planned trajectory** is done similarly with step 2, except we project points from the realized trajectory onto the planned trajectory. After this step, points on both trajectories are 'synchronised' i.e. each planned point has a realized, closest counterpart, so their vertical components can be compared.
4. **Obtain the vertical component of the new points by linear interpolation.** Each  $w_{i,k}^r$  point can be defined by its vertical component  $z_{i,k}^{r'}$  and its distance along the trajectory  $da_k^r$  (referenced to the TOC<sup>r</sup>). The projected points, which belong to the M1 trajectory ( $w_{i,j}^r$ ) are characterized by the same components and will always appear between two planned points:  $\exists j$  s.t.  $w_{i,k}^r \in [w_{i,j}^p, w_{i,j+1}^p]$ ,  $\forall j$ . Thus, we obtain the vertical component of the projected point by linear interpolation:

$$z_k^{r'} = \frac{(d_k^{r'} - d_j^p)(z_j^p - z_{j+1}^p)}{(d_{j+1}^p - d_j^p)} + z_{j+1}^p \quad (29)$$

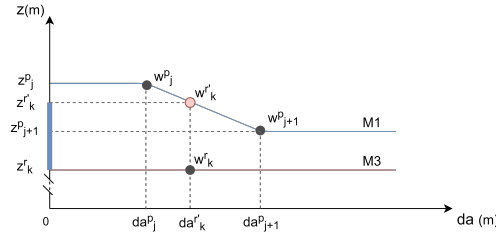


Figure 15: Z-component interpolation example. The x-axis represents the distance along the trajectory, while the y-axis represents the FL in meters.

5. **Definition of the total deviation area  $A_i$**  along the realized trajectory, as described by Eq. 24 by summing deviations from all intervals.
6. **Division of the obtained area by the length of the realized trajectory:** by this last step, the length of the trajectory is incorporated in the index.

### 5.5. FAIR Results

This section presents the FAIR results, starting with a high-level view on the average FAIR per flight for each airline group, the total impact at network level and FAIR distributions. The second part focuses on the comparison between major European Low-Cost Carriers (Group 8) and Network Carriers (Group 7). We present an analysis of vertical deviations for each flight level and an analysis of FAIR per hour. We notice that LCCs deviate considerably more than the NCs, the opposite of the efficiency results in Section 5.1.

First, Table 15 presents the average FAIR per groups identified by the clustering methodology presented in Section 4 and listed in Table 10. Groups 2 and 8 display the highest average FAIR values, while NCs in group 7 exhibit the 3rd lowest FAIR. This means that, on average, per flight, LCCs deviate 38% more than Network Carriers present in Group 7. However, it is noteworthy that Group 2, which also consists of mainly Network Carriers, exhibits FAIR values similar to the LCCs. The total impact on the network is however, much to have an idea on the network-wide impact each airline type has, the FAIR values must be correlated with the total area of deviations. It gives an indication on the magnitude of the total deviation that also takes into account the average cruise phase (in km) and the total number of flights for each airline:

$$A_g = FAIR_{\mu,g} \cdot F_{\mu,g} \cdot l_{\mu,cr}, g \in [1, 8] \quad (30)$$

where the double subscript refers to the average values within a group. i.e:

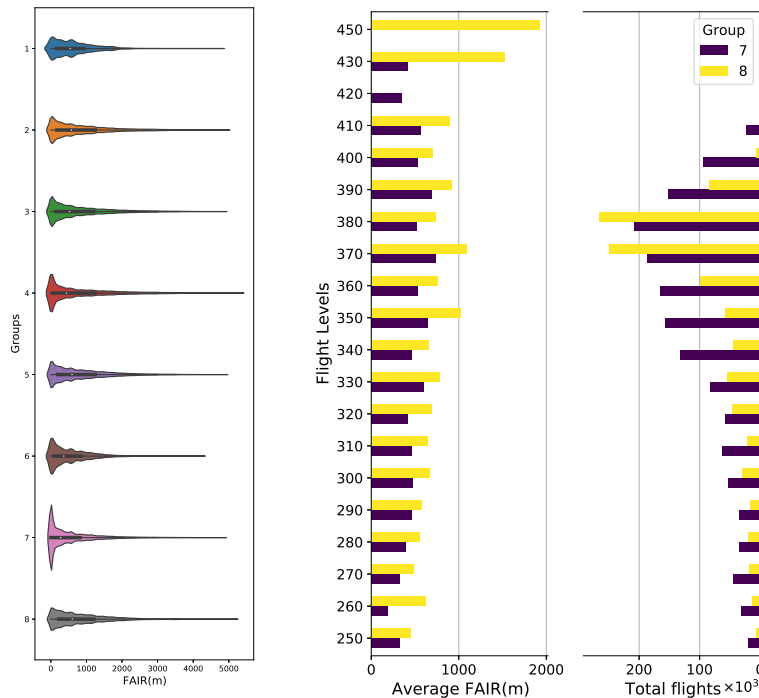
$$FAIR_{\mu,g} = \sum_{i=1}^n \frac{FAIR_i}{n}, n = \text{total flights in a group} \quad (31)$$

Table 15 shows that the major LCCs in Europe deviate on average, per flight 34% more than major NCs in Group 7. On the other hand, smaller NCs in Group 2 show a 2.5% larger FAIR, on average, compared to

Group	1	2	3	4	5	6	7	8
Average FAIR(m)	635	854	803	794	832	551	551	832
Total flights	16648	783918	645826	629946	1027827	71683	1544967	1032561
Average cruise [km]	361258	903720	1004111	1129634	690861	968992	943920	866640
Total deviation area	3,82E+12	6,05E+14	5,21E+14	5,65E+14	5,91E+14	3,82E+13	8,04E+14	7,45E+14
Average flights	3329	71265	13454	52495	128478	7964	308993	516280
Total average deviation area	7,63806E+11	5,5E+13	1,08E+13	4,71E+13	7,38E+13	4,25E+12	1,61E+14	3,72E+14

Table 15: The average FAIR per flight, for each group. The total deviation area is the product of all rows beforehand and gives an indication on the magnitude of the total area of deviations per groups of airlines, across the entire European ATM network. The last row points to a similar measure, but for the average number of flights for an airline within each group.

Group 8. The total deviation area gives a more precise sense of the impact of each group by multiplying the FAIR with the number of flights and the average cruise length. However, the number of airlines within each group differs, so to capture this effect, the last two rows indicate the average number of flights for an airline within each group, and consequently what impact the *average airline* within each group, has. Figure E.26 provides more details on the differences between flight numbers. Finally it is clear that the LCCs have nearly a 50% higher impact network-wide than NCs, partially because of the high frequency of flights, but also because of a much higher FAIR per flight. Such differences between groups are also visible when comparing the FAIR value distributions, shown by the violin plots in Figure 16.a.



(16.a) Violin Plots

(16.b) FAIR/Flight Level.Groups 7, 8

Figure 16: a) Probability density functions in the shape of violin plots for all groups. The interquartile range is defined between the extremes of the thicker, black lines, while the median value is marked by a white dot. b) An overview on the FAIR per flight level, coupled with the number of flights planned to cruise at that particular FL. The planned FL is identified as the most common FL in the en-route phase of the M1 trajectory. On the right side, the corresponding total number of flights per group which planned to cruise at that particular FL are shown. Only flights planned at primary cruise levels have been included, i.e. flights at FL251 have been discarded.

### 5.6. Case study and discussion

We turn our focus again at Groups 7 and 8. At a first glance, the probability density of group 7 stands out because of its higher width in the area of lower FAIR values, indicating there is a higher probability of flights adhering to their Flight Level. It is the only group that shows such behaviour, reinforcing the difference between the Network Carriers in Group 7 and the rest of the groups.

The primary ordinate in Figure 16.b references the most common FL in the planned trajectory i.e. the cruise level, while the right axis illustrates the average number of planned flights at that respective cruise FL. LCCs deviate more on average per flight, and this behaviour is consistent for all flight levels. The two groups share some similarities: a trend in increasing FAIR with the increase in FL, and higher FAIR values for odd FL compared to even FLs. Such difference might point to the impact of the 'hemispherical rule', as eastbound flights eastbound are assigned odd FLs, and westbound even FLs. This is easily explained for group 7 as most NCs operate transoceanic flights that deviate less when flying westbound on the oceanic tracks, but need to adjust their trajectories when entering the busy EU airspace, eastbound. The LCCs, on the other hand, might be exhibiting more deviations on odd FLs simply as a reaction to the high amount of traffic already present at those FLs. Finally, high and unexpected values for the uppermost FLs underline that, on average, LCCs halt their climb on average 2000 meters (80 FLs) sooner, when planning to cruise between FL 410–450. However, their impact on the network is insignificant, as only a few flights are planned to cruise that high.

The secondary vertical axis in Figure 16.b depicts the total number of flights planned to cruise at each FL. Here, we notice that LCCs focus the majority of their cruise FLs between FL 370 – 380 most likely because of a more narrow range of optimal cruise level due to a significant lower diversity in their fleet, as seen also in Table 4. The NCs on the other hand, spread their optimal cruise levels in a different manner, most likely due to a more heterogeneous aircraft fleet.

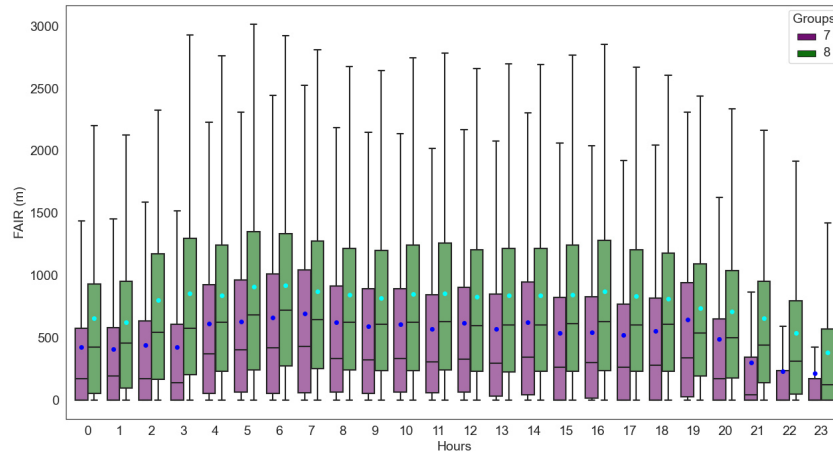


Figure 17: Boxplots showing the hourly FAIR values for groups 7 and 8 (outliers are not shown). The dots represent the averages.

The temporal aspect of FAIR is analysed next. Figure 17 shows the FAIR hourly boxplot for LCCs and NCs with higher values overall for LCCs. Similarly to the efficiency results in Figure 11, this plot points to the fact that vertical deviations follow an hourly pattern easily attributed to the amount of aircraft already airborne or preparing to depart at that time. In the case of FAIR, however, the higher values of Group 8 show that LCCs deviate consistently more than their NC counterparts.

## 6. Conclusion

In this paper, we have shown that Low-Cost airlines deviate more than Network Carriers in the vertical plane and have a larger fraction of flights with a negative efficiency difference i.e. their actual efficiency is higher than the planned one, pointing to more deviations from the planned route in the interest of the aircraft operator. On the other hand, Network carriers have on average, more efficient trajectories in the horizontal plane. The vertical deviations have been assessed by means of a novel deviation metric, the Flight Level Adherence Index for Realized trajectory (FAIR). FAIR provides a precise measure of vertical deviations during the cruise phase, and its flight-centric approach makes it a good candidate for assessing both the individual performance of a trajectory, and the impact each aircraft operator has on the network. This would allow in turn an objective measure by which airline deviation 'behaviour' is monitored or taken action upon, if needed. Future research into this area can correlate the reasons for deviations, i.e. ATCO request vs. pilot request (weather, safety), with data stemming from other sources (weather radar); or can develop the FAIR further to look specifically at YoYo flights [4]. Another interesting avenue is to use the FAIR to assess whether the change in route charges [2] had an effect on planning practices and thus, on deviations. The other focus in this paper, the Unsupervised Airline Clustering, provides a framework to objectively cluster airlines in groups and to assess whether the current marketing narrative is reflected in the actual business model. It is the first use of Unsupervised Machine Learning on airline clustering, and proves also that both operational and Complex Network metrics are relevant indicators of airline business models.

In conclusion, this research represents a closer step to the fair and equal use of the EU airspace and furthers with one step the precise performance-based assessment of aircraft operators trajectories. Such assessment will be of utmost importance when the 'first-come first-served' rule in trajectory planning will evolve, and a measure to gauge the credibility of airlines to fly their desired routes will be critical.

## References

- [1] P. R. Unit, Yearly Network Operations Report 2017, Technical Report, EUROCONTROL, 2009.
- [2] C. R. C. Office, Conditions of Application of the Route Charges System and Conditions of Payment, Technical Report, EUROCONTROL, 2010.
- [3] EASA, Note for the attention of aircraft operators and air traffic services (ats): Adherence to filed flight plans in european airspace, 2019.
- [4] ERAA - European Regions Airline Association, Eurocontrol requests for flight plan adherence, 2020. URL: <https://www.eraa.org/policy/overview-and-news/eurocontrol-request-flight-plan-adherence>.
- [5] Performance Review Unit, ATM Airport Performance (ATMAP) Framework - Measuring Airport Airside and Nearby Airspace Performance, Technical Report, EUROCONTROL, 2009.
- [6] C. Mayer, T. Sinai, Network effects, congestion externalities, and air traffic delays: Or why not all delays are evil, *American Economic Review* 93 (2003) 1194–1215.
- [7] J. J. Rebollo, H. Balakrishnan, Characterization and prediction of air traffic delays, *Transportation research part C: Emerging technologies* 44 (2014) 231–241.
- [8] P. Pasutto, E. Hoffman, K. Zeghal, Adherence to best descent profiles-an analysis of the relative vertical (in) efficiency at four major european airports, in: *AIAA Aviation 2019 Forum*, 2019, p. 3623.
- [9] S. Shresta, D. Neskovic, S. S. Williams, Analysis of continuous descent benefits and impacts during daytime operations, in: *8th USA/Europe Air Traffic Management Research and Development Seminar (ATM2009)*, Napa, CA, 2009.
- [10] C. Bongiorno, G. Gurtner, F. Lillo, R. Mantegna, S. Miccichè, Statistical characterization of deviations from planned flight trajectories in air traffic management, *Journal of Air Transport Management* 58 (2017) 152–163.
- [11] G. Gurtner, C. Bongiorno, M. Ducci, S. Miccichè, An empirically grounded agent based simulator for the air traffic management in the sesar scenario, *Journal of Air Transport Management* 59 (2017) 26–43.
- [12] EUROCONTROL, Aviation intelligence Unit Portal, 2020. URL: <http://ansperformance.eu>.
- [13] G. G. Sam Peeters, Analysis of en-route vertical flight efficiency - Edition 00-04 - Submitted for consultation, Technical Report, EUROCONTROL, 2017.
- [14] L. Hunter, Low cost airlines: Business model and employment relations, *European Management Journal* 24 (2006) 315–321. doi:10.1016/j.emj.2006.08.001.
- [15] V. Morandi, P. Malighetti, S. Paleari, R. Redondi, Codesharing agreements by low-cost carriers: An explorative analysis, *Journal of Air Transport Management* 42 (2015) 184–191. doi:10.1016/j.jairtraman.2014.10.004.
- [16] L. Graf, Incompatibilities of the low-cost and network carrier business models within the same airline grouping, *Journal of Air Transport Management* 11 (2005) 313–327. doi:10.1016/j.jairtraman.2005.07.003.
- [17] M. Dziedzic, D. Warnock-Smith, The role of secondary airports for today’s low-cost carrier business models: The european case, *Research in transportation business & management* 21 (2016) 19–32.
- [18] P. Belobaba, A. R. Odoni, C. Barnhart, *The global airline industry*, Wiley, 2009.
- [19] D. Warnock-Smith, A. Potter, An exploratory study into airport choice factors for european low-cost airlines, *Journal of Air Transport Management* 11 (2005) 388–392. doi:10.1016/j.jairtraman.2005.05.003.
- [20] K. Frenken, S. V. Terwisga, T. Verburg, G. Burghouwt, Airline competition at european airports, *Tijdschrift voor Economische en Sociale Geografie*-2004 95 (2004) 233–242.
- [21] S. A. Morrison, Actual, adjacent, and potential competition estimating the full effect of southwest airlines, *Journal of Transport Economics and Policy (JTEP)* 35 (2001) 239–256.
- [22] G. Francis, I. Humphreys, S. Ison, M. Aicken, Where next for low cost airlines? a spatial and temporal comparative study, *Journal of Transport Geography* 14 (2006) 83–94.
- [23] A. Cook, H. A. Blom, F. Lillo, R. N. Mantegna, S. Miccichè, D. Rivas, R. Vázquez, M. Zanin, Applying complexity science to air traffic management, *Journal of Air Transport Management* 42 (2015) 149–158. doi:10.1016/j.jairtraman.2014.09.011.
- [24] R. Pastor-Satorras, A. Vázquez, A. Vespignani, Dynamical and correlation properties of the internet, *Physical review letters* 87 (2001) 258701.
- [25] S. Porta, P. Crucitti, V. Latora, The network analysis of urban streets: a primal approach, *Environment and Planning B: planning and design* 33 (2006) 705–725.
- [26] P. Sen, S. Dasgupta, A. Chatterjee, P. Sreeram, G. Mukherjee, S. Manna, Small-world properties of the indian railway network, *Physical Review E* 67 (2003) 036106.
- [27] R. Pastor-Satorras, A. Vespignani, Epidemic spreading in scale-free networks, *Physical review letters* 86 (2001) 3200.
- [28] H.-B. Hu, K. Wang, L. Xu, X.-F. Wang, Analysis of online social networks based on complex network theory, *Complex Systems and Complexity Science* 2 (2008) 1214.
- [29] D.-D. Han, J.-H. Qian, J.-G. Liu, Network topology of the austrian airline flights, arXiv preprint physics/0703193 (2007).
- [30] A. Bombelli, B. F. Santos, L. Tavasszy, Analysis of the air cargo transport network using a complex network theory perspective, *Transportation Research Part E: Logistics and Transportation Review* 138 (2020) 101959.
- [31] C. Kai-Quan, Z. Jun, D. Wen-Bo, C. Xian-Bin, Analysis of the chinese air route network as a complex network, *Chinese Physical Society and IOP Publishing Ltd* (2011).
- [32] R. Guimerà, L. A. Amaral, Modeling the world-wide airport network, volume 38, 2004, pp. 381–385. doi:10.1140/epjb/e2004-00131-0.
- [33] M. M. Hossain, S. Alam, A complex network approach towards modeling and analysis of the australian airport network, *Journal of Air Transport Management* 60 (2017) 1–9. doi:10.1016/j.jairtraman.2016.12.008.
- [34] G. Bagler, Analysis of the airport network of india as a complex weighted network, *Physica A: Statistical Mechanics and its Applications* 387 (2008) 2972–2980.
- [35] Z. Xu, R. Harriss, Exploring the structure of the u.s. intercity passenger air transportation network: A weighted complex network approach, *GeoJournal* 73 (2008) 87–102. doi:10.1007/s10708-008-9173-5.
- [36] M. Zanin, F. Lillo, Modelling the air transport with complex networks: A short review, *European Physical Journal: Special Topics* 215 (2013) 5–21. doi:10.1140/epjst/e2013-01711-9.

- [37] EUROCONTROL, Demand data repository web portal, 2020. URL: <https://www.eurocontrol.int/ddr>.
- [38] T. C. Melike Atik, DDR2 Reference Manual for General Users 2.9.5, Technical Report, EUROCONTROL, 2018.
- [39] J. Gllavata, R. Ewerth, B. Freisleben, Text detection in images based on unsupervised classification of high-frequency wavelet coefficients, in: Proceedings of the 17th International Conference on Pattern Recognition, 2004. ICPR 2004., volume 1, IEEE, 2004, pp. 425–428.
- [40] H. Wang, S. Sen, A. Elgohary, M. Farid, M. Youssef, R. R. Choudhury, No need to war-drive: Unsupervised indoor localization, in: Proceedings of the 10th international conference on Mobile systems, applications, and services, 2012, pp. 197–210.
- [41] R. G. Wijnhoven, P. H. de With, Unsupervised sub-categorization for object detection: Finding cars from a driving vehicle, in: 2011 IEEE International Conference on Computer Vision Workshops (ICCV Workshops), IEEE, 2011, pp. 2077–2083.
- [42] H. XIAOFEI, C. DENG, Laplacian score for feature selection, Advances in Neural Information Processing Systems 18 (NIPS) (2005).
- [43] M. Belkin, P. Niyogi, Laplacian eigenmaps and spectral techniques for embedding and clustering, in: Advances in neural information processing systems, 2002, pp. 585–591.
- [44] X. He, P. Niyogi, Locality preserving projection, neural information processing symposium, vancouver, British Columbia, Canada (2003).
- [45] Z. Zhao, H. Liu, Spectral feature selection for supervised and unsupervised learning, in: Proceedings of the 24th international conference on Machine learning, ACM, 2007, pp. 1151–1157.
- [46] A. Fred, Finding consistent clusters in data partitions, in: International Workshop on Multiple Classifier Systems, Springer, 2001, pp. 309–318.
- [47] R. Tibshirani, G. Walther, T. Hastie, Estimating the number of clusters in a data set via the gap statistic, Journal of the Royal Statistical Society: Series B (Statistical Methodology) 63 (2001) 411–423.
- [48] N. X. Vinh, J. Epps, A novel approach for automatic number of clusters detection in microarray data based on consensus clustering, in: 2009 Ninth IEEE International Conference on Bioinformatics and BioEngineering, IEEE, 2009, pp. 84–91.
- [49] N. X. Vinh, J. Epps, J. Bailey, Information theoretic measures for clusterings comparison: Variants, properties, normalization and correction for chance, Journal of Machine Learning Research 11 (2010) 2837–2854.
- [50] M. Granger, Python implementation of the gap statistic, [https://github.com/milesgranger/gap\\_statistic/](https://github.com/milesgranger/gap_statistic/), 2019. [Online; accessed 10-January-2020].
- [51] L. Hubert, P. Arabie, Comparing partitions, Journal of classification 2 (1985) 193–218.
- [52] N. X. Vinh, J. Epps, J. Bailey, Information theoretic measures for clusterings comparison: is a correction for chance necessary?, in: Proceedings of the 26th annual international conference on machine learning, ACM, 2009, pp. 1073–1080.
- [53] W. M. Rand, Objective criteria for the evaluation of clustering methods, Journal of the American Statistical association 66 (1971) 846–850.
- [54] T. Ronan, S. Anastasio, Z. Qi, P. H. S. V. Tavares, R. Sloutsky, K. M. Naegle, Openensembles: A python resource for ensemble clustering, Journal of Machine Learning Research 19 (2018) 1–6. URL: <http://jmlr.org/papers/v19/18-100.html>.
- [55] F. Pedregosa, G. Varoquaux, A. Gramfort, V. Michel, B. Thirion, O. Grisel, M. Blondel, P. Prettenhofer, R. Weiss, V. Dubourg, J. Vanderplas, A. Passos, D. Cournapeau, M. Brucher, M. Perrot, E. Duchesnay, Scikit-learn: Machine learning in Python, Journal of Machine Learning Research 12 (2011) 2825–2830.
- [56] L. McInnes, J. Healy, S. Astels, hdbscan: Hierarchical density based clustering, The Journal of Open Source Software 2 (2017). URL: <https://doi.org/10.211052Fjoss.00205>. doi:10.21105/joss.00205.
- [57] D. Arthur, S. Vassilvitskii, k-means++: The advantages of careful seeding, in: Proceedings of the eighteenth annual ACM-SIAM symposium on Discrete algorithms, Society for Industrial and Applied Mathematics, 2007, pp. 1027–1035.
- [58] D. Reynolds, Gaussian Mixture Models, Springer US, Boston, MA, 2009, pp. 659–663. URL: [https://doi.org/10.1007/978-0-387-73003-5\\_196](https://doi.org/10.1007/978-0-387-73003-5_196). doi:10.1007/978-0-387-73003-5\_196.
- [59] T. Zhang, R. Ramakrishnan, M. Livny, Birch: an efficient data clustering method for very large databases, ACM Sigmod Record 25 (1996) 103–114.
- [60] J. H. Ward Jr, Hierarchical grouping to optimize an objective function, Journal of the American statistical association 58 (1963) 236–244.
- [61] A. Strehl, J. Ghosh, Cluster ensembles—a knowledge reuse framework for combining multiple partitions, Journal of machine learning research 3 (2002) 583–617.
- [62] Y. Jeon, J. Yoo, J. Lee, S. Yoon, Nc-link: A new linkage method for efficient hierarchical clustering of large-scale data, IEEE Access 5 (2017) 5594–5608.
- [63] B. Desgraupes, Clustering indices, University of Paris Ouest-Lab Modal’X 1 (2013) 34.
- [64] Student, The probable error of a mean, Biometrika (1908) 1–25.
- [65] ATC-Network, New procedures help optimise air traffic management over the alps in adverse weather conditions, 2020. URL: <https://www.atc-network.com/atc-news/fabec/new-procedures-help-optimise-air-traffic-management-over-the-alps-in-adverse-weather-conditions>.



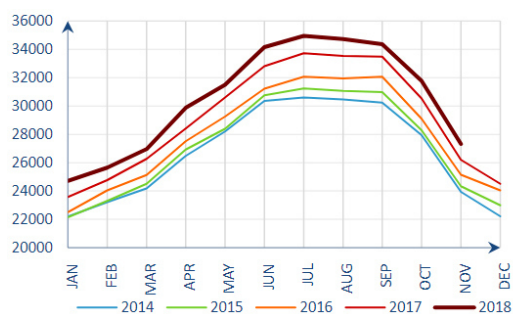
III  
Literature Review  
as graded for AE4020 Literature Study



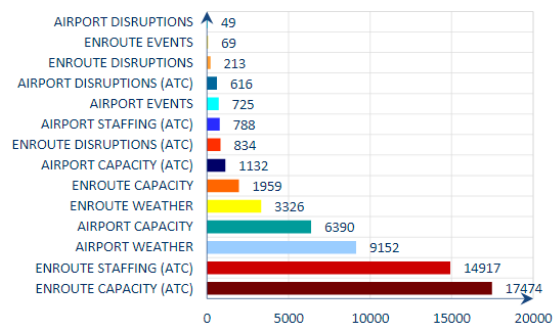
# Introduction

The Air Traffic Network is an intricate and complex system, comprised of airports, navigation points, air traffic control, aircraft and many technical systems supporting the delivery of a safe and efficient service to its customers. In such a vast enterprise, characterized by dynamic interactions and unforeseen events, deviations from the planned trajectory occur often. Until now, the network has been able to support the increase in traffic and has shown remarkable resilience to the events causing deviations. However, traffic is expected to grow and order to accommodate the extra capacity, the Single European Sky (SES) initiative was launched in 2004, together with its research-oriented body, SESAR. Under the umbrella of SESAR and Air Navigation Service Providers (ANSPs), operational experts together with research bodies are working towards enabling a three-fold increase in capacity, however this increase can be rendered useless if aircraft do not stick to their planned trajectory.

A deviation can be defined as an aircraft not following its intended flight path. Deviations are closely linked to airspace capacity and delays, and can occur due to a multitude of factors. In November 2018 it has been reported that roughly 11% of delays are caused by weather EUROCONTROL [27]. Particularly in the en-route phase, there has been an increase of more than 125% in weather driven delays. These are highly linked to en-route deviations, however at the level of the entire Air Traffic Management (ATM) system, one must take into account that not all of them are caused by deviations, as some of them occur on ground, at airports.



(1.1.a) Average daily traffic year-to-date as reported in November 2018



(1.1.b) Reasons for En-route ATFM delays in November 2018

Figure 1.1: Network Performance: traffic and en-route ATFM delays. EUROCONTROL [27]

Capacity is at large, influenced by a number of factors, however the focus of this report will be on deviations and indirectly, on delays. Deviations occur during flights almost all the time, be it due to other traffic, air traffic control, Air Traffic Flow measures (ATFM) and in some cases, weather. The deviations are considered as is and, even if their operational effect at network level translates to delays, they are merely a symptom and a metric for the management of the network.

Weather is at large, unpredictable, although notable advancements have been made in modelling and predicting weather events especially for the ATM industry Rubnich and DeLaura [58], DeLaura et al. [23], Hauf et al. [39]. A report EUROCONTROL [26] captures European stakeholders strategy on severe weather avoidance, as well as a summary of the available resources and the impacts of each actor involved in ATM. Moreover, it includes the results of a survey sent to the Member States which clearly states the risks added by the increase of adverse weather events, specifically, for the en-route and TMA ATC the most relevant weather hazards are: severe turbulence, lightning and in-flight icing. Typically, these hazards are associated with the existence and the development of convective weather. Typical procedures identified to cope with these situations provide sub-optimal trajectories and contribute to ATC workload increase and are further detailed in section 4.1.

This report presents a literature review of the analysis on LCC and NC approach on deviations and possibly dealing with small-to medium severe weather events in Europe, using Complex Network Theory and operational metrics. The remainder of this report is organized as follows: Chapter 2 presents the data to be used in the project: the types of information obtained from EUROCONTROL's Demand Data Repository and the weather data used to validate the results obtained in the first stage of the thesis. It also presents the weather phenomena most relevant to the Air transportation industry. Chapter 3 delves into Complex Network Theory and describes some of the basic theories in graph network and percolation, highlighting their use in Air Transportation. A subsection deals also with Agent-Based Modelling techniques and some platforms supporting such modelling. Chapter 4 describes the various airline types and some of their particularities, followed by a detailed analysis on trajectory deviation. This chapter underlines some of the key research advancements until now and highlights the most relevant metrics and methodologies in flight deviations. Chapter 5 draws the conclusion of this Literature Study.

# 2

## Data Description

### 2.1. Flight Trajectory data

Data expected to be used is stored in an online repository owned by EUROCONTROL called the Demand Data Repository 2 (DDR2). Historical traffic can be downloaded from here for research purposes. At the moment of writing this report, flight data type of ALLFT+ covering the whole year of 2017 have been obtained.

ALLFT+ data contains information on the M1 planned, M2 ATFM regulated and M3 realized trajectories. Below a sample of such data fields relevant for the thesis project, with additional explanations.

Origin	Destination	Aircraft ID	Operator	Aircraft type	IFPS ID	AIRAC	M1 Points	M1 Profile
LSZH	EDDC	SWR918	SWR	F100	AA63375970	425	67	Table 2.2

Table 2.1: DDR2 ALLFT+ Planned Trajectory (M1) data sample.

Table 2.2 below details the content of the M1 point profiles relevant to analyse the trajectories. The first row contains the actual data, whereas the second one explains the content above.

20170508164700	LSZH	DEGES2W	14	0	A	472729N0083253E
yyyymmddhhmmss	Navpoint	Sector	FL	Speed[kts]	Navpoint type	latlong

Table 2.2: M1 point profile detailed

### 2.2. Weather data

Two major sources of weather data have been investigated, the first one being the European Centre for Medium-Range Weather Forecasts (ECMWF), which offers extensive weather data ensembles and forecasts. These cover vast surfaces and contain a high number of data related to pressure, moisture, temperature and others. However, there are some challenges in processing the data, since it is in GRIB and NETCDF file format, which are a binary file format that can be read using either UNIX -based programming languages or dedicated weather analysis and data manipulation software such as METView. The second, source is the European Severe Weather Database (ESWD) that contains weather reported by National Agencies as well as volunteers. It is easier to read however the weather data is most likely reported at ground level, with no indication of altitude.



# 3

## Complex Network Theory

Complex Networks Theory deals with today's intricate and large systems, allowing us to understand previously unknown ways our world behaves. Examples of such networks are the Internet, the World Wide Web, the roads in a country, even a cell, the human organism or the navigation points making up the ATM infrastructure. This chapter dives into the mathematical background of such networks, known as graph theory, and then proceeds to define some of the useful Complex Network properties and also presents interesting or well-known types of networks and their use. Finally, the discussion takes on how communities can emerge in networks, and how they can be identified, both in more traditional ways and in novel ways (i.e.: modularity - based detection).

A review by Albert\* and Barabási [3] on the statistical mechanics of complex networks makes a good starting point for the literature review on this section. The research commences by making a case for the 3 main model types:

- Random graphs
- Scale-free networks, having to the so-called "hub" property of a network in which some nodes play a particular role. These exhibit a deviation from the Poisson distribution one would expect from the random network, usually in the form of a power-law tail or an exponential behaviour. (Barabassi, Albert 1999)
- Models with the small-world property, which are defined by networks with nodes of high degree and a short average path length

A number of empirically analyzed networks present give ground to the following comparisons, some of which are worth mentioning. For example, a network of high-energy particle where the nodes are the particles and the edges are the physical relationship between them, developed in the mid '90s by Newman , appears with an almost perfect power law distribution, which in practice is nearly impossible. Food Networks elicit high clustering, with Montoya and Solé [48] showing that the degree distribution follows a power law with an unusually small exponent, leaving room to challenging their findings, as the distribution might be considered exponential (perhaps also due to the low number of nodes in their analysis). Thus becomes important that the analysed network has sufficient data points; for example in this case the nodes are the species and the edges represent one of predator - prey relationships.

Language presents itself as a particular network. One unpublished study by Yook, Jeong and Barabassi considers words as nodes, connected to their synonyms by links. The resulting network unveils a major cluster of words forming the heart of the network, with a few of the words that that do not have synonyms. Such networks can be found also in other areas of interest. Cook et al. [21] identifies a similar topology in the delay causality of airport, where a supercluster of airports consisting of most delays "forced" into one another, emerges, with few airports not heavily impacted. Figure 3.1 shows how such supercluster is organized.

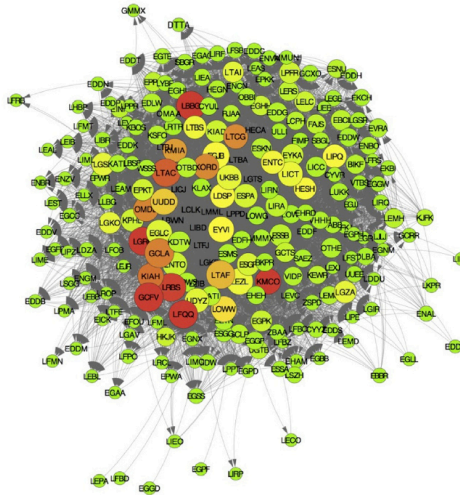


Figure 3.1: Supercluster example of airports delay causality. Cook et al. [21]

### 3.1. Graph Theory

A graph is made up of vertices, nodes, or points which are connected by edges, arcs, or lines. A graph may be undirected or directed, meaning that there is no direction defined on the edges between two points or the relationship between the two nodes is applicable in both directions.

Graph theory was first developed by the work of Leonhardt Euler, who thought about small, usually highly regulated graphs in his work in the 18<sup>th</sup> century. A few hundreds of years later, graph theory has evolved, as the mathematical backbone of the ever - expanding networks. A particular interest has been gauged towards the study of random graphs - as most complex networks seemed arbitrary without the proper instruments to investigate them. In their work, Albert\* and Barabási [3] refer to a number of real-life networks and review a number of concepts, among them the inception of random graphs and their most appealing features as found out by Erdős and Rényi [24].

The model developed by Erdős and Rényi [24] remains the basis for any random graph: defining a random graph with  $N$  nodes and  $n$  edges out of the potential  $N(N-1)/2$  edges that can form. The probability space is made up of  $C_{N(N-1)/2}^n$  equiprobable realizations. The greatest discovery of the authors was how swift and unannounced some properties may appear in the graph, depending on whether the connection probability  $P(N)$  rises slower or faster compared to a critical probability  $P_c(N)$  while  $N \rightarrow \infty$ . Many properties in random graphs are not  $N$ -independent, however, as proven by Erdős and Rényi [24], the average degree of a graph has a critical value independent of the graph size:

$$\langle k \rangle = 2n/N = p(N - 1) = pN, \quad (3.1)$$

with  $p$  the probability of the edges to exist between any two nodes.

### 3.2. Random subgraphs and random graph evolution

In this section, the main types of structures are presented and mathematically defined: trees and cycles. As their names suggest, cycles consist of subgraphs with the average degree of 2, as each node is connected with the next node only by one edge. Trees on the other hand, cannot form cycles by definition and have an average degree of  $2 - 2k$  with  $k$  number of edges.

The most important aspect of random graphs are the critical probabilities. These are probabilities that edges exist and mark the sudden change of topology of random graphs. If we consider  $Z = -k/l$  with  $k$  nodes and  $l$  number of edges, therefore  $p \sim N^Z$ . Depending on the number of edges and nodes, various critical probabilities have been outlined, as defined in the table below:

Z	Subgraph characteristics
$-\infty$	Inexistent Graph
-2	Separate edges start to appear, forming random, individual lines
$-\frac{3}{2}$	Trees of order 2 start appearing, with higher orders as z moves closer to -1
-1	Trees of all orders are present, and at the same time cycles appear
$-\frac{2}{3}$	Complete cycles of order 4 start appearing; as Z gets closer to 0, higher order complete cycles appear
$> 0$	Most nodes belong to cycles and trees. Every new edge means one less cluster. Super-tree is forming
1	Graph changes behaviour abruptly. $N^{2/3}$ nodes belong to one giant, complex structure
$> 1$	Smaller, disconnected trees connect to the larger, already existing structure

Table 3.1: Random Graph evolution with increase of  $Z = \frac{z}{T}$  Erdős and R enyi [25].

Generalizing, the critical probability of having specific structures translates into:

- Tree of order k:

$$p_c(N) = cN^{-k/(k-1)} \quad (3.2)$$

- Cycle of order k:

$$p_c(N) = cN^{-1} \quad (3.3)$$

- Complete subgraph of order k:

$$p_c(N) = cN^{(k-2)/(k-1)} \quad (3.4)$$

## 3.3. Complex Network properties

### 3.3.1. Degrees and degree distributions

The degree of a node reflects the number of edges or links connected to it. In a directed graph, the in-degree represents the number of edges arriving at the node and the out-degree represents the number of edges going out. Studying degree distributions allows a quick and precise analysis of the graph. It offers important insights about the heterogeneity of the network and highlights functionality aspects of specific nodes (i.e. hubs), as explained in section 3.6 on scale-free networks and section 3.5 on networks with small-world property. Most common distributions are presented in Table 3.2 below:

Distribution	Definition	Description
Poisson	$P(x) = e^{-\lambda} \frac{\lambda^x}{x!}$	Discrete; Characterizes random graphs degree distribution, with $\lambda$ the average number of events / interval, $e$ being Euler's number; $x$ taking values $0, 1, 2, \dots$ and $x!$ is the factorial of $x$
Power law	$P(x) = Cx^{-\alpha}$	Not found in empirical scale-free networks, rather in theoretical scale-free networks, where: $\alpha$ is the scaling factor, usually $2 < \alpha < 3$ $x$ is the variable of interest $C$ is a constant
Power law w/ exponential cutoff	$P(x) = x^{-\alpha} e^{-\lambda x}$	Usually found in real-life scale-free networks, where $\alpha$ is the scaling factor $\lambda$ is the average value, $x$ is the variable of interest.

Table 3.2: Most encountered degree distributions in Complex Network Theory. Clauset et al. [20]

If we are to consider the degree, for any given navigation point  $nav_i$ , its degree can be written as

$$deg_{nav_i} = \sum_{k \in Kl_{ik}} k \quad (3.5)$$

where  $l_{ik}$  is any link connecting the navigation point  $i$  with its neighbours. Power law distributions have been intensely studied in recent years as they offer a model to study the dynamics of scale-free networks, i.e. networks whose characteristics do not scale up with an increase in time span or with the addition of nodes. Power laws characterize networks in that just a few nodes have large amounts of connections, whereas the vast majority of nodes exhibit a low amount of links. Some examples are the link distribution of the World Wide Web Clauset et al. [20] or the degree distribution of the outgoing calls of the AT&T service provider Faloutsos et al. [28], class hierarchy in programming by Wheeldon and Counsell [68] are just a few of the examples of empirical networks exhibiting such characteristics. Some types of power-law distributions are particularly interesting for developing search algorithms by using the nodes with higher degree connectivity, as explained in Adamic et al. [1]. This has lately become a relevant issue, especially with the change in electronic networks architecture and peer-to-peer file sharing. A more traditional and well-known study on power-law distributions is related to the dynamics of the networks, or how the underlying distribution of the graph ultimately becomes characterized by a power law.

The underlying principle at the basis of forming a power law distribution is the preferential attachment, known also as the rich getting richer principle or informally, the 'Yule Distribution'. In essence, the preferential attachment law posits that nodes with higher number of links tend to increase their degrees faster than the ones with less number of connected edges. Similar to power law distributions, Gibrat's law or 'Gibrat's rule of proportionate growth' is another example of log-linear distribution used in growth rate analysis. It is commonly associated with Zipf's Law - which states that in some processes, sets, or more commonly corpuses of natural languages, the frequency of words is inversely proportional to their rank in the frequency table Sen and Wang [61]. More details on power laws and scale-free networks is presented in section 3.6, whereas a visual representation of such power law in comparison with the classical Gaussian distribution or "Bell Curve" is shown in Figure 3.2 below.

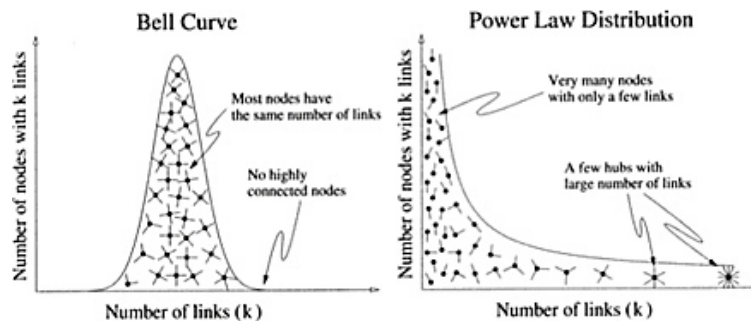


Figure 3.2: Example Power law distribution and Gaussian distribution. Barabási [6]

The Poisson distribution is one of the most common probability distributions. It is of discrete type and counts how many events happen in a given time-frame or fixed environment, given that the events occur arbitrarily and are independent, i.e. they do not depend on each other Erdős and Rényi [25]. It is at the basis of the random graph theory Erdős and Rényi [25], and considers that graph links (connections) can occur with a certain probability  $p$  which, for some particular value ranges, generates specific and highly predictable types of graphs.

### 3.3.2. Node strength

The strength of a node in a network represents the sum of the weights of all the links connected to it. By looking at an Air Route Network, the strength of some nodes can highlight potential hubs, with higher values meaning more traffic. For example, Kai-Quan et al. [43] show that for the Chinese Air Route Network, the distribution of routes is rather homogeneous, as only a few routes connect each two points, and the routes are spread in order to cover most of the Chinese Territory. When looking at the traffic passing through these routes, we find that a high fraction of traffic passes through only a few routes: a clear example on how degree distribution can offer a different type of information compared to strength distribution. Another relevant example on node strength analysis is mentioned in Barrat et al. [8], where a network of scientists (nodes) and the number of collaborations (weighted edges) can offer at a glance the entire scientific productivity of

an author.

### 3.3.3. Clustering Coefficient

The clustering coefficient of a node  $i$  with  $k_i$  connections to its adjacent  $k$  nodes in a complex network is given by the following formula:

$$C_i = \frac{2E_i}{k_i(k_i - 1)}, \quad (3.6)$$

where  $E_i$  is the actual number of edges present between all the number of nodes linked to the original node  $k_i$  Albert\* and Barabási [3] An example of specific clustering coefficients is a situation in which in a group of nodes, are all connected between themselves, such as triangles or 'cliques' - forming a so-called maximal complete subgraph. Another common clustering coefficient variant found in literature and proposed by Watts and Strogatz [67] is given by:

$$C' = \frac{3 \times \text{number of triangles}}{\text{number of triples}}, \quad (3.7)$$

where triples are composed of 3 nodes with 2 links. This definition is linked to the concept of "fraction of transitive triples", highly studied in sociology. The clustering correlation of a network is found out by averaging all the coefficients of all nodes. Therefore, for random graphs, the network clustering coefficient is given by its  $p$ , or the probability that a link exists between two nodes:

$$C_{rand} = p = \frac{\langle k \rangle}{N}, \quad (3.8)$$

It is a common metric among social network studies and has been used in various studies involving physical or food networks. Empirical (or real) networks usually exhibit high clustering correlations and also form communities, a form of clustering identified also in the study of the air navigation infrastructure, further detailed in Section 3.8

### 3.3.4. Average path length

The average path length is a network indicator of how many steps are needed on average, to reach any point in the network, starting at a random location. One of the most famous applications of this concepts is Stuart's Milgram 'Six degrees of separation' which postulates that on average, a person needs to go through 6 people and their connections to reach almost anyone in the United States.

The average path length is defined in Eq. 3.9. For the sake of clarity, we give also the definition of a path, i.e. a set of vertices and links passed through when going from an initial vertice to a final vertice without passing twice through the same vertice.

$$l_G = \frac{1}{n \cdot (n - 1)} \cdot \sum_{i \neq j} d(v_i, v_j), \quad (3.9)$$

where,  $d(v_1, v_2)$  denotes the shortest distance between the two vertices of a graph  $G$ , with  $v_1, v_2 \in V$ . We consider  $d(v_1, v_2) = 0$  if  $v_2$  has no link to  $v_1$  to  $v_2$  i.e. it cannot be reached. The average path length is one of the 3 most important network topology characteristics, together with degree distribution and clustering coefficient. It is a measure of efficiency in a network, and internet networks are primarily build with this condition in mind, as it reduces costs and speeds up any operations carried throughout the network. Albert and Barabási [2] A visual representation of the concept is given in section 3.5, where the Walter- Strogatz model that made it famous is also shown.

### 3.3.5. Connectedness and diameter

The diameter of the graph is defined as the maximal distance between any pairs of its nodes, or, in simpler terms, the longest shortest path between any two nodes in a network. Connectedness is also a topological feature in graphs, and refers to the fact that each vertex or node is connected with a link. A much stronger characteristic is path connectedness, which intuitively refers to the fact that there is a way to get to each vertex in the graph. The Air Traffic Management network is a path connected network.

### 3.3.6. Centrality measures

There are several measures of centrality useful to identify nodes with various functions in a network. One of them is betweenness-centrality, which measures the number of times a node acts as a bridge along the shortest path between two other nodes. First introduced by Linton Freeman as a measure for quantifying the control of a human on the communication between other humans in a social network, it also highlights the important nodes in the exchange of any type of information exchange. Fig 3.3 depicts the betweenness-centrality of a small graph.

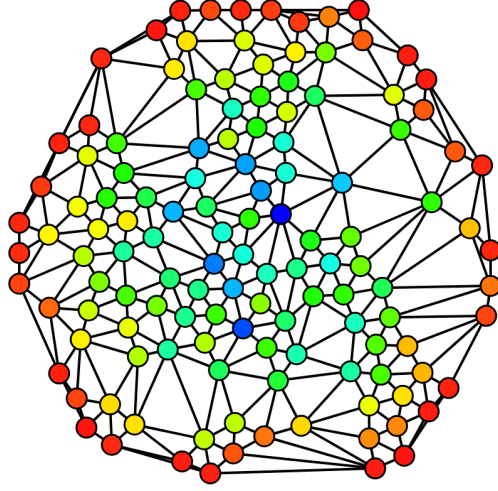


Figure 3.3: Betweenness-centrality increase from red to dark blue hue. Author: Claudio Rocchini

Eq. 3.10 defines the mathematical formalism to compute the betweenness-centrality:

$$C_B(v) = \sum_{s \neq v \neq t \in V} \frac{\sigma_{st}(v)}{\sigma_{st}}, \quad (3.10)$$

where  $\sigma_{st}$  represents the total number of shortest paths from node  $s$  to node  $t$  and  $\sigma_{st}(v)$  is the number of those paths that pass through node  $v$ . There are other types of centrality measures existing in literature, such as, closeness centrality, which measures the extent to which a node is close to all other nodes along the shortest path. It reflects the node's accessibility in a given network and can be viewed as the inverse of the average shortest path from that particular node to all nodes in the network Wang et al. [66]:

$$C_C(i) = \frac{n-1}{\sum_{v_j \in V, i \neq j} d_{ij}} \quad (3.11)$$

Degree centrality refers to the number of edges that a node shares with others, and thus symbolizes the importance of the node in a network. Depending on the degrees of the nodes it connects to, it can be either assortative or disassortative, meaning it tends to connect to nodes that have either high or low degrees, analysis used by several authors to reflect geographical, economic and political implications. Bagler [5]; Kai-Quan et al. [43]; Wang et al. [66]:

$$C_D(i) = \sum_{j=1}^n a_{ij} \quad (3.12)$$

Another centrality measure geared towards Air Transport Networks can be defined relative to the Origin-Destination pair as in Monechi et al. [47], taking into consideration only the nodes that are passed by travelling from an Origin to a Destination:

$$B_i^{OD} = \sum_{j \neq k \neq i} \sigma_{kj} |i| / \sigma_{kj} OD_{kj} \quad (3.13)$$

This adaptation allows to compute centrality for nodes actually used by specific O-D pairs and not of the entire network.

Finally, random-walks betweenness centrality (RWBC) is an adaptation of centrality measure defined by Newman [50] which generalizes the usual betweenness centrality considering other paths beside the shortest ones as relevant. This betweenness centrality is defined as:

$$B_i^{RW} = \sum_{j \neq k \neq i} r_{jk}(i) \quad (3.14)$$

where  $r_{jk}(i)$  is the probability that a walk originating in vertex  $v_j$  and ending in vertex (node)  $v_k$  passes through node  $i$ . This version might be useful to address centrality for specific en-route air navigation points.

### 3.3.7. Graph spectra

The graph spectra can be used to obtain many characteristics of a graph as it is made of the sets of eigenvalues of the adjacency matrix. The Adjacency Matrix of a graph is a square matrix with values of 1 if a link exists between the nodes on the two matrix sides, or 0 if there aren't. Albert\* and Barabási [3]. Spectral density is written as:

$$\rho(\lambda) = \frac{1}{N} \sum_{j=1}^N \delta(\lambda - \lambda_j) \quad (3.15)$$

The  $k$ th spectral moment gives information about the networks topological structure, with the first moments in a graph offering statistical information on degree distribution for example:

- First moment - Mean of the degree distribution
- Second moment - Variance of the degree distribution
- Third moment - Skewness of the distribution
- Fourth moment - Kurtosis of the distribution

The more popular statistical instruments, mean and variance, are defined as the expected value and the expected squared deviation from the mean in a random variable, respectively. The skewness is defined as the asymmetry of the distribution with respect to its mean, so if the 'fatter' tail is to the left of the mean towards the x-axis, it is called 'positive' - skewed, and negative it is to the right. Finally, kurtosis is a measure of the arching of a distribution - simpler put, it is a property of the shape of the tails of a distribution.

## 3.4. Generating function

The Generating function formalism is defined as the function at the basis of the of the probability distribution for the degree of a network, for example. It is usually in the form of a power function,  $x^n$ , and is particularly useful because the coefficient of an element gives the probability of having a node with the degree equal to the power of the considered element (Albert\* and Barabási [3]).

## 3.5. Small-world networks

The small-world property is usually found in the real-world networks, as they exhibit a high degree of clustering and a short average path. The Watts-Strogatz model Watts and Strogatz [67] posited that while rewiring a regular lattice to become a random graph, a small-world network appears: the local clustering is preserved and it takes a few links to reach any node from any other node, as seen in Figure 3.4 below.

Small-worlds can be grouped under three types as Amaral et al. [4] proposes (Scale-free, broad-scale and single-scale), whereas Kai-Quan et al. [43], Barabási and Albert [7] and others consider them as a single class or even a property on its own. Small worlds are found also in other instances, for example the network of collaborating actors, but also in the World Airport Network, as detailed more in Section 3.8.

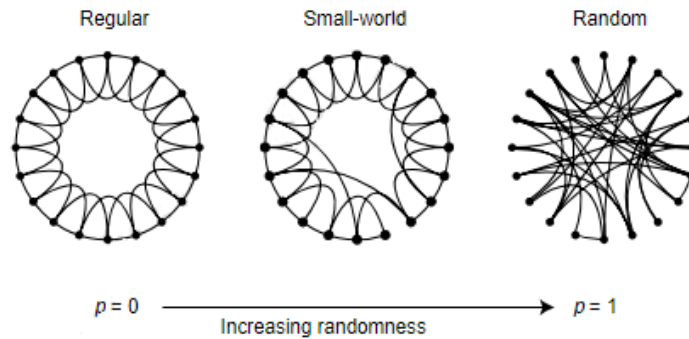


Figure 3.4: Example of regular lattice randomization with small-world instances. Watts and Strogatz [67]

### 3.6. Scale-free networks

Scale-free networks are a type of network with at least one characteristic, usually the degree distribution or node strength distribution, following a type of power law. They have attracted much research interest lately as several real-life networks or distributions follow such power-laws, where a few nodes are responsible for the major part of the information flow in the network. Examples include biological networks Jeong et al. [41], [64], wealth distribution in the world and the Internet. These networks have a few particular characteristics, such as a high degree of decentralization and highly resilient. However, error tolerance comes at a high price, as they are extremely vulnerable to attacks. This stems from the fact that the removal of important nodes will lead to a serious decrease in network capabilities.

At the basis of the scale-free concept is the power-law distribution (Eq.3.16) which emerges as a property of the network following the 'preferential attachment', better described as the probability that nodes with already higher degrees have a higher chance of getting new connections.

$$P(k) \sim k^{-\gamma}, \quad (3.16)$$

with usually  $\gamma \in (2, 3)$ , denoting the level of curvature that the power law describes.

### 3.7. Percolation Theory

Percolation theory refers to networks rather than graphs, and is primarily concerned by the probability of a certain network to percolate, that is, the network to connect into one large cluster. However, several properties apply to regular lattice as they apply to graphs, the reason being that, as Albert\* and Barabási [3] clearly explains, the infinite-dimensional limit ( $d \rightarrow \infty$ ) is the meeting point of the graphs and lattices. As several properties hold for percolation in such infinite dimension, it is possible to use them in graph theory as well.

The percolation theory has multiple applications in natural and engineering sciences, having been developed by Broadbent and Hammersley [16] as a method of analysing crystals and dealing with random media, it is now used in hydrology and analysis and modelling of porous media such as soil Berkowitz and Balberg [10], landscape and coastline analysis. Percolation can be associated also with fractal structures, as they exhibit a large, connected cluster, which develops after a certain critical percolation probability is attained. This is commonly referred to as phase transition and is yet another field where percolation theory is highly used. Such transitions can, for example, change the chemical structure of elements or physical topology, marking the birth of new elements as further elaborated in Berkowitz and Balberg [10]. One novel use in traffic systems of percolation is proposed by Shang et al. [62] with an ABM model consisting of 2 layers, one of virtual (cyber) nature and one of physical nature. The model uses percolation theory as the basis for information sharing between car drivers in a network, and calculates the total cost of travel function of the time it takes for the network to converge. The paper concludes that a high, positive correlation between the percolation rate and the convergence time is a clear indication of the utility of information-sharing in clusters, with agents having a local overview on the situations.

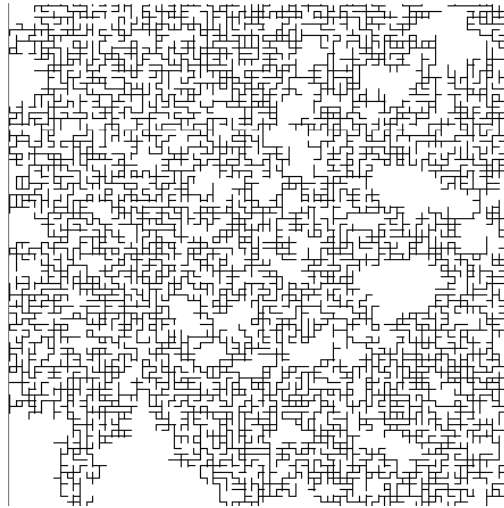


Figure 3.5: Percolation example of a 2d lattice network. Chen et al. [18]

### 3.8. Complexity Science in Air Transport

All concepts applicable in Complex Network Theory mentioned in Chapter 3 have been applied in ATM or in air transport operations with various different purposes. A network is defined by links and nodes and thus can be built in several ways, by considering airports as nodes, connected by non-stop flights Bagler [5], Cook et al. [21]. Other studies consider the network made of navigation points and air routes Kai-Quan et al. [43]. Irrespective of the choice of network elements, Network Science is a useful paradigm to assess the current network topology and its performance but also the evolution in time, identifying trends and bottlenecks. This section presents first how has Complex Network Theory been used by studying multiple real networks and their topology, by well known indices (degree distributions, betweenness, average path length, clustering coefficients, and others). In addition, a separate subsection is focusing on the dynamics of the networks or comparisons between air transport networks and between different modes of transportation. The known CNT KPIs of real ATM networks are presented and compared to the same KPIs of a random model in order to understand the attributes of the real-world system.

Topological aspects of the network are a much researched avenue in ATM and network science. Topology can be physical or logical: The first one refers to how the layout of the nodes and links is done, whereas the second one refers to how data is carried around the network. In the case of ATM studies, logical topology can be considered as aircraft flow across nodes (be they airports or nodes). For example, from the physical topology perspective, the literature shows that the European ATM network can be characterized as a scale-free, small world network with communities at multiple scales Amaral et al. [4]; Guimera and Amaral [31]; Guimera et al. [32]. Research in ATM has been carried out at national Bagler [5]; Han et al. [36], local-regional Han et al. [37] or at the level of entire regions Guimera and Amaral [31], Guimera et al. [32]).

One example of national networks by Guida and Funaro [30] investigates the topology of the Italian Airport Network, considering the nodes as airports, linked by non-stop flights. The out-degree of a node, i.e., an airport, is defined as the number of trajectories departing from this airport to all other airports in the Italian airspace. Based on this network representation, the authors computed and showed that the node distribution and the correlation of degrees and 'betweenness', follow a Double Pareto Law, fitted by two different exponents. However, the authors fail to completely align the Italian Network with all the characteristics of a small-world network: there is no conclusion on whether the average path length of the IAN is characteristic for small-worlds, and the resulting clustering coefficients are notably lower than those of random networks, whereas real world networks exhibit considerable higher clustering Coefficients due to the natural tendency to form communities Gurtner et al. [33].

Kai-Quan et al. [43] on the other hand, provide a consistent analysis of the Chinese Air Route Network (CARN) in comparison with the Chinese Airport Network (CAN): the first network consists of air navigation waypoints connected by air routes, whereas the second one is defined by airports connected by non-stop

flights. It provides a complete analysis by a one-to-one topological comparison of both transport structures and highlights the critical waypoints in the air Route Network, the exponential distribution of the degrees, low clustering coefficient, large shortest path length in the Chinese Air Route Network (CARN) as well as the traffic distribution and the traffic increase patterns in East and West China. Moreover, it goes in depth by cross-comparing degree-degree correlations, concluding that CARN tends to resemble more a regular lattice whereas CAN is surely a small-world network due to its higher clustering and lower average path (in this case being 2, a value which does not surprise, as most passengers fly a 2-flight trip). The traffic aspect has been analysed in a time window of 8 years (2002 – 2010) and sheds light on different aspects of air transportation in China by analysing and comparing the Air Route Segments with the Airline routes, as well as by looking at the traffic flowing through each waypoint. The authors find that traffic flow through waypoints spans 4 orders of magnitude and despite the rather homogeneous topology of CARN, and highlight a linear degree-strength correlation of the waypoints with a few exceptions, for which operational and geographical arguments clearly explain why they do not fit.

Bagler [5] finds out that Airport Network of India (ANI) also exhibits the small-world property, when considering airports as vertices and direct flights as the connections. The article does a fine analysis of in-out degree correlations of airports and reinforces the disassortative mixing of the higher degree nodes with the lower degree ones, while also emphasizing the connections between the higher ranking nodes as a byproduct of airport manager decisions. This fact is also apparent by the analysis of the clustering coefficient and the weighted clustering coefficient reinforcing the 'rich-club' phenomenon. One interesting aspect of the ANI is that most nodes can be reached from any other node using just one layover, as 78% of the nodes are connected by a path of 2. Using the cyclic nature of flights and an approach oriented towards 'transport' with the support of complex network theory, Li and Cai [45] investigate the degree variation across days or weeks, with the nodes being airports in China, linked by non-stop flights. A remarkable discovery is that a significant positive correlation has been found between the frequency of the flights between two nodes and the degrees of said nodes. Upon a closer look the, authors seem to have confused the calculations of diameter and average shortest path, reporting the value of the latter for both KPIs.

To begin with, Zanin and Lillo [71] describe the metrics and the topology of a network shedding light on various business strategies adopted by low-cost of network carriers. Such business choices are thought to have a direct impact on passenger mobility analysis and on the network evolution in time, while the former adapts and is changing the latter.

Woolley-Meza et al. [69] perform an initial, comparative study between the Global Cargo Ship Network (GCSN) and the World Airport Network (WAN) both at global and a few local sites. An interesting feature of the paper is displayed below in Figure 3.6: the logarithm of the shortest path from specific airports or harbours to all other points in the network shows that the closest points are always the ones with higher flux or traffic (blue), whereas the furthest ones are the ones with less traffic (flux in the case of GCSN and air traffic in the case of WAN).

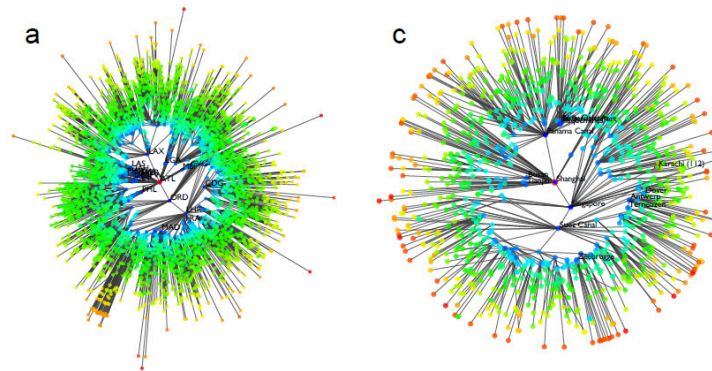


Figure 3.6: Shortest path trees for Atlanta airport and Shanghai harbour. Woolley-Meza et al. [69]

Pien et al. [53] propose a new index, the Relative Area Index (RAI), to assess more consistently the robustness of the European Air Traffic Network, consisting of Airports and airspaces, being one of the few that integrate the two in a network representation. The authors define a robustness index by calculating the

influence of nodal capacity-reductions on network capacity, based on lagrangian exponents is rounded up by a quantitative analysis of the network topology, highlighting its apparent hierarchy, and a degree-strength correlation analysis considered a weighted network.

One paper that deserves a separate mention is investigating the Air Transport Network by considering countries as nodes, and aggregate the flights from one country to another into one link with weights depending on the number of flights between the countries. Wandelt and Sun [65] It investigates the evolution of traffic during 9 years by looking at ticket data and performs a topological and functional assessment of the network. Countries are assessed based on their criticality in the overall global network, with complex network KPIs such as degree and density correlated with GDP, Country Area, population, GDP, GNI per capita, life expectancy, and CO2 emission. In addition, the authors describe 3 different kinds of betweenness: hops, distance-based and passenger-based betweenness, concluding that the hops-betweenness is highly correlated to the distance based betweenness. Other aspects worth mentioning are the MDS (Minimum Dominating Set), defined for a network with the set of nodes  $N$ , as a set of nodes  $S$  with  $S \subseteq N$  such that for each  $n \in N$  we have  $n \in S$  or  $n$  is a neighbor of at least one  $s \in S$ . The MDS is the dominating set with the smallest size Nacher and Akutsu [49], in other words, the smallest set of nodes controlling the network or adjacent to the nodes controlling the network. For scale-free networks, usually this amounts to 20% of the nodes.

Another particular approach is taken by Bongiorno et al. [13], who carry out a network study of the central-south-west European countries over an AIRAC cycle, in which network topological aspects are analysed and compared. The proposed network consists of navigation points and the flights connecting them, and yields an exponential function for its degree distribution with a rather heterogeneous waypoints distribution. Such heterogeneity stems from geographical peculiarities but also from individual nations choices: for example in France there are a higher number of waypoints, thus reducing the local complexity and but chooses to route traffic on a much smaller number of waypoints, whereas in UK the traffic spread is more balanced across the entire airspace. The unique aspect of the article is that it is able to link the network topology to the flight efficiency and hence the strategic choices that airlines take when choosing to fly a specific route.

Table 3.3 displays a summary of the topology aspects of different networks, how these networks were constructed and how they were analysed. A short explanation of the meaning of the columns is given in the table description. The last column contains specific analyses or aspects, that were not found in other papers mentioned in the table.

Table 3.4 shows the main Complex Network KPIs measured in some of the surveyed literature. As expected, average shortest path and clustering are two of the most studied metrics. What comes as a surprise is the apparent absence of average degree measure - however some articles mentioned in Table 3.3 do highlight the degree distributions, showing that degree is still largely employed to characterize a network. Another noteworthy aspect is the networks themselves: a large portion consists of airports, with air navigation points representing a small fraction of the studies.

### 3.9. Agent-Based Modelling in ATM

Agent-Based Modelling (ABM) has become one of the most robust modelling paradigms of complex systems. In most aspects, it can compete with equation-based modelling, being particularly useful to capture the emerging behaviour of a system. Agent-based modelling is considering individual agents that can interact with their peers and with the environment, being a particular useful modelling paradigm for socio-technical systems, such as the ATM or in general in Air Transportation systems.

A few examples of ABM being used in the Air Transportation System is that of a decentralized taxi model proposed by Udluft [63] to implement, analyze, and evaluate a decentralized control approach in the context of taxiing aircraft. Because it is unclear if the emergent behavior of decentralized control will result in safe and efficient operations, the amount of information to be shared with the local agents or in this case, ATCOs, on the state of the runways and the taxiways is critical. The author demonstrates that a decentralized control for aircraft taxiing operation can result in stable operations.

Janssen et al. [40] Perform an analysis on Schiphol Airport to assess the trade-off between security and efficiency, considering an external attack in one of the terminals. Besides emergent properties, ABM allows for heterogeneity at multiple levels, including agent types, their actions and interactions, in order to model realistic operations.

Multi-agent systems have been extensively used also in Safety Analyses in ATM, Blom et al. [11] developing a Multi-Agent Dynamic Risk Modelling framework called TOPAZ, encompassing Agent-based Modelling, Human performance modelling, Petri Net modelling syntax, rare event Monte Carlo (MC) simulation and Sensitivity and Bias and uncertainty analysis. Using the petri nets as methodology and the Monte-Carlo simulation for rare events, this variant of ABM proposes hazard identification for safety assessment by taking into consideration the multitude of options in ATM operations design.

ABM covers several facets of the ATM operations, one of them being En-route ATC: Bongiorno et al. [12] have developed an ABM capable of simulating Air Traffic using real trajectory data over a portion of the entire ECAC area. Besides showing the capabilities of the model and the reliable statistical analysis produced, the same authors propose an initial Agent Based-model to simulate and study the 'directs' given by ATCOs in the En-route phase of flights - all while ensuring a conflict-free trajectory Bongiorno et al. [15].

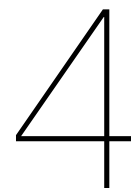
This is to show that ABM is used as a modelling paradigm to go one step further than equation-based modelling, in order to capture emergent behaviour, model information exchange and investigate resilience principle in socio-technical environments such as the Air Traffic Management system.

Network	Nodes	Links	Topology (distr.)	Correlation	Coeff.	Specifics	Ref.
China	1.Arpts 2.Wpts	1.Flights 2.RT segment	Degree Clustering Avg path Betweeness Diameter Edge length Min max edge*	degree-degree degree-strength degree-clustering degree-betweeness air segment - flight leg betweeness - strength traffic evolution - economic, geographic, political	Mixing	Temporal analysis (weekly, seasonal and yearly) Geographical disparity	[43]
India	Arpts	Flights	Unweighted: Degree Avg. path Weighted (cdf): Strength* Clustering Coeff.	Degree k- avg strength of vertice w/ degree k; Weighted C - Unweighted C	Mixing Scaling Correl.	hierarchicy truncated scale-free degree distribution	[5]
China	Arpts	Flights	In-out degree (Un-directed) Directed: Flight weight Clustering Coeff Connectivity Density Efficiency	Subcluster diameter - connection density Weight - degree Degree - degree	Mixing	Double pareto law fitting	[45]
Italy	Arpts	Flights 1 week	Degree (cdf) <i>Betweeness<sub>rand</sub></i>	degree-centrality	-	Double Pareto law fitting Seasonal comparisons	[30]
EU countries	Wpts	Flights	Nr of nodes* Avg degree* Max degree* Avg, max strength*	Traffic - Fork	Pearson	Efficiency (traj./ grand circle) Predictability (negative delay [sec/km]) Analysis on deviations at waypoint network level	[33]
World	Arpts	Flights	Degree Betweeness Norm. Betweeness Clustering	Betweeness - Connectedness	-	Multi-community analysis (within-community degree and participation factors: 7 different roles for nodes)	[55]
Austria	Arpts	Flights	Avg degree* Nr. flights* Flight weight expon.* Clustering coeff. Degree (weekly) In/out flights	Degree-degree Flights- weight distributions In-out degree Out degree - out degree exponent	Mixing	Airline perspective, network subset	[36]

Table 3.3: Table with main topology aspects of various papers. Columns 2 and 3 explain the meaning of nodes and links. In column 4, starred \* elements represent a value, not a distribution. Column 5 refers to different coefficients used to characterize the correlations.

Network	Period	Nodes/Links	Avg. Degree	C	$C_{rand}$	L	$L_{rand}$	D	$D_{rand}$	Connect.	Eff.	Ref.
Chinese Air Route Network	2002-2010	1013/1586	3,13	0,08	-	14,08	-	39	-	-	-	[43]
China	2002-2010	147/1055	14,35	0,79	-	2,2	-	4	-	-	-	[43]
China	1 Week	128/1165	14	0,733	0,6	2,067	-	2,067*	-	0,1433	0.484	[45]
India(unweighted)	-	79/442	5,77	0,6574	0,00731	2,2593	2,493	4	-	-	-	[5]
India	12/2010	84/13909(f)	-	0,645	0,18	2,17	2,55	-	-	-	-	[59]
Italy	1.06.2005 - 31.05.2006	42/310	-	0,09	0,16	-	-	-	-	-	-	[30]
Italy	16.7.2005-14.8.2005	42/310	-	0,1	0,17	1,987	3,74	-	-	-	-	[54]
Italy	-	33/105	-	0,418	-	1,92	-	-	-	-	-	[72]
WAN	1.11.2000- 31.10.2001	3883/27,051	-	0,62	0,049	4,4	-	-	-	-	-	[55]
WAN	11/2002	3880/18810	-	-	-	4,37	-	-	-	-	-	[8]
Austrian Airline	-	134/9560(f)	1,3	0,206	0,01	d	-	2,383	18,67	-	-	[36]
US	-	215/116725(f)	-	0,618	0,065	1,403	-	-	-	-	-	[46]
US	10/2005 - 12/2005	272/6566	-	0,73	0,19	1,9	1,8	-	-	-	-	[70]
Spain	-	35/123	-	0,738	-	1,84	-	-	-	-	-	[72]

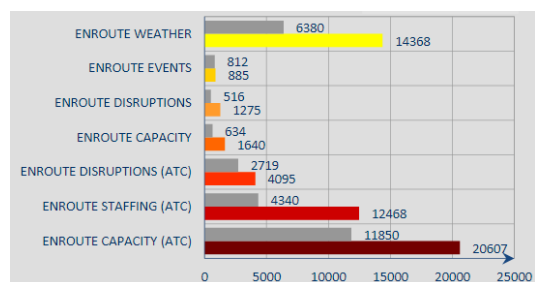
Table 3.4: Table containing quantitative aspects of surveyed literature. All networks assume airports as nodes and direct flights as existing links, except those with an additional(f) in Column 3 who refer to number of flights in the network (traffic). Columns 5 and 6 show the Clustering Coefficient at entire network level, with the randomized counter parts. Columns 7,8 and 9,10 do the same for average path length and network diameter



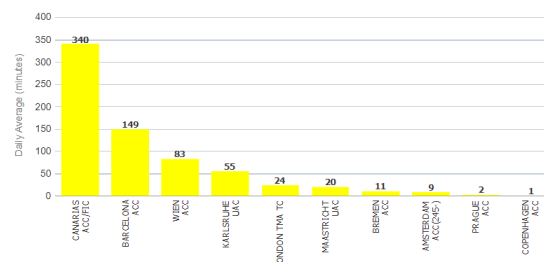
# Trajectory Deviations

## 4.1. Flight Deviations

En-route flight delays added up to an average of 340 minutes per day last year in November in some FIRs, with central EU FIRs such as Maastricht or Karlsruhe experiencing usually such issue. Avoiding en-route weather plays an important role in the amount of delay experienced by the airspace users, as shown in subpicture 1.1.b below.



(4.1.a) November 2018 En-route delay reasons compared with previous year



(4.1.b) Top 20 FIRs with weather delay november 2018

Figure 4.1: En-route weather ATFM delay statistics EUROCONTROL [27]

Following suit, the research community has mainly investigated delays as a whole Rebollo and Balakrishnan [56] or how do they propagate through the network Jetzki [42]. Comparably little research effort has been put into understanding the effects of weather at European level for the ATM en-route delays.

One of the research papers found focusing specifically on this topic is that of Bongiorno et al. [14], which perform an in-depth analysis on the flight deviations in the German Airspace during an AIRAC cycle. Deviations are considered from the realized trajectory compared with the filed flight plan by assessing whether the aircraft has flown through the air navigation route point ( or simply referred to as waypoint). The statistical approach underlies traffic deviations characteristics, such as an inclination for introducing deviations during night-time compared to day-time, and in lower traffic situations. Furthermore, these deviations seem to occur more frequently and at larger angle-to-destination closer to the departure airport. The metric used to measure the said deviations is called "di-fork" (directional fork), and is a development of the "fork" Bongiorno et al. [13]. The di-fork takes into consideration the traffic direction and is defined as:

$$F_{\Delta t}(P) = dF_{\Delta t}(P)/pF_{\Delta t}(P) \quad (4.1)$$

where  $pF_{\Delta t}(P)$  is the number of flights passing through P as observed in the planned flight trajectories and  $dF_{\Delta t}(P)$  the number of flights passing through P, as observed in the realized flight trajectories, and missing the next navigation point as indicated in the corresponding planned flight trajectory. The authors

provide a rigorous analysis of flight deviations by referring to the waypoints network and the di-fork by characterizing pairs of points between which aircraft are most likely not to follow their planned trajectory spatially and temporally. One of the conclusions is that deviations frequently occur close to the beginning of the flight trajectory, thus indicating that they might not occur to recover from accumulated en-route delay but rather due to ATC action to speed flights up, especially if the trajectory is has started with a high angle-to-destination value. Additionally, an intra-day deviation pattern is proven due to the variation in traffic levels, but it is also dependant on the particular airspace structure and operational procedures in place.//

A survey EUROCONTROL [26] lists the identified operational weather avoidance strategies with their associated impact on sector capacity and the associated risks.

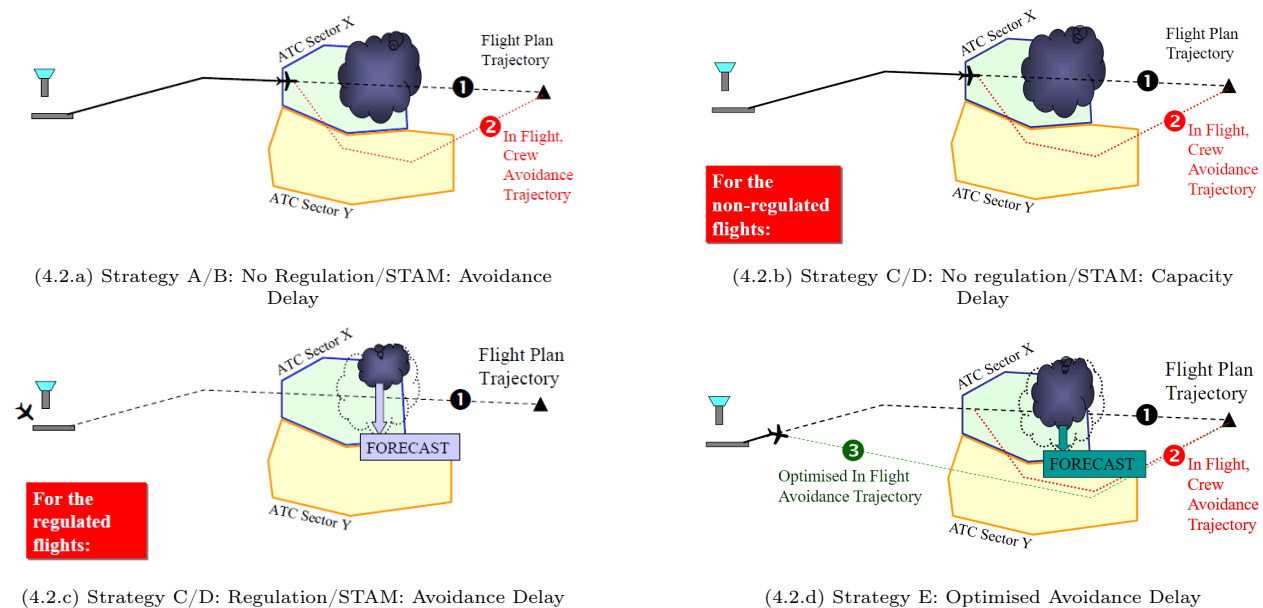


Figure 4.2: En-route weather avoidance strategies EUROCONTROL [26]

The survey analysed a spectrum of available and used strategies for en-route and TMA ATC severe weather impact management. The strategies are differentiated depending on the timeliness of notification and communication, its potential/actual impact on ATC operations and the application of flow measures. STAMs (Short-term ATCFM Measures) is a collaborative procedure which allows flight management positions (FMPs) across different sectors to identify hotspots that need to be regulated with more time in advance:

- Strategy A: lack of communication with other ATC units or the Network Manager about the forecasted/reported severe weather and related impact; traffic flow measures or STAM are not implemented; severe weather risk is managed locally at tactical ATC level.
- Strategy B: systematic communication with other ATC units or the Network Manager about the forecasted/reported severe weather and the related impact; traffic flow measures or STAM are not implemented; severe weather risk is managed locally at tactical ATC level.
- Strategy C: lack of communication at network level (with other ATC units or the Network Manager) about the forecasted/reported severe weather and related impact; implementation of traffic flow measures or STAM in addition to tactical ATC mitigation measures.
- Strategy D: systematic communication at network level (with other ATC units or the Network Manager) about the forecasted/reported severe weather and related impact; implementation of traffic flow measures or STAM in addition to tactical ATC mitigation measures.

- Strategy E (an upgrade of Strategy D): systematic communication at network level about the forecasted/ reported severe weather; implementation of traffic flow measures or STAM. Based on a collaborative decision making process, the in-flight weather avoidance of specific flights may be optimised.

## 4.2. Weather in ATM

The survey cited in section 4.1 by EUROCONTROL [26] carried out in 2013 determined that for the en-route and TMA Air Transport Control, airspace users rate as the most relevant weather hazards severe turbulence, lightning and in-flight icing. Such hazards are usually associated with the existence and the development of convective weather. Figures 1.1.a and 1.1.b highlight another characteristic of weather: its randomness and high degree of unpredictability, which yearly generate hundreds of thousands of minutes in delay and loss of revenue. One key factor that affects ATM is uncertainty, which is an inherent property of real-world socio-technical complex systems. Rivas et al. [57]

The analysis of weather uncertainty has been addressed by many authors, using different methods. For instance, Nilim et al. [51] consider a trajectory-based air traffic management scenario to minimize delays under weather uncertainty. In this publication, weather processes are modeled as stationary Markov chains. Pepper et al. [52] present a method, based on Bayesian decision networks, for taking into account uncertain weather information in air traffic flow management. Its focus is on convective weather with coverage and probability data taken from the US Aviation Weather forecast, however little information is given on the data source. Clarke et al. [19] develop a methodology to study airspace capacity in the presence of weather uncertainty, which in turn stems from the 1 – 6 hour National Convective Weather Forecast (NCWF). Zheng and Zhao [73] develop a statistical model of wind uncertainties and apply it to stochastic trajectory prediction in the case of straight, level flight trajectories.

### 4.2.1. Convective events analysis and modelling

DeLaura and Evans [22] NASA Study dealing with convective storms over two large US sectors. Hauf et al. [38] DIVMET : modelling trajectories with severe weather information. In table 4.1 below, Gelhardt et al. [29] present the weather severity levels with associated parameter thresholds. Such data are a good indication for the data extraction from the ECMWF (European Centre for Medium-Range Weather Forecasts). Details on such data are described in more detail in section 2.2

Category	Attributes
Heavy Rain	>37 dBZ (30 or 35 also encountered in literature, without lightning)
Warning Level 1 (light)	thunderstorm with wind gusts up to 40 kt
Warning level 2 (moderate)	thunderstorm with wind gusts up to 55 kt and/or heavy rain (15-25 mm/h)
Warning level 3 (heavy)	- thunderstorm with wind gusts more than 56 kt, optionally heavy rain - thunderstorm with hail - thunderstorm with heavy rain (25-40 mm/h)
Warning level 4 (extreme)	- thunderstorm with wind gusts more than 56 kt and heavy rain, optionally hail - thunderstorm with extrem heavy rain (more than 40 mm/h), optionally hail

Table 4.1: Different weather severity thresholds Gelhardt et al. [29]

Hydrostatic equilibrium describes the atmospheric state in which the upward directed pressure gradient force (the decrease of pressure with height) is balanced by the downward-directed gravitational pull of the Earth. On average the Earth's atmosphere is always close to hydrostatic equilibrium. This has been used to approximate the Euler equations underlying weather prediction models and successfully applied in NWP and climate prediction. Non-hydrostatic dynamical effects start to become important below horizontal scales of about 10km.

#### 4.2.2. Alpine Weather Operations

Air Navigation Service Providers are tackling operations during severe weather: DFS, Austrocontrol, ENAV and Skyguide have formed a consortium and have devised strategic re-routing procedures in case of severe weather affecting the geographical area around the Alps. The partners devised the new procedures with the aim of reducing delays at Munich airport, stabilizing the network and air traffic flows, reducing the workload in the Karlsruhe Upper Area Control Center (UAC), and increasing safety under adverse weather conditions. Areas of uncertainty remain, however. The atmospheric variables with the most effect on aviation and ATM are driven by smaller scales of atmospheric motion, i.e. fronts, rapidly developing cyclones and, most importantly, by thunderstorms and the effect of mountains and coasts.

The number of thunderstorms in the Alps has grown over the last years, and the first six months of 2018 weather affected traffic to Munich airport on 17 days, compared with 16 days for the whole of 2017. As adverse weather often occurs unexpectedly, controllers routinely have routed inbound flights to Munich airport to the upper airspace controlled by the Karlsruhe UAC at short notice. The flights increased the complexity in already overloaded sectors. Under the new procedures, controllers working in Padova, Vienna, or Zurich distribute the traffic to three additional fixed routings via airspace controlled by Karlsruhe, Zurich, or Vienna. In addition, the procedures include defined descent areas to ensure a smooth inbound flow to Munich airport, while a new automated data exchange increases predictability.

### 4.3. Airline Types

The most defining characteristic of airlines nowadays is their business strategy, which can be divided roughly in two major categories: Low-Cost Carriers (LCCs) and Network Carriers, also known as Network Carriers (NC). NCs use a network of connected flights and make use of hubs to use economies of scale, reduce maintenance and crew costs, rather than LCCs who operate usually on short -to -medium routes and consider individual Origin-Destination (O-D) as separate markets Belobaba et al. [9]. A visual representation of a point-to-point network (left) and a hub-and-spoke (right) can be seen in Figure 4.3 below. A list of European LCCs is presented in Appendix A.

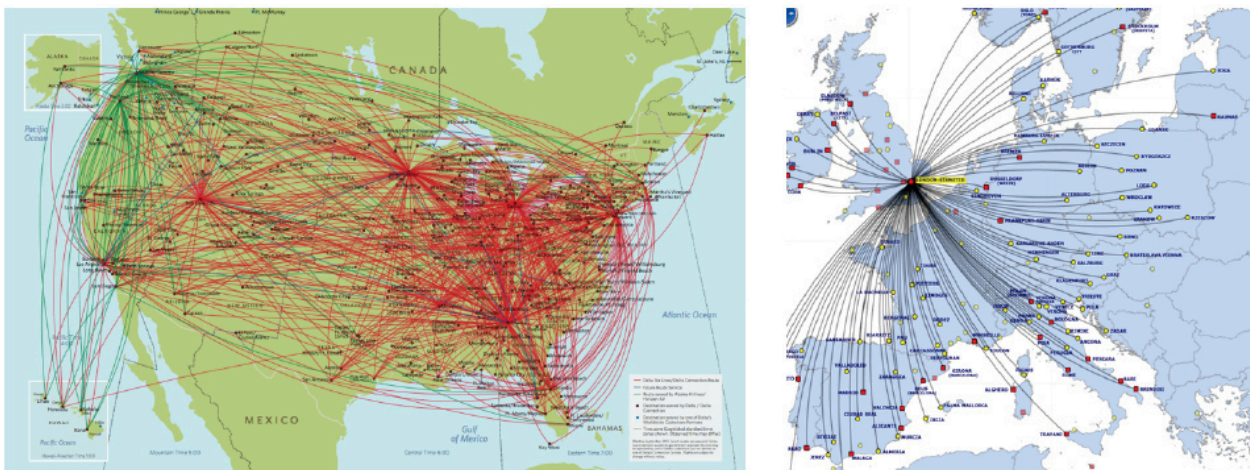


Figure 4.3: Point-to-point Network (left) and Hub-and-spoke network model (right). AE4423 TU Delft

LCCs may also implement different flight management strategies during severe weather situations in order

to optimize the route at the expense of passenger comfort; whereas the NCs are expected to value passenger comfort more than the cost -saving associated with a shorter flight time with few minutes.

## 4.4. Deviation KPIs

Another similar article by the some of the previous authors comes from 2016, Gurtner et al. [35]. The author's secondary focus is in fact on traffic complexity and safety, analysing the Free-route scenario and developing new metrics for measuring ATC complexity and potential conflicts. By measuring complexity, the paper touches also on trajectory deviations, mentioning the geometric efficiency of the trajectory, and the maximum angle of deviation between the planned and modified trajectory as two parameters relevant for the management of flight trajectories. Some previously developed complexity metrics that could be adapted to the scope of this study are presented in Table 4.2 in section 4.4.

Some of the already developed metrics for air traffic complexity are presented in Table 4.2 below, adapted for the analysis of deviations. The fourth column contains information for which point of view the metrics will be useful.

Code	Short Description	Unit	Source
C1	Density	AC/hour/sector	[17]
C2	Geometric Trajectory efficiency (Planned/actual) also per segment	Ratio	[17]
C3	Angle-to destination	Degrees	[35]
C4	Number of AC with Heading changes of angles greater than 15 degrees	Count	[44]
C5	di-Fork	Count	[14]
C6	Angle between last planned and first deviated segment	Degrees	[14]

Table 4.2: Deviation metrics derived from the original table in Gurtner et al. [35]. The respective table provides a summary from the metrics found by the authors in literature, mainly from Chatterji and Sridhar [17], Laudeman et al. [44], Gurtner et al. [34], C11 Di-fork is an original metric developed by the authors in Bongiorno et al. [14]

Novel metrics that capture the behaviour of airlines related to the deviations, together with complex network concepts applied to specific components of the network are presented in Table 4.3. The third column coding refers to the metric description applicability:

- D - Deviation characterization
- U - User Characterization
- N - Network characterization

Below, the details on the mathematical definition on the computation of the KPIs presented Table 4.3 and Table 4.2 are shown.

KPI 1 refers to the number of aircraft flying in a given sector, and can be defined as

$$C1 = \int_{t_1}^{t_2} \sum_{FL_{min}}^{FL_{max}} AC_{sect_i}^{FL_x}, \quad (4.2)$$

with  $AC_{sect_i}^{FL_x}$  the unit variable referring to an aircraft flying at a given  $FL_x$  in a sector( $sect_i$ ) with limits  $FL_{min}$ ,  $FL_{max}$  in a given period  $T \in (t_1, t_2)$ .

$$C2 = E_i = \frac{l_i}{l_i^{nvp}}, \quad (4.3)$$

Code	Short Description	Unit	Applicable
C7	Beginning and ending points of the deviation	x,y,z	D
C8	Volume/surface of deviations	$NM^3$	D,U
C9	Number and size of vertical deviations at a node	count	U,N
C10	Number and size of horizontal deviations at a node	count	U,N
C11	Temporal efficiency	count	U
C12	Deviation as a percentage of the entire flight path	count	D,U
C13	Horizontal distance from A/C to weather event at the point of deviation	NM	U
C14	Correlation: number of planned and deviated trajectories at a node	count	N
C15	Correlation: number of planned and deviated trajectories in a sector	count	N

Table 4.3: Possible novel deviation metrics.

where C2 refers to the efficiency of a single flight  $i$  between Origin of flight  $i$ , denoted  $O_i$  and destination of flight  $i$ , denoted  $D_i$  and is computed using  $l_i$ , defined as the grand circle between OD. The  $l_i^{nvp}$  is defined as the trajectory of flight  $i$  (planned or flown) consisting of navigation points, with  $E_i \in (0, 1]$

$$C3 = \alpha_j^i = \angle (P_j, P_{j+1}), \quad (4.4)$$

where we define the angle-to-destination for each flight  $f_i$  we calculate the angle between the segment consisting of the current navigation point  $P_j$  and next point  $P_{j+1}$  and the segment connecting  $P_j$  with destination  $D_i$

$$C4 = \sum AC_{hdg}, \text{ if } hdg \geq 15^\circ \quad (4.5)$$

Where C4 represents the sum of aircraft with heading changes greater than  $15^\circ$

$$C5 = di - fork_{j,j+1}^{t_1,t_2} = \frac{f_{P_j} - f_{P_{j+1}}}{f_{P_j}}, \quad (4.6)$$

where the di-fork for a given time-frame  $(t_1, t_2)$  and for a given segment  $(P_j, P_{j+1})$  is calculated as the ratio between the difference of flights that have flown past by both navpoints and flights that have flown past the first but not the second, and the number of total flights that have flown through both.

$$C6 = \alpha_{nav_i}^{dev}, \quad (4.7)$$

where the deviation angle at a specific navigation point  $nav_i$  between last planned segment  $s_{nav_i}$  and next deviated segment  $s_{nav_{i+1}}^{dev}$  is computed.

$$C7 = dev_{f_i}^i = (nav_i, \dots, nav_j, t_1, t_2, date), \quad (4.8)$$

Each deviation for each flight  $f_i$  is characterized by a tuple consisting of the start and end navigation points as well as the navigation points in between, the date, the start time and end time of the deviation.

$$C8 = \int_{nav_i}^{nav_{i+k}} F_s, \quad (4.9)$$

where function F is a function of surface. C8 is the cumulative displacement along a deviation with respect to a reference trajectory, with  $nav_i$  and  $nav_{i+k}$  being the beginning and the end of the deviation in terms of crossed navigation points. In other terms, the additional airspace volume or surface that has been used in addition to the flown volumes according to the flight plan.

$$C9 = \int_{nav_i}^{nav_{i+k}} V_s, \quad (4.10)$$

where  $V$  is a function of the distance from the reference trajectory at each navigation point in the vertical plane, with  $C9$  the cumulative vertical deviations at a given segment.

$$C10 = \int_{nav_i}^{nav_{i+k}} H_s, \quad (4.11)$$

where  $V$  is a function of the distance from the reference trajectory at each navigation point in the horizontal plane, with  $C10$  the cumulative horizontal deviation at a given segment.

$$C11 = Et_i = \frac{t_a}{t_p}, \quad (4.12)$$

where the temporal efficiency of a flight  $f_i$  is given by actual duration of flight divided by planned duration of flight

$$C12 = dev_i = \frac{C8}{f_i}, \quad (4.13)$$

where  $C12$  is the deviation of a flight seen as a fraction of that flight, both planned and realized.

$$C13 = d(pos_1, pos_2), \quad (4.14)$$

where  $pos_1 = (x, y, z)_i$  of  $AC_i$  and in a similar way,  $pos_2 = (x, y, z)_j$  of weather event  $j$ , signifying the distance at which the first deviation occurred with respect to the position of the weather event.

$$C14 = \rho F'_{nav_i}, F_{nav_i}, \quad (4.15)$$

where it refers to the correlation of the planned and deviated trajectories at a given navpoint, and where the sum of planned and deviated trajectories from at a specific navigation point  $nav_i$ , are:

$$F = \sum_i f_i \quad (4.16)$$

$$F' = \sum_i f'_i \quad (4.17)$$

Some of the KPIs to be used in this MSc. Thesis stem directly from Complex Network Theory and will be instrumental in analysing the variations at entire Network level, or for a particular area of nodes. A list with the KPIs can be observed in Table 4.4 with an indication of the type of analysis they might be used for. The mathematical definition and a more detailed explanations on the concepts of Complex Network Theory are presented in the sections of Chapter 3. As shown in Kai-Quan et al. [43] and further in Chapter 4, insights on Air Traffic Networks are obtained by analysis of correlation between Complex Network metrics.

Code	Short Description	Deviations	Network
CX1	Clustering Coefficient Distribution	Y	Y
CX2	Degree Distribution	Y	Y
CX3	Strength distribution	Y	Y
CX4	Betweenness distribution	N	Y
CX5	Average path length distribution	N	Y
CX6	Betweenness-centrality distribution	Y	N

Table 4.4: Complexity Network metrics, surveyed from Albert\* and Barabási [3] and Erdős and Rényi [24]

Code	Short Metric Description	daily	weekly	per season
CP1	(Cumulative) Number and size of vertical deviations	yes	yes	yes
CP2	(Cumulative) Number and size of horizontal deviations	yes	yes	yes
CP3	C1 and C2 depending on geography	yes	yes	yes
CP4	Geometric Trajectory efficiency	yes	yes	yes
CP5	Temporal Trajectory efficiency	yes	yes	yes
CP6	Angle-to-destination	yes	yes	yes
CP7	Number of A/C with heading changes greater than 15 degrees	yes	yes	yes
CP8	Deviation segment length	yes	yes	yes
CP9	Trajectory characterization(min, max and average length)	yes	yes	yes
CP10	Deviation length as a percentage of the trajectory	yes	yes	yes

Table 4.5: Deviation metrics for the initial characterization of Airlines. Columns 3,4,5 mention if they will have a Probability Distribution Function attributed over various time scales. Column 3 will show the PDF for 24h to distinguish day and night variation, column 4 will present the probabilities every day of the week to show weekend variations and finally the last column will integrate season variability.

Table 4.5 shows the planned metrics to be used as a way of behaviour definition for the major 2 types of airlines: Low-Cost Carriers (LCC), Network Carriers (NC). Other types of airlines might be added for the study, such as Cargo (C) and Feeder airlines (F).

# 5

## Research Questions

Deviations from planned trajectory occur often as they are normal to some extent, however such deviations have not been extensively characterized and their effect on airspace capacity has not been fully understood. After writing this Literature Review report, the main research question can be constructed in the following way:

How can the differences between the Planned trajectory and Realized trajectory of European Low-Cost and Non-Low Cost carriers be quantified and characterized, assuming Air Traffic Control Officers (ATCOs) manage the trajectories in a similar fashion?

The research question can be structured into several sub-questions:

- How do the planned and realized trajectories compare considering the type of airline but also geographical and temporal aspects?
- How can deviations be defined considering the differences between the planned and realized trajectory?
- How can the aircraft trajectory deviations between be computed and characterized using a network representation of the European Air Navigation Points?
- How to define new metrics and adapt existing ones to characterize trajectory deviations?
- Can trajectory deviations due to weather be distinguished from other types of deviations? If so, how can they be characterized? Is the statistical profile different than the ones not caused by weather?



# Bibliography

- [1] Lada A Adamic, Rajan M Lukose, Amit R Puniyani, and Bernardo A Huberman. Search in power-law networks. *Physical review E*, 64(4):046135, 2001.
- [2] Réka Albert and Albert-László Barabási. Statistical mechanics of complex networks. *Reviews of modern physics*, 74(1):47, 2002.
- [3] Réka Albert\* and Albert László Barabási. 'Statistical mechanics of complex networks'. *Previews of Modern Physics*, VOLUME 74, JANUARY 2002, 48-94, 2017.
- [4] Lus A Nunes Amaral, Antonio Scala, Marc Barthelemy, and H Eugene Stanley. Classes of small-world networks. *Proceedings of the national academy of sciences*, 97(21):11149–11152, 2000.
- [5] G. Bagler. Analysis of the airport network of india as a complex weighted network. *Physica A: Statistical Mechanics and its Applications*, 387(12):2972–2980, 2008.
- [6] Albert-László Barabási. *Linked: The new science of networks*, 2003.
- [7] Albert-László Barabási and Réka Albert. Emergence of scaling in random networks. *science*, 286(5439): 509–512, 1999.
- [8] Alain Barrat, Marc Barthelemy, Romualdo Pastor-Satorras, and Alessandro Vespignani. The architecture of complex weighted networks. *Proceedings of the national academy of sciences*, 101(11):3747–3752, 2004.
- [9] Peter Belobaba, Amedeo Odoni, and Cynthia Barnhart. *The global airline industry*. John Wiley & Sons, 2015.
- [10] Brian Berkowitz and Isaac Balberg. Percolation theory and its application to groundwater hydrology. *Water Resources Research*, 29(4):775–794, 1993.
- [11] Henk AP Blom, Sybert H Stroeve, and Tibor Bosse. Modelling of potential hazards in agent-based safety risk analysis. In *Proc. 10th USA/Europe Air Traffic Management Research and Development Seminar (ATM2013)*, 2013.
- [12] C. Bongiorno, Miccichè S., Mantegna R. N., Gurtner G., Lillo F., ValoriL., Ducci M. Monechi B., and Pozzi S. 'An agent based model of air traffic management'. In *SESAR Innovation Days 2013 - Proceedings of the SESAR Innovation Days*, 2013.
- [13] C. Bongiorno, S. Miccichè, R. N. Mantegna, G. Gurtner, F. Lillo, and S. Pozzi. 'Adaptive air traffic network: statistical regularities in air traffic management'. *Proceedings in 11th USA/Europe Air Traffic Management Research and Development Seminar, ATM 2015. EUROCONTROL*, 2015.
- [14] C. Bongiorno, G. Gurtner, F.Lillo, R.N. Mantegna, and S. Micchicè. 'statistical characterization of deviation from planned flight trajectories in air traffic management'. *Journal of Air Transport Management*, 2016.
- [15] C Bongiorno, S Miccichè, and RN Mantegna. 'An empirically grounded agent based model for modeling directs, conflict detection and resolution operations in air traffic management'. *PLoS ONE* 12(4): e0175036, 2017. doi: 10.1371/journal.pone.0175036.
- [16] Simon R Broadbent and John M Hammersley. Percolation processes: I. crystals and mazes. In *Mathematical Proceedings of the Cambridge Philosophical Society*, volume 53, pages 629–641. Cambridge University Press, 1957.

- [17] Gano Chatterji and Banavar Sridhar. Measures for air traffic controller workload prediction. In 1st AIAA, Aircraft, Technology Integration, and Operations Forum, page 5242, 2001.
- [18] Zhen-Qing Chen, David Croydon, and Takashi Kumagai. Quenched invariance principles for random walks and elliptic diffusions in random media with boundary. 43, June 2013.
- [19] John-Paul B Clarke, Senay Solak, Y Chang, Liling Ren, and A Vela. Air traffic flow management in the presence of uncertainty. In Proceedings of the 8th USA/Europe Air Traffic Seminar (ATM09), 2009.
- [20] Aaron Clauset, Cosma Rohilla Shalizi, and Mark EJ Newman. Power-law distributions in empirical data. *SIAM review*, 51(4):661–703, 2009.
- [21] A. Cook, H. A. P. Blom, S. Miccichè, F. Lilla, RN. Mantegna, D. Rivas, R. Vazquez, and M. Zanin. 'applying complexity science to air traffic management'. *Journal of Air Transport Management*, 2014.
- [22] R. DeLaura and J. Evans. 'an exploratory study of modeling enroute pilot convective storm flight deviation behavior'. In 86th AMS Annual Meeting, 2006.
- [23] Rich DeLaura, Mike Robinson, Margo Pawlak, and Jim Evans. Modeling convective weather avoidance in enroute airspace. In 13th Conference on Aviation, Range, and Aerospace Meteorology, AMS, New Orleans, LA. Citeseer, 2008.
- [24] P. Erdős and Alfred Rényi. 'On random graphs I'. *Publ Math. Debrecen* 6, 290297, 1959.
- [25] P. Erdős and Alfred Rényi. "on on the evolution of random graphs i". *Publ. Math. Inst. Hung. Acad. Sci.* 5, 1761., 1960.
- [26] EUROCONTROL. Sever weather risk management survey, 2013.
- [27] EUROCONTROL. Monthly network operations report, 2018.
- [28] Michalis Faloutsos, Petros Faloutsos, and Christos Faloutsos. On power-law relationships of the internet topology. In *ACM SIGCOMM computer communication review*, volume 29, pages 251–262. ACM, 1999.
- [29] Ulrike Gelhardt, Jürgen Lang, and Stefan Schwanke. An approach to define adverse wx zones based on the flight management performed by pilots in convective weather events. In 2nd International Workshop on Meteorology and Air Traffic Management, Salzburg,, 2018.
- [30] Michele Guida and Maria Funaro. Topology of the italian airport network: A scale-free small-world network with a fractal structure? *Chaos, Solitons and Fractals*, 31(3):527–536, 2007.
- [31] Roger Guimera and Luis A Nunes Amaral. Modeling the world-wide airport network. *The European Physical Journal B*, 38(2):381–385, 2004.
- [32] Roger Guimera, Stefano Mossa, Adrian Turtchi, and LA Nunes Amaral. The worldwide air transportation network: Anomalous centrality, community structure, and cities' global roles. *Proceedings of the National Academy of Sciences*, 102(22):7794–7799, 2005.
- [33] G. Gurtner, Vitali S., Cipolla M, Lillo F, Mantegna RN, Salvatore Miccichè, and Simone Pozzi. 'multi-scale analysis of the european airspace using network community detection'. *PLoS ONE* 9(5): e94414, 2014. doi: 10.1371/journal.pone.0094414.
- [34] G. Gurtner, C. Bongiorno, M. Ducci, S. Miccichè, and S. Pozzi. 'elsa d2.4 sesar agent based model', 2015.
- [35] G. Gurtner, C. Bongiorno, M. Ducci, S., and Miccichè. 'an empirically grounded agent based simulator for the air traffic management in the sesar scenario'. *Journal of Air Transport Management*, 2016.
- [36] Ding-Ding Han, Jiang-Hai Qian, and Jin-Gao Liu. Network topology of the austrian airline flights. *arXiv preprint physics/0703193*, 2007.

- [37] Ding-Ding Han, Jiang-Hai Qian, and Jin-Gao Liu. Network topology and correlation features affiliated with european airline companies. *Physica A: Statistical Mechanics and its Applications*, 388(1):71–81, 2009.
- [38] Thomas Hauf, Ludmila Sakiew, and Manuela Sauer. Adverse weather diversion model divmet. *Journal of Aerospace Operations*, 2(3-4):115–133, 2013.
- [39] Thomas Hauf, Patrick Hupe, Manuela Sauer, Carl-Herbert Rokitansky, Jürgen Lang, Daniel Sacher, Pak Wai Chan, and Ludmila Sakiew. Aircraft route forecasting under adverse weather conditions. *Meteorologische Zeitschrift* 26 (2017), Nr. 2, 26(2):189–206, 2017.
- [40] Stef Janssen, Alexei Sharpanskykh, and Richard Curran. Agent-based modelling and analysis of security and efficiency in airport terminals. *Transportation Research Part C: Emerging Technologies*, 100:142–160, 2019.
- [41] Hawoong Jeong, Bálint Tombor, Réka Albert, Zoltan N Oltvai, and A-L Barabási. The large-scale organization of metabolic networks. *Nature*, 407(6804):651, 2000.
- [42] Martina Jetzki. The propagation of air transport delays in europe. Master’s thesis, RWTH Aachen University, Airport and Air Transportation Research, 2009.
- [43] Cai Kai-Quan, Zhang Jun, Du Wen-Bo, and Cao Xian-Bin. Analysis of the chinese air route network as a complex network. Chinese Physical Society and IOP Publishing Ltd, 2011.
- [44] Irene Vincie Laudeman, SG Shelden, R Branstrom, and CL Brasil. Dynamic density: An air traffic management metric. 1998.
- [45] Wei Li and Xu Cai. Statistical analysis of airport network of china. *Physical Review E*, 69(4):046106, 2004.
- [46] Chi Li-Ping, Wang Ru, Su Hang, Xu Xin-Ping, Zhao Jin-Song, Li Wei, and Cai Xu. Structural properties of us flight network. *Chinese physics letters*, 20(8):1393, 2003.
- [47] B Monechi, M Ducci, M Cipolla, S Vitali, S Micciché, RN Mantegna, G Gurtner, F Lillo, L Valori, and S Pozzi. Exploratory analysis of safety data and their interrelation with flight trajectories and network metrics. In ATOS-ISI ATM conference, 2013.
- [48] Jose M Montoya and Ricard V Solé. Small world patterns in food webs. *Journal of theoretical biology*, 214(3):405–412, 2002.
- [49] Jose C Nacher and Tatsuya Akutsu. Analysis of critical and redundant nodes in controlling directed and undirected complex networks using dominating sets. *Journal of Complex Networks*, 2(4):394–412, 2014.
- [50] Mark EJ Newman. A measure of betweenness centrality based on random walks. *Social networks*, 27(1):39–54, 2005.
- [51] Arnab Nilim, Laurent El Ghaoui, Vu Duong, and Mark Hansen. Trajectory-based air traffic management (tb-atm) under weather uncertainty. In Proc. of the Fourth International Air Traffic Management R&D Seminar ATM, 2001.
- [52] Joshua W Pepper, Kristine R Mills, and Leonard A Wojcik. Predictability and uncertainty in air traffic flow management. In 5th USA/Europe Air Traffic Management R&D Seminar (ATM-2003), Metrics and Performance Management, Budapest, Hungary, 2003.
- [53] Kuang-Chang Pien, Ke Han, Wenlong Shang, Arnab Majumdar, and Washington Ochieng. Robustness analysis of the european air traffic network. *Transportmetrica A: Transport Science*, 11(9):772–792, 2015. doi: 10.1080/23249935.2015.1087233. URL <https://doi.org/10.1080/23249935.2015.1087233>.

- [54] Joseph Quartieri, Michele Guida, Claudio Guarnaccia, Salvatore D'Ambrosio, and Davide Guadagnuolo. Topological properties of the Italian airport network studied via multiple addendials and graph theory. *International Journal of Mathematical Models and Methods in Applied Sciences*, 2:312–316, 2008.
- [55] A. Turtschi L.A.N. Amaral R. Guimera, S. Mossa. The worldwide air transportation network: Anomalous centrality, community structure, and cities' global roles. *Proc. Nat. Acad. Sci.*, (102):7794–7799, 2005.
- [56] Juan Jose Rebollo and Hamsa Balakrishnan. Characterization and prediction of air traffic delays. *Transportation research part C: Emerging technologies*, 44:231–241, 2014.
- [57] Damián Rivas, Rafael Vazquez, and Antonio Franco. Probabilistic analysis of aircraft fuel consumption using ensemble weather forecasts. In *7th International Conference on Research in Air Transportation (ICRAT)*, Philadelphia, PA, pages 1–8, 2016.
- [58] Mikhail Rubnich and Rich DeLaura. An algorithm to identify robust convective weather avoidance polygons in en route airspace. In *10th AIAA Aviation Technology, Integration, and Operations (ATIO) Conference*, page 9164, 2010.
- [59] Manasi Sapre and Nita Parekh. Analysis of centrality measures of airport network of India. In *International Conference on Pattern Recognition and Machine Intelligence*, pages 376–381. Springer, 2011.
- [60] Mare Sarr, Erwin Bulte, Chris Meissner, and Tim Swanson. On the looting of nations. *Public choice*, 148(3-4):353–380, 2011.
- [61] Subhabrata Sen and Jia Wang. Analyzing peer-to-peer traffic across large networks. In *Proceedings of the 2nd ACM SIGCOMM Workshop on Internet measurement*, pages 137–150. ACM, 2002.
- [62] Wenlong Shang, Ke Han, Washington Ochieng, and Panagiotis Angeloudis. Agent-based day-to-day traffic network model with information percolation. *Transportmetrica A: Transport Science*, 13(1):38–66, 2017. doi: 10.1080/23249935.2016.1209254. URL <https://doi.org/10.1080/23249935.2016.1209254>.
- [63] H Udluft. Decentralization in Air Transportation. PhD thesis, Delft University of Technology, 2017.
- [64] Andreas Wagner. The yeast protein interaction network evolves rapidly and contains few redundant duplicate genes. *Molecular biology and evolution*, 18(7):1283–1292, 2001.
- [65] Sebastian Wandelt and Xiaoqian Sun. Evolution of the international air transportation country network from 2002 to 2013. *Transportation Research Part E: Logistics and Transportation Review*, 82:55–78, 2015.
- [66] Jiaoe Wang, Huihui Mo, Fahui Wang, and Fengjun Jin. Exploring the network structure and nodal centrality of China's air transport network: A complex network approach. *Journal of Transport Geography*, 19(4):712–721, 2011.
- [67] Duncan J Watts and Steven H Strogatz. Collective dynamics of small-world networks. *nature*, 393(6684):440, 1998.
- [68] Richard Wheeldon and Steve Counsell. Power law distributions in class relationships. arXiv preprint [cs/0305037](https://arxiv.org/abs/cs/0305037), 2003.
- [69] Olivia Woolley-Meza, Christian Thiemann, Daniel Grady, Jake Jungbin Lee, Hanno Seebens, Bernd Blasius, and Dirk Brockmann. Complexity in human transportation networks: a comparative analysis of worldwide air transportation and global cargo-ship movements. *The European Physical Journal B*, 84(4):589–600, 2011.
- [70] Zengwang Xu and Robert Harriss. Exploring the structure of the US intercity passenger air transportation network: a weighted complex network approach. *GeoJournal*, 73(2):87, 2008.
- [71] Massimiliano Zanin and Fabrizio Lillo. Modelling the air transport with complex networks: A short review. *The European Physical Journal Special Topics*, 215(1):5–21, 2013.

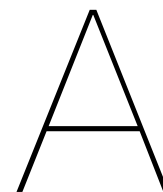
- 
- [72] Massimiliano Zanin, Javier M Buldú, P Cano, and S Boccaletti. Disorder and decision cost in spatial networks. *Chaos: An Interdisciplinary Journal of Nonlinear Science*, 18(2):023103, 2008.
- [73] Qian Zheng and Yiyuan Zhao. Modeling wind uncertainties for stochastic trajectory synthesis. In 11th AIAA Aviation Technology, Integration, and Operations (ATIO) Conference, including the AIAA Balloon Systems Conference and 19th AIAA Lighter-Than, page 6858, 2011.



# IV

## Annexes to Scientific Article





# Airline Clustering

Group	Name	$n_L$	$n_A$	$\bar{U}$	$n_F$	$n_{AC}$	$n_K$	$\bar{k}$	$\bar{L}$	$\bar{S}$	$\bar{C}$
1	CityJet	207	111	3,13	5216	45	8	3,73	2,86	49,21	0,35
1	Chalair Aviation	42	29	2,34	629	12	4	2,90	2,57	82,89	0,23
1	Adria Airline	43	30	2,67	1410	11	3	2,87	2,64	50,36	0,33
1	Eastern Airways	288	99	3,92	10435	39	9	5,82	2,67	108,71	0,36
1	Sun Air of Scandinavia	224	131	3,75	4208	20	7	3,42	3,21	34,49	0,24
1	Twin Jet	61	42	3,32	698	17	4	2,90	3,09	76,68	0,18
2	Air Europa	192	96	11,34	34723	71	13	3,94	2,43	385,89	0,23
2	Austrian Airlines	188	144	8,90	55103	100	11	2,61	2,08	390,84	0,28
2	Ukraine Airlines	107	78	9,53	23630	53	10	2,74	2,06	306,95	0,27
2	Brussels Airlines	135	126	7,77	35815	105	12	2,14	2,01	298,47	0,14
2	Air Baltic	97	76	8,23	20320	43	13	2,53	2,09	270,93	0,18
2	Aer Lingus	123	82	11,00	31849	60	10	3,00	2,01	388,41	0,29
2	Finnair	154	136	9,60	49364	102	12	2,26	2,04	362,99	0,13
2	Iberia Airlines	131	111	14,00	40779	87	9	2,36	2,03	374,21	0,25
2	LOT Polish Airlines	116	92	9,65	44817	78	18	2,52	2,14	498,00	0,22
2	Swiss Air Lines	146	114	10,65	62640	123	16	2,56	2,15	554,39	0,28
2	TAP Portugal	171	102	12,56	53439	99	16	3,35	2,02	529,56	0,48
3	Aigle Azur	111	57	6,56	7021	27	7	3,89	2,31	127,71	0,40
3	Adria Airways	216	120	5,41	8583	28	9	3,60	2,33	71,53	0,45
3	Aegean Airlines	175	105	7,09	21204	59	7	3,33	2,15	209,98	0,27
3	Air Malta	58	54	8,15	5745	15	5	2,15	2,00	110,50	0,19
3	Air Nostrum	271	94	6,93	32113	45	5	5,67	2,30	345,32	0,43
3	Air Serbia	84	81	9,25	13725	21	6	2,07	2,00	169,44	0,10
3	Aurigny Air Services	24	20	3,79	6241	13	7	2,40	1,87	312,10	0,37
3	Astra Airlines Regional	74	49	5,46	2842	5	3	3,02	2,19	58,00	0,42
3	Blue Islands	28	23	3,59	4174	6	3	2,43	2,19	208,70	0,26
3	Belair Airlines	11	11	5,60	146	15	3	2,00	2,35	14,60	0,19
3	Blue Air	143	68	9,07	15769	29	5	4,21	2,35	235,36	0,44
3	Blue Panorama Airlines	107	57	8,98	4129	20	6	3,75	2,37	75,07	0,33
3	Braathens Regional Airlines	26	16	3,97	9476	43	9	3,25	2,01	592,25	0,49
3	Air Corsica	52	29	1,50	81	12	4	3,59	1,97	104,24	0,47
3	BA CityFlyer	94	52	6,60	15474	28	6	3,62	2,24	297,60	0,31
3	Czech Airlines	75	59	6,86	13793	48	7	2,54	1,99	233,78	0,33
3	Croatia Airlines	92	55	7,27	11706	17	5	3,35	2,35	234,12	0,32
3	Edelweiss Air	61	60	7,14	4524	37	5	2,00	2,00	75,43	0,04

Group	Name	$n_L$	$n_A$	$\bar{U}$	$n_F$	$n_{AC}$	$n_K$	$\bar{k}$	$\bar{L}$	$\bar{S}$	$\bar{C}$
3	Ellinair	76	63	5,52	1691	10	6	2,41	2,11	27,27	0,20
3	Cobalt	26	25	8,07	2437	8	2	2,08	2,13	101,54	0,16
3	Fly One	23	21	6,59	1433	14	4	2,19	1,89	71,70	0,22
3	Atlantic Airways	59	39	5,79	1575	5	3	3,03	2,28	40,38	0,42
3	Sky Wings Airlines	55	48	7,24	1396	9	3	2,29	2,07	29,70	0,31
3	Iberia Express	60	49	8,76	13968	24	2	2,45	2,06	297,19	0,26
3	Icelandair	56	47	6,65	7066	32	3	2,38	2,26	153,61	0,23
3	Meridiana	169	76	8,83	8649	26	8	4,45	2,38	121,83	0,40
3	AlbaStar	22	16	4,85	98	8	2	2,48	2,51	4,90	0,57
3	Luxair	211	129	8,53	12735	17	3	3,27	2,16	101,08	0,41
3	Loganair	86	36	5,30	7815	23	10	4,78	2,19	536,06	0,48
3	Bulgaria Air	49	36	8,04	4684	15	6	2,72	2,02	130,11	0,26
3	Montenegro Airlines	41	29	4,15	2847	10	4	2,83	2,03	98,17	0,45
3	Air Moldova	36	31	7,29	4857	19	5	2,32	1,98	167,48	0,25
3	Laudamotion	276	99	8,55	16648	117	11	5,49	2,54	175,28	0,33
3	NextJet	70	34	4,85	6729	22	5	4,12	2,27	203,91	0,41
3	Olympic Air	62	35	2,87	23161	62	6	3,54	1,99	702,12	0,53
3	Helvetic Airways	67	54	4,49	430	13	3	2,48	2,19	8,11	0,33
3	People's Vienna	41	31	3,82	1303	8	3	2,65	2,24	43,43	0,43
3	Primera Air	93	45	7,78	1688	19	5	4,13	2,23	38,39	0,49
3	Tarom	56	41	8,76	15065	23	7	2,73	2,04	367,54	0,32
3	Malmö Aviation (Braathens)	180	73	4,26	9753	37	7	4,93	2,38	137,37	0,53
3	Sky Express	74	38	5,34	6214	8	7	3,89	2,17	168,03	0,49
3	Stobart Air	62	39	6,20	14107	32	10	3,18	2,37	361,72	0,31
3	Sunexpress DE	145	47	9,83	3937	17	5	6,17	2,30	85,61	0,35
3	Sunexpress TK	152	62	9,83	20338	49	3	4,90	2,14	328,03	0,42
3	Thomas Cook	52	42	7,64	2040	43	4	2,48	1,98	49,78	0,37
3	Transavia NL	230	122	9,76	24339	62	5	3,77	2,24	204,58	0,44
3	Transavia France	159	88	7,24	14716	54	8	3,61	2,07	175,26	0,40
4	Condor Flugdienst	302	121	11,86	16538	74	10	4,99	2,17	143,81	0,39
4	Jet2.com	359	84	9,51	24386	77	6	8,55	2,07	301,22	0,55
4	Germania	645	171	10,31	11480	31	5	7,54	2,48	67,56	0,53
4	Germanwings	335	125	6,60	36545	92	3	5,36	2,16	292,38	0,59
4	TUIFly	499	152	10,03	14741	54	10	6,57	2,23	104,57	0,49
4	Monarch Airlines	150	58	10,59	13034	36	4	5,17	2,07	224,76	0,61
4	Neos	238	95	12,17	3445	13	5	5,01	2,24	37,48	0,52
4	Pegasus	296	121	10,61	66518	81	5	4,89	2,11	554,36	0,43
4	TUI Airways	650	140	13,78	27430	66	9	9,07	2,19	197,42	0,54
4	Volotea	322	103	8,83	16964	29	4	6,25	2,60	169,75	0,33
4	Widerøe	232	61	7,79	52597	41	4	7,61	2,30	862,25	0,67
4	Wizz Air	696	158	12,17	68770	86	2	8,81	2,36	440,90	0,32
5	Alitalia	229	121	9,14	83067	134	11	3,79	2,03	698,06	0,49
5	Flybe	346	98	6,14	66256	113	13	7,06	2,26	690,27	0,59
5	Air Berlin	327	115	7,99	59155	216	15	5,61	2,28	510,00	0,50
5	Eurowings	408	154	7,20	45669	176	9	5,30	2,28	296,56	0,45
5	Hop!	263	84	2,48	6543	153	20	6,26	2,33	376,44	0,46
5	Norwegian Air Shuttle	663	178	10,64	91038	182	11	7,45	2,30	520,26	0,55
5	Scandinavian Airlines	526	179	8,81	133969	205	19	5,88	2,19	761,23	0,58
5	Vueling Airlines	437	151	8,82	80715	127	8	5,79	2,08	534,58	0,41
6	Albawings	13	14	3,08	794	8	4	1,86	1,86	66,17	0,00
6	Bergen Air Transport	6	6	1,79	117	1	1	2,00	1,73	19,50	0,25
6	Dreamjet	10	8	15,00	504	3	2	2,50	1,64	63,00	0,46

Group	Name	$n_L$	$n_A$	$\bar{U}$	$n_F$	$n_{AC}$	$n_K$	$\bar{k}$	$\bar{L}$	$\bar{S}$	$\bar{C}$
6	Air Dolomiti	10	11	4,66	5052	11	2	1,82	1,96	459,27	0,00
6	Hahn Air	14	12	1,52	95	3	2	2,33	2,12	7,92	0,17
6	British Airways Shuttle	15	11	3,23	16679	148	5	2,73	1,98	1516,27	0,54
6	Siavia	8	6	4,74	562	3	1	2,25	1,47	80,29	0,00
6	Virgin Atlantic Airways	52	41	17,99	11629	40	4	2,54	2,29	298,21	0,24
6	XL Airways	35	31	15,28	1236	9	3	2,26	2,04	44,14	0,11
7	Air France	263	193	10,86	106979	305	31	2,73	2,09	680,74	0,28
7	British Airways	334	217	11,85	113440	311	18	3,06	2,28	522,82	0,28
7	Lufthansa	450	249	11,49	217921	355	20	3,61	2,26	875,23	0,49
7	KLM	215	188	12,60	107340	190	19	2,29	2,19	586,62	0,16
7	Turkish Airlines	604	286	11,84	201871	353	17	4,22	2,02	726,29	0,41
8	EasyJet	1120	172	10,36	225365	288	5	13,02	2,17	1318,11	0,51
8	Ryanair	1982	222	10,57	306676	413	3	17,86	2,15	1394,11	0,51

Table A.1: All airline features. Intercontinental flights and weekends included.

	Ac Types	Avg Clustering	Avg Degree	Avg Path	Links	Nodes	Avg Strength	dailyAvg Util[hrs]	Fleet size	totalFlights Monthly
PC-1	0,22	0,24	0,35	0,11	0,38	0,38	0,35	0,22	0,39	0,4
PC-2	0,43	-0,21	-0,39	-0,52	-0,27	-0,16	0,4	0,04	0,26	0,16
PC-3	-0,6	0,04	0,26	-0,65	0,24	-0,22	0,09	0,09	-0,05	0,15
PC-4	0,06	0,54	-0,03	0,01	-0,27	-0,14	0,15	0,69	-0,26	-0,21
PC-5	0,2	0,7	0,11	-0,21	-0,06	-0,1	-0,05	-0,6	0,1	-0,15

Table A.2: PC features correlation. ECAC flights, weekends included. An example of the amount of correlation between each of the 10 features and the resulting 5 principal components.

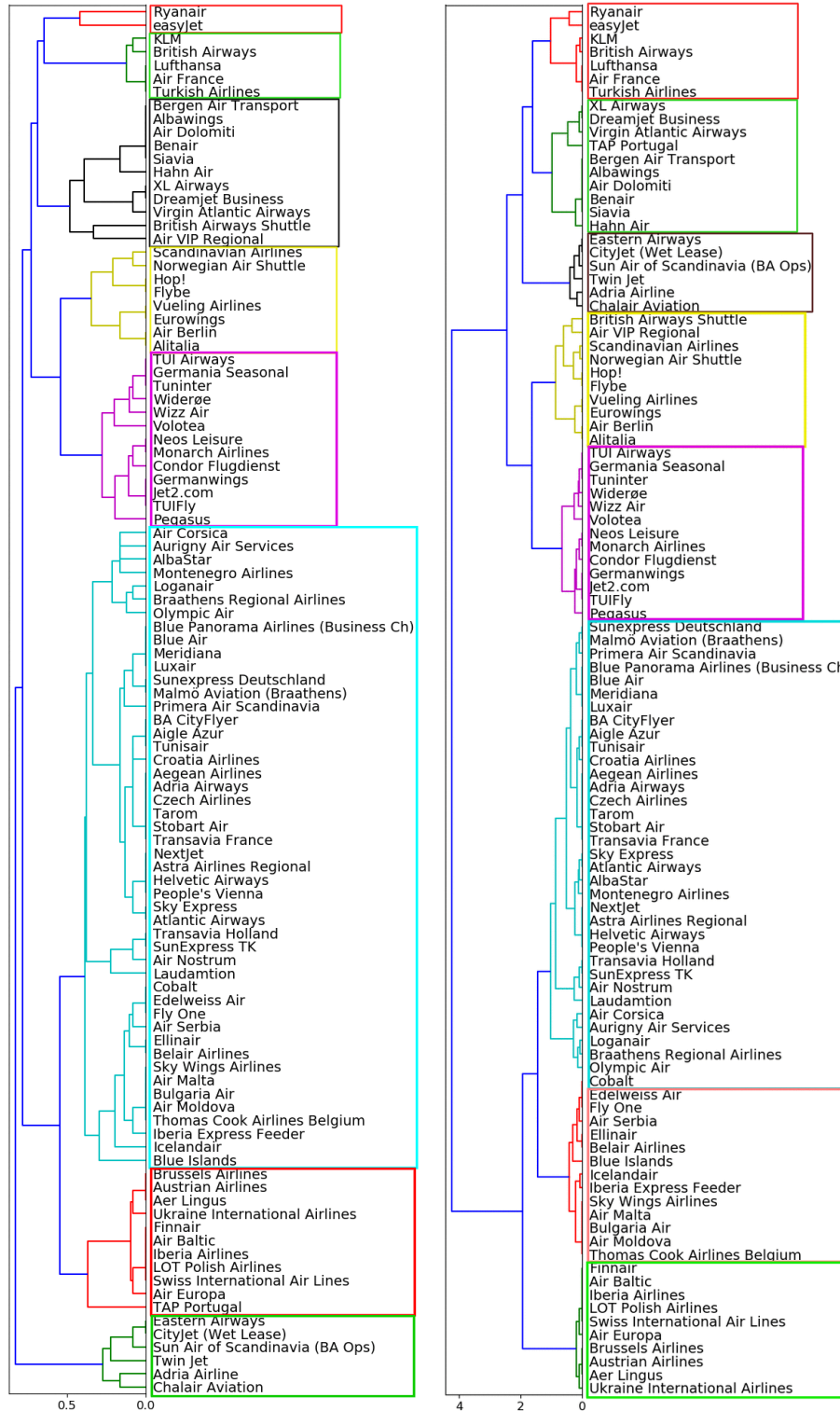
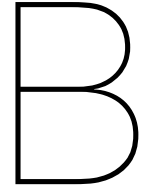


Figure A.1: Left: Clustering dendrogram of the final result with average linkage and a cut at 0.5. Right: Clustering dendrogram with Ward Linkage and a cut at 1.05.



# Efficiency

Group	1		2		3		4		5		6		7		8	
Hour	$\mu$	$\sigma$														
0	0,97	0,0018	0,96	0,0035	0,98	0,0005	0,98	0,001	0,97	0,0014	0,99	0,0001	0,98	0,0004	0,97	0,0027
1	0,98	0,0009	0,97	0,0025	0,98	0,0004	0,98	0,0007	0,98	0,0004	0,99	0,0001	0,98	0,0003	0,98	0,0004
2	0,97	0,0002	0,97	0,0027	0,98	0,0004	0,97	0,0012	0,98	0,0006	0,99	0,0001	0,98	0,0004	0,97	0,0007
3	0,97	0,0008	0,98	0,0008	0,97	0,0009	0,97	0,0009	0,98	0,0007	0,99	0,0003	0,98	0,0006	0,98	0,0003
4	0,94	0,0005	0,98	0,0007	0,97	0,0008	0,98	0,0007	0,97	0,0008	0,98	0,0006	0,98	0,0006	0,97	0,0007
5	0,96	0,0012	0,97	0,0007	0,97	0,0008	0,97	0,0008	0,97	0,0008	0,98	0,0004	0,97	0,0007	0,97	0,0007
6	0,97	0,001	0,97	0,0007	0,97	0,0008	0,97	0,0008	0,98	0,0008	0,97	0,0014	0,97	0,0007	0,97	0,0008
7	0,97	0,0009	0,97	0,001	0,97	0,0008	0,97	0,0007	0,97	0,0009	0,98	0,0005	0,97	0,0008	0,97	0,0009
8	0,97	0,0014	0,97	0,0008	0,97	0,0007	0,97	0,0007	0,97	0,0008	0,98	0,0003	0,97	0,0008	0,96	0,0009
9	0,96	0,0013	0,97	0,0008	0,97	0,0006	0,97	0,0009	0,97	0,0009	0,98	0,0004	0,97	0,0006	0,96	0,0008
10	0,97	0,0012	0,97	0,0007	0,97	0,0006	0,97	0,0007	0,97	0,0009	0,98	0,0004	0,97	0,0007	0,97	0,001
11	0,96	0,0015	0,97	0,0008	0,97	0,0008	0,97	0,0009	0,97	0,0009	0,98	0,0004	0,97	0,0007	0,96	0,0009
12	0,96	0,0013	0,97	0,0009	0,97	0,0007	0,97	0,0007	0,97	0,0008	0,98	0,0003	0,97	0,0007	0,96	0,0011
13	0,97	0,0012	0,97	0,0008	0,97	0,0007	0,97	0,0006	0,97	0,0009	0,98	0,0004	0,97	0,0007	0,97	0,0009
14	0,97	0,0009	0,97	0,0008	0,97	0,0007	0,97	0,0007	0,98	0,0009	0,98	0,0004	0,97	0,0007	0,97	0,0009
15	0,96	0,0011	0,97	0,0007	0,97	0,0009	0,97	0,0007	0,98	0,0009	0,98	0,0005	0,97	0,0007	0,97	0,0009
16	0,96	0,0012	0,97	0,0009	0,97	0,0008	0,97	0,0007	0,98	0,0009	0,98	0,0006	0,97	0,0007	0,97	0,0008
17	0,96	0,0009	0,97	0,0011	0,97	0,0008	0,97	0,0007	0,98	0,0008	0,98	0,0005	0,97	0,0007	0,97	0,0008
18	0,97	0,0008	0,97	0,0013	0,97	0,0009	0,97	0,0008	0,98	0,0008	0,97	0,0014	0,97	0,0007	0,97	0,0007
19	0,97	0,0006	0,97	0,0013	0,97	0,0009	0,97	0,0007	0,98	0,0007	0,98	0,0009	0,97	0,0007	0,97	0,0007
20	0,97	0,0006	0,97	0,0009	0,97	0,0007	0,97	0,0008	0,98	0,0006	0,98	0,0003	0,98	0,0005	0,97	0,0006
21	0,97	0,0006	0,98	0,0007	0,97	0,0008	0,98	0,0006	0,98	0,0006	0,98	0,0002	0,98	0,0004	0,97	0,0006
22	0,96	0,0015	0,98	0,0015	0,97	0,0006	0,98	0,0008	0,97	0,0007	0,99	0,0003	0,98	0,0002	0,97	0,0007
23	0,96	0,0019	0,97	0,0032	0,98	0,0004	0,97	0,0012	0,97	0,0005	0,99	0,0002	0,98	0,0004	0,97	0,0009

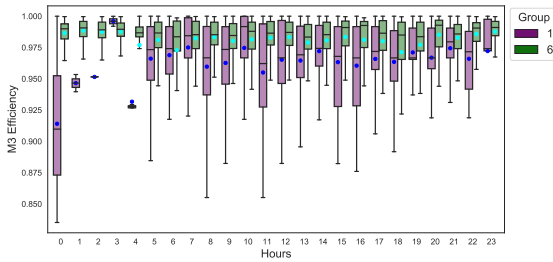
Table B.1: Variance and average planned (M1) efficiency for every hour per airline group.

Group	1		2		3		4		5		6		7		8	
Day	$\mu$	$\sigma$														
Mon	0,966	0,035	0,972	0,032	0,971	0,027	0,972	0,028	0,974	0,03	0,98	0,024	0,974	0,025	0,966	0,029
Tue	0,966	0,034	0,971	0,035	0,971	0,029	0,973	0,027	0,975	0,029	0,981	0,023	0,974	0,026	0,966	0,029
Wed	0,965	0,033	0,972	0,032	0,972	0,028	0,973	0,028	0,974	0,029	0,982	0,023	0,974	0,027	0,966	0,029
Thu	0,966	0,033	0,972	0,032	0,972	0,027	0,973	0,028	0,974	0,029	0,981	0,022	0,975	0,026	0,967	0,028
Fri	0,966	0,034	0,972	0,033	0,971	0,027	0,972	0,028	0,974	0,03	0,981	0,023	0,975	0,025	0,967	0,029
Sat	0,956	0,038	0,973	0,031	0,973	0,024	0,974	0,025	0,973	0,027	0,983	0,018	0,977	0,023	0,969	0,025
Sun	0,959	0,037	0,973	0,03	0,973	0,025	0,974	0,027	0,976	0,027	0,982	0,021	0,976	0,024	0,969	0,026

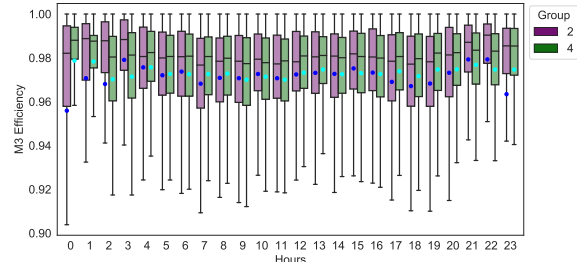
Table B.2: Variance and average of planned (M1) efficiency for every day per airline group

Groups	1		2		3		4		5		6		7		8	
	$\mu$	$\sigma$														
Mon	0,978	0,026	0,981	0,026	0,981	0,019	0,979	0,023	0,983	0,022	0,982	0,019	0,981	0,02	0,977	0,022
Tue	0,979	0,023	0,979	0,031	0,98	0,022	0,979	0,024	0,983	0,021	0,982	0,019	0,98	0,021	0,976	0,023
Wed	0,978	0,025	0,98	0,027	0,981	0,02	0,979	0,024	0,983	0,021	0,983	0,019	0,981	0,022	0,976	0,022
Thu	0,978	0,024	0,98	0,027	0,981	0,02	0,979	0,024	0,983	0,022	0,983	0,019	0,981	0,021	0,977	0,022
Fri	0,98	0,024	0,98	0,028	0,981	0,02	0,979	0,024	0,983	0,021	0,983	0,019	0,981	0,02	0,977	0,021
Sat	0,976	0,025	0,981	0,027	0,981	0,019	0,98	0,022	0,982	0,022	0,985	0,015	0,982	0,019	0,979	0,019
Sun	0,979	0,023	0,981	0,025	0,982	0,02	0,98	0,023	0,984	0,02	0,984	0,017	0,982	0,019	0,979	0,02

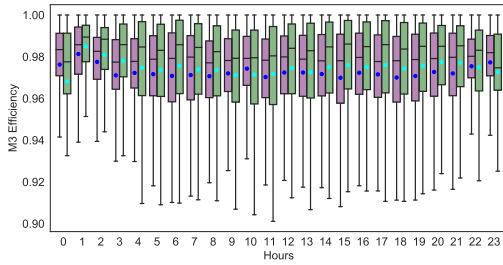
Table B.3: Variance and average of realized (M3) efficiency for every day per airline group



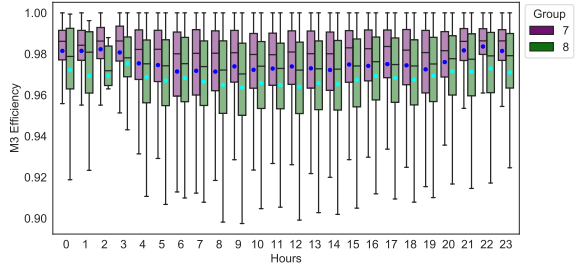
(B.1.a) Group 1-6



(B.1.b) Groups 2-4

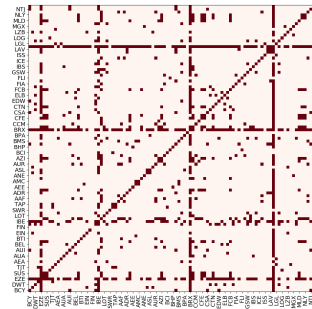


(B.1.c) Group 3-5

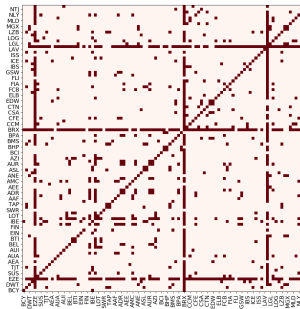


(B.1.d) Groups 7-8

Figure B.1: M3 efficiency comparison between groups.



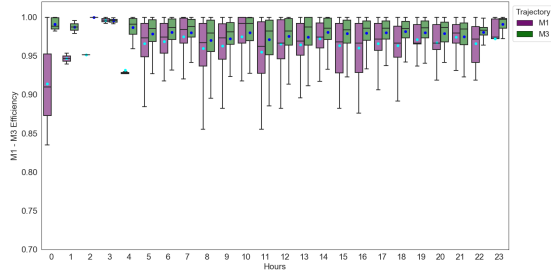
(B.2.a) M1 efficiency T-test between all operators



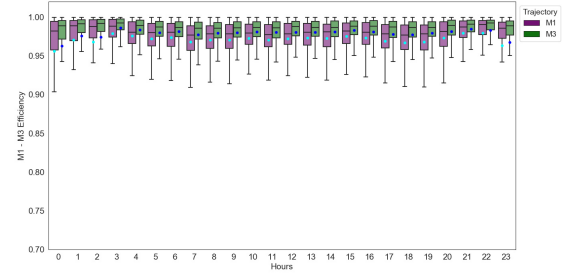
(B.2.b) M3 efficiency T-test between all operators

Red means p-value > 0.05, thus we accept the null hypothesis that the distributions are similar. White means they are different. The appearance of vertical and horizontal red lines is explained by operators with few flights, leading to an apparent similarity with most other airlines. If only airlines within each group would have similar efficiency distributions, then the plots would be red only along the secondary diagonal, and would form a chain of squares. We see, however, that this is not the case.

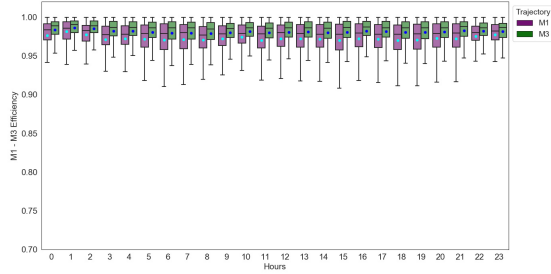
Figure B.2: Efficiency T-tests between all operators. Left (M1) and right (M3).



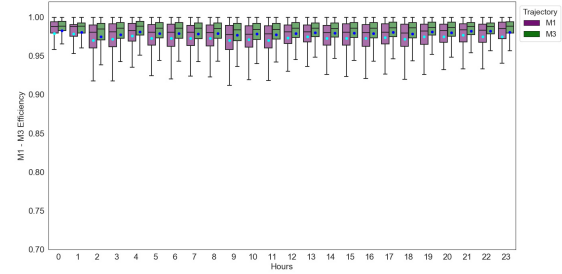
(B.3.a) Group 1



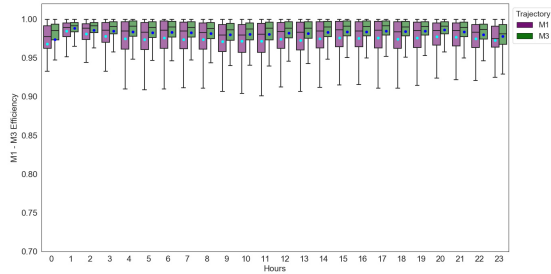
(B.3.b) Group 2



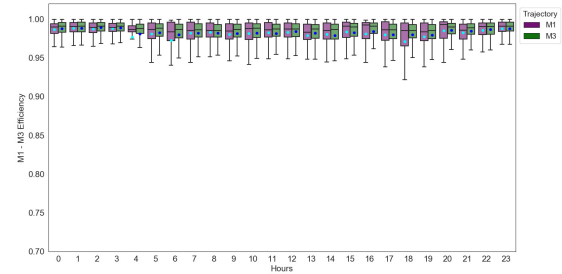
(B.3.c) Group 3



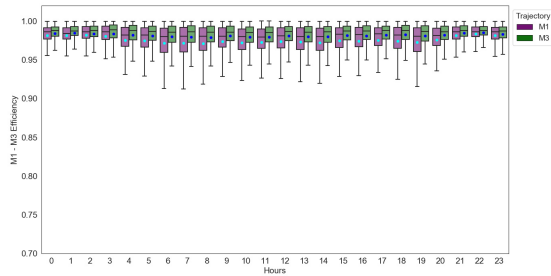
(B.3.d) Group 4



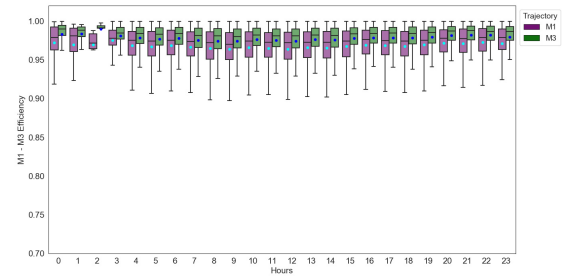
(B.3.e) Group 5



(B.3.f) Group 6

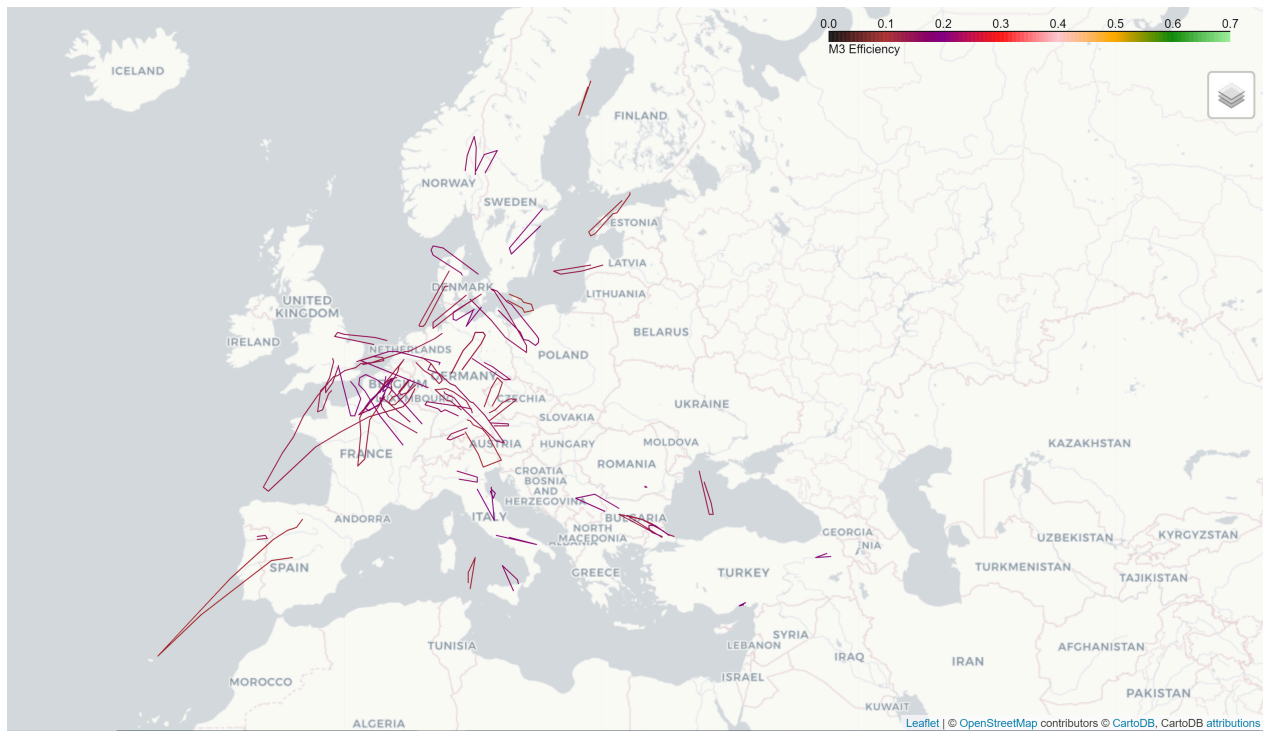


(B.3.g) Group 7

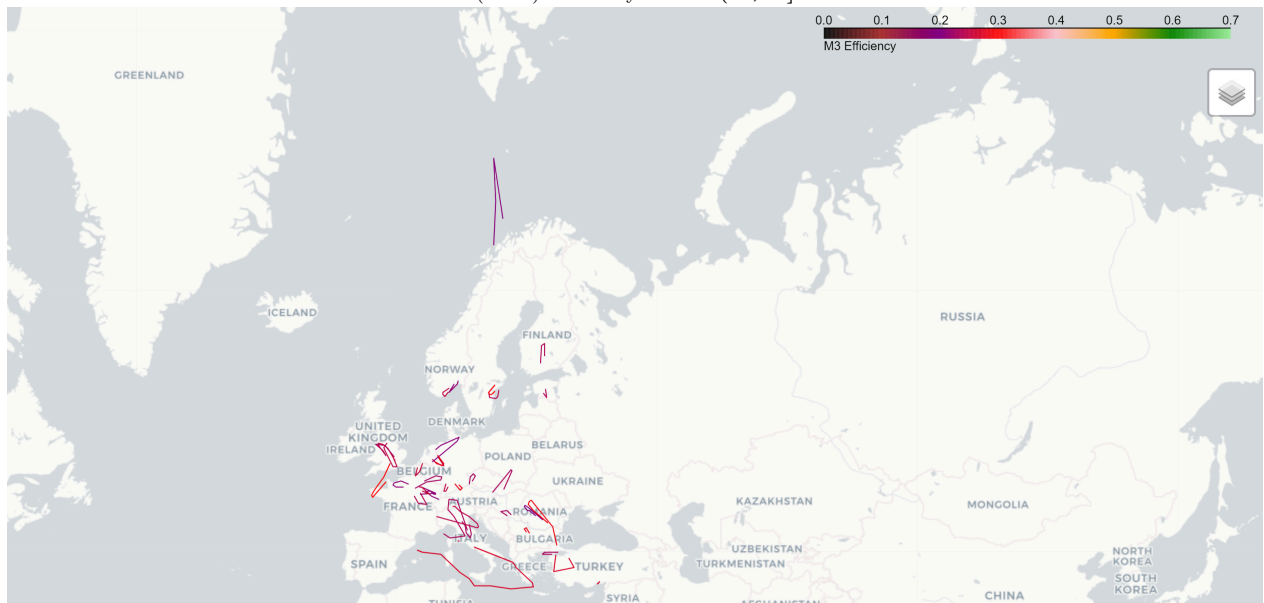


(B.3.h) Group 8

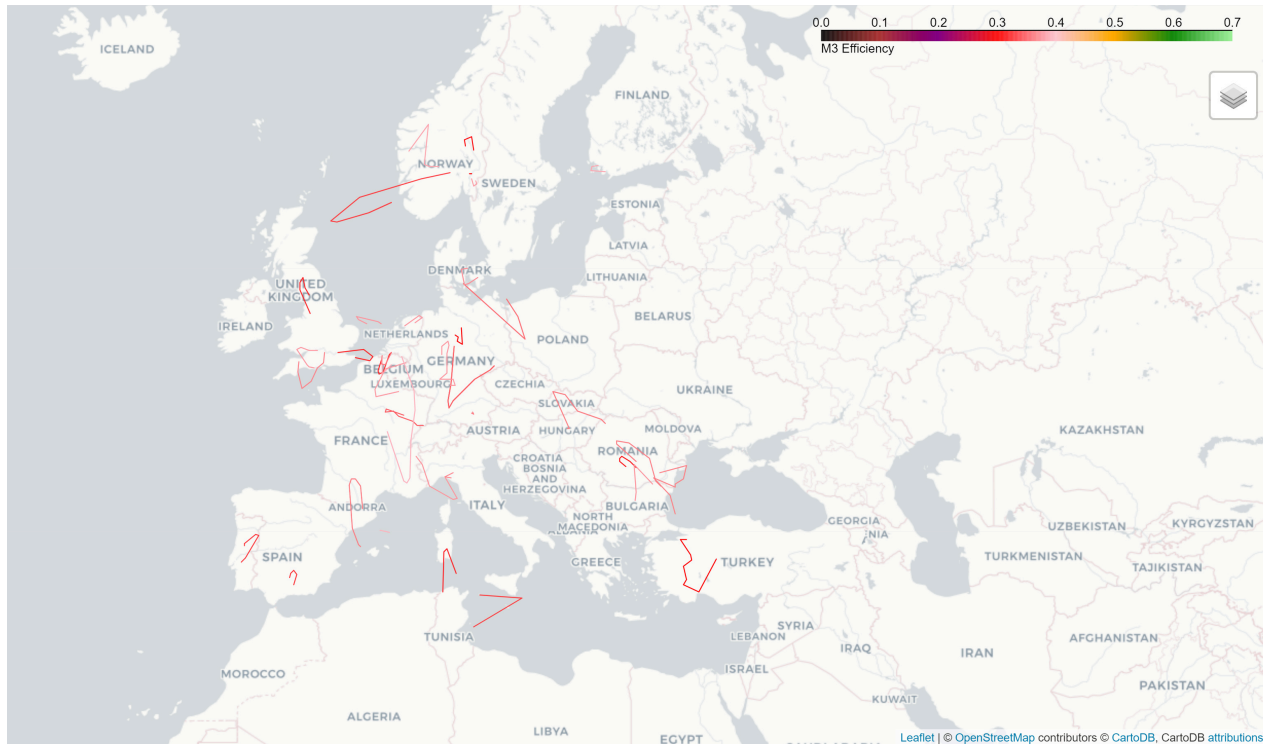
Figure B.3: M1 and M3 efficiency comparison per groups of airlines per hour. All eight groups are presented here.



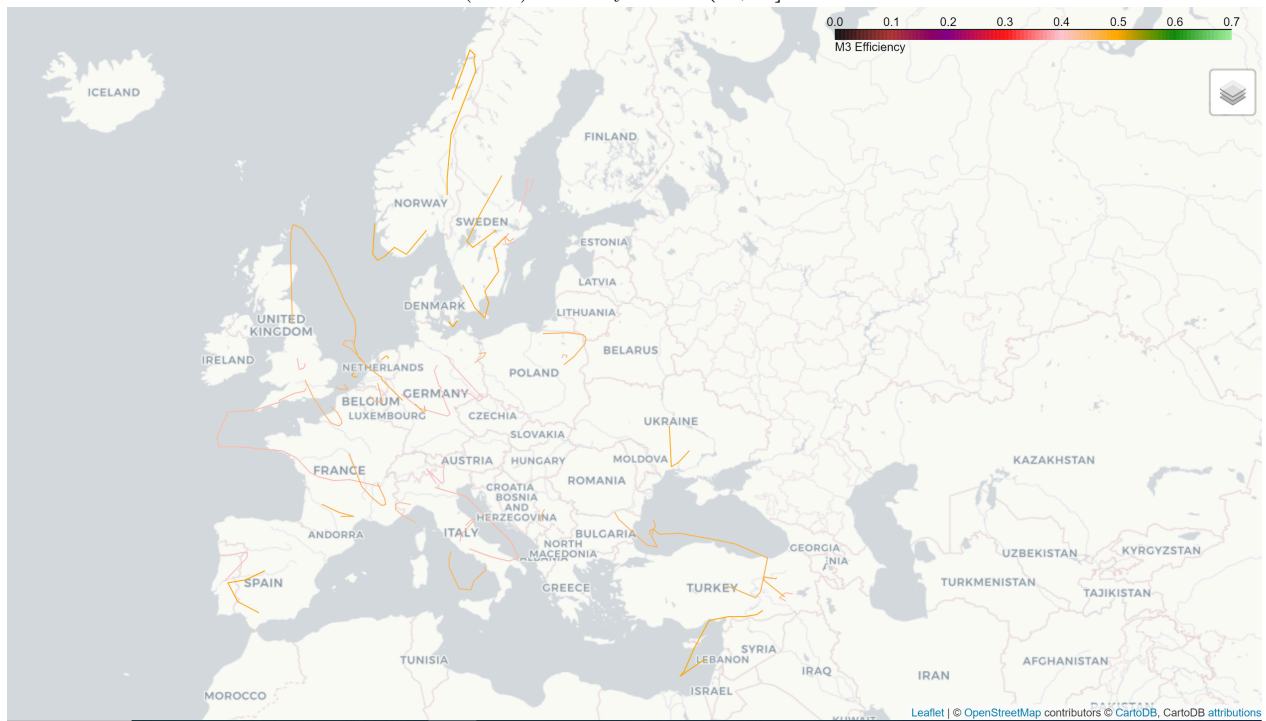
(B.4.a) Efficiency bracket (0.1,0.2]



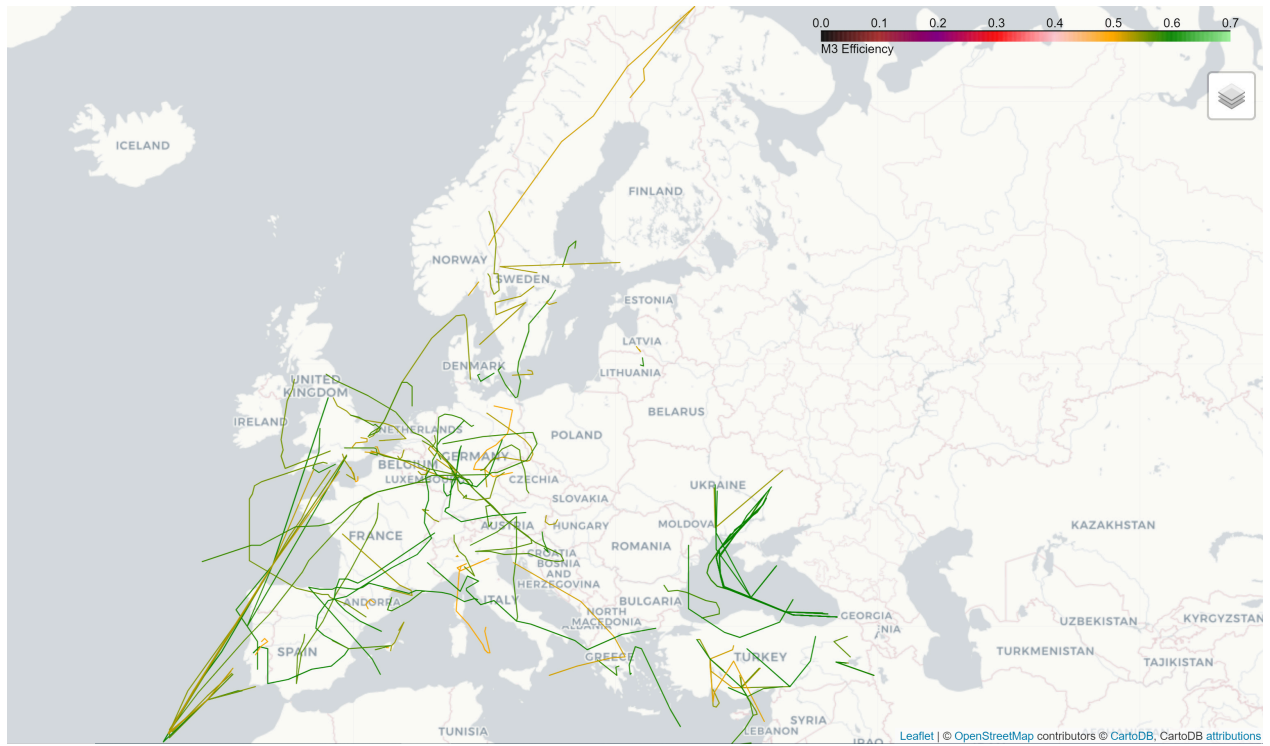
(B.4.b) Efficiency bracket (0.2,0.3]



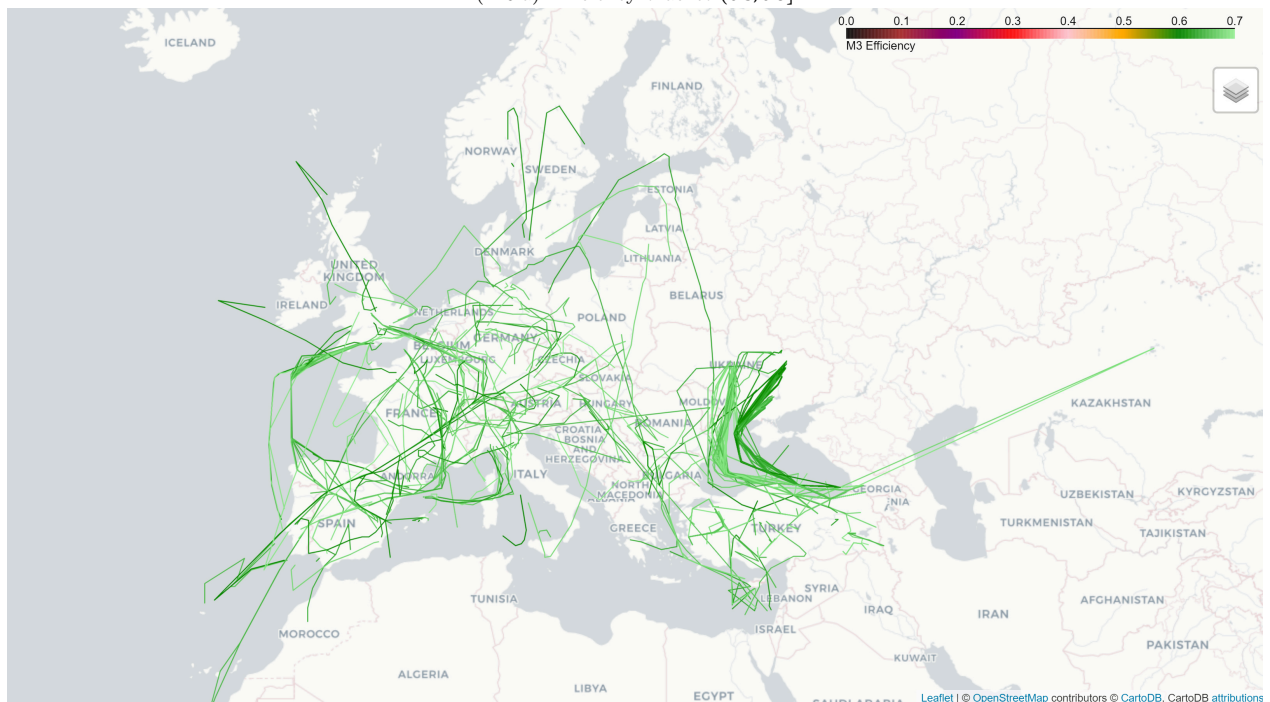
(B.5.a) Efficiency bracket (0.3,0.4]



(B.5.b) Efficiency bracket (0.4,0.5]



(B.6.a) Efficiency bracket (0.5,0.6]



(B.6.b) Efficiency bracket (0.6,0.7]

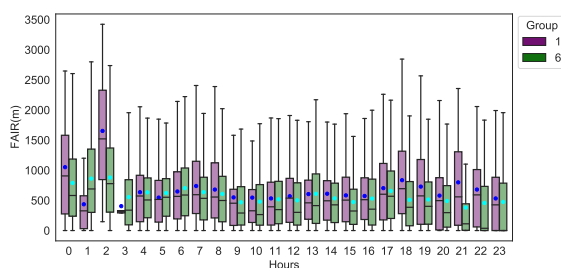
Name	Code	$E_h$							FAIR			
		$\delta_E^-$	$\delta_E^+$	$\delta_E^0$	$\delta_E^-\%$	$\delta_E^+\%$	$\delta_E^0\%$	Flights	$E_h$	$\overline{cruise[km]}$	$\overline{FAIR}$	Flights
1	BCY	3064	3053	10	0,5	0,5	0	6127	0,82	419192	347	4084
1	DWT	376	582	1	0,39	0,61	0	959	0,83	542414	585	882
1	EZE	3119	2956	40	0,51	0,48	0,01	6115	0,83	275725	668	5259
1	SUS	3209	4327	9	0,43	0,57	0	7545	0,83	369180	801	6390
1	TJT	5	20	1	0,19	0,77	0,04	26	0,81	446172	15	33
2	AEA	22764	36610	464	0,38	0,61	0,01	59838	0,81	835711	737	56018
2	AUA	39440	58737	941	0,4	0,59	0,01	99118	0,82	758752	750	92279
2	AUI	21192	36578	290	0,37	0,63	0	58060	0,83	1025744	977	54521
2	BEL	24615	46317	1693	0,34	0,64	0,02	72625	0,81	790404	741	68077
2	BTI	15939	15303	1290	0,49	0,47	0,04	32532	0,81	758180	628	29568
2	EIN	30114	40136	1035	0,42	0,56	0,02	71285	0,87	932066	782	62117
2	FIN	44929	33522	676	0,57	0,42	0,01	79127	0,82	923109	1231	73170
2	IBE	32974	51209	2359	0,38	0,59	0,03	86542	0,9	885443	706	83093
2	LOT	29223	45277	164	0,39	0,61	0	74664	0,82	806411	1293	70334
2	SWR	45332	67345	2336	0,39	0,59	0,02	115013	0,47	904069	654	99922
2	TAP	33067	63491	1308	0,34	0,65	0,01	97866	0,83	1195863	877	94819
3	AAF	4458	11352	75	0,28	0,71	0,01	15885	0,82	884413	506	15342
3	ADR	7463	10333	12	0,42	0,58	0	17808	0,8	458253	597	15874
3	AEE	18371	30291	69	0,38	0,62	0	48731	0,83	1242407	868	46707
3	AMC	4792	6897	2	0,41	0,59	0	11691	0,99	1141822	1234	11543
3	ANE	14753	23790	34	0,38	0,62	0	38577	0,98	387613	637	34628
3	ASL	8681	11270	17	0,43	0,56	0,01	19968	0,82	861539	839	18749
3	AZI	253	743	6	0,25	0,74	0,01	1002	0,87	1151970	729	878
3	BCI	46	188	0	0,2	0,8	0	234	0,83	1381205	696	206
3	BHP	14140	23616	16	0,37	0,63	0	37772	0,89	1054433	1138	32932
3	BMS	2637	7561	121	0,26	0,73	0,01	10319	0,81	803920	816	9606
3	BPA	269	326	6	0,45	0,54	0,01	601	0,79	434492	598	527
3	BRX	40	96	2	0,29	0,7	0,01	138	0,81	490401	578	6193
3	CCM	12974	17140	26	0,43	0,57	0	30140	0,81	468928	945	28513
3	CFE	7261	10854	10	0,4	0,6	0	18125	0,83	728414	1112	17686
3	CSA	7151	8344	11	0,46	0,54	0	15506	0,8	527158	631	12799
3	CTN	4182	6379	174	0,39	0,59	0,02	10735	0,81	1628198	640	9758
3	EDW	1221	3983	24	0,23	0,76	0,01	5228	0,84	1149355	874	5056
3	ELB	2545	2910	6	0,47	0,53	0	5461	0,8	1363060	1008	4992
3	FCB	1518	2206	5	0,41	0,59	0	3729	0,81	840544	927	3653
3	FIA	1453	2043	152	0,4	0,56	0,04	3648	0,9	946181	1042	3404
3	FLI	1480	1709	1	0,46	0,54	0	3190	0,8	1196165	867	2832
3	GSW	12875	19760	9	0,39	0,61	0	32644	0,79	966282	783	30184
3	IBS	7166	9803	16	0,42	0,58	0	16985	0,84	1642018	619	16341
3	ICE	6782	12097	210	0,36	0,63	0,01	19089	0,8	820956	640	16711
3	ISS	651	2479	8	0,21	0,79	0	3138	0,81	1143711	732	2854
3	LAV	3613	7213	6	0,33	0,67	0	10832	0,85	965643	518	10026
3	LGL	1828	1582	6	0,54	0,46	0	3416	0,83	195008	424	3132
3	LOG	4567	7566	42	0,38	0,62	0	12175	0,82	945907	982	11428
3	LZB	2628	3873	3	0,4	0,6	0	6504	0,79	556355	676	4314
3	MGX	3735	7883	29	0,32	0,68	0	11647	0,8	996491	1001	11433
3	MLD	12672	26732	73	0,32	0,68	0	39477	0,8	1297399	772	37544
3	NLY	880	239	4	0,78	0,21	0,01	1123	0,97	230261	260	979
3	NTJ	7244	6461	13	0,53	0,47	0	13718	0,83	120656	573	8968
3	OAL	315	620	2	0,34	0,66	0	937	0,82	1009486	870	832
3	OAW	1136	1283	1	0,47	0,53	0	2420	0,83	336116	1119	1399

3	PEV	1126	3042	3	0,27	0,73	0	4171	0,83	2070775	815	3826
3	PRI	6493	13934	16	0,32	0,68	0	20443	0,84	1027108	1195	19227
3	ROT	12752	4561	25	0,74	0,26	0	17338	0,8	272211	465	10741
3	SCW	1060	1098	2	0,49	0,51	0	2160	0,96	558141	938	1952
3	SEH	3908	5543	60	0,41	0,58	0,01	9511	0,79	2081279	751	9123
3	STK	20640	20873	7635	0,42	0,42	0,16	49148	0,83	1381400	518	44703
3	SXD	10194	16009	782	0,38	0,59	0,03	26985	0,82	846284	509	26540
3	SXS	1220	3263	0	0,27	0,73	0	4483	0,85	1882605	953	4280
3	TAR	19158	38425	31	0,33	0,67	0	57614	0,84	1285592	1103	54455
3	TCW	11881	22845	67	0,34	0,66	0	34793	0,82	1107929	697	32949
4	TRA	13723	24005	1237	0,35	0,62	0,03	38965	0,84	2012134	799	36792
4	TVF	23870	33366	31	0,42	0,58	0	57267	0,81	1668281	885	52299
4	CFG	8262	17700	55	0,32	0,68	0	26017	0,74	1823660	1071	24398
4	EXS	30300	35317	23	0,46	0,54	0	65640	0,85	506718	782	59689
4	GMI	9516	22649	324	0,29	0,7	0,01	32489	0,99	1551969	901	30001
4	GWI	10131	18443	15	0,35	0,65	0	28589	0,87	1491424	967	27381
4	JAF	2380	4958	200	0,32	0,66	0,02	7538	0,82	1575954	702	7174
4	MON	65097	49213	46267	0,41	0,31	0,28	160577	0,81	656379	236	141805
4	NOS	23559	36919	1758	0,38	0,59	0,03	62236	0,81	1925528	822	58038
4	PGT	17308	25881	37	0,4	0,6	0	43226	0,8	559713	669	38977
4	TOM	2638	2601	50	0,5	0,49	0,01	5289	0,83	395194	21	4201
4	VOE	64815	97608	131	0,4	0,6	0	162554	0,8	995896	1244	149191
5	WIF	68740	110683	1127	0,38	0,61	0,01	180550	0,82	583039	1045	170220
5	WZZ	34463	20860	51	0,62	0,38	0	55374	0,84	357775	295	48368
5	AZA	37284	46726	1423	0,44	0,55	0,01	85433	0,79	770466	610	76885
5	BEE	49708	61492	411	0,45	0,55	0	111611	0,81	625155	855	103022
5	BER	5308	8674	29	0,38	0,62	0	14011	0,79	312611	600	47579
5	EWG	93512	107511	436	0,46	0,53	0,01	201459	0,84	1085827	884	182703
5	HOP	143946	119449	1150	0,54	0,45	0,01	264545	0,91	619715	839	238279
5	NAX	68407	103174	200	0,4	0,6	0	171781	0,81	677802	856	160771
6	SAS	504	1320	3	0,28	0,72	0	1827	0,78	425401	824	1563
6	VLG	2	10	1	0,15	0,77	0,08	13	0,8	241613	91	10
6	AWT	542	534	140	0,45	0,44	0,11	1216	0,83	2497105	179	1214
6	BGT	5612	6481	3	0,46	0,54	0	12096	0,83	172838	637	10256
6	DJT	36	196	0	0,16	0,84	0	232	0,83	665893	978	211
6	DLA	23021	8349	5	0,73	0,27	0	31375	0,82	179406	648	28146
6	SHT	442	1075	8	0,29	0,7	0,01	1525	0,98	500314	1051	1343
6	VIR	11415	12058	3457	0,42	0,45	0,13	26930	0,8	2037003	410	26184
6	XLF	1067	1588	142	0,4	0,6	0	2797	0,79	1738007	312	2756
7	AFR	89604	145789	10688	0,36	0,59	0,05	246081	0,79	962413	467	261088
7	BAW	99841	134810	9749	0,41	0,55	0,04	244400	0,84	1337956	644	235092
7	DLH	183461	237689	9330	0,43	0,55	0,02	430480	0,8	829887	691	399787
7	KLM	92330	116370	7153	0,43	0,54	0,03	215853	0,82	886719	892	202584
7	THY	199518	166988	109622	0,42	0,35	0,23	476128	0,9	853676	271	446416
8	EZY	203180	288585	218	0,41	0,59	0	491983	0,81	783893	739	444430
8	RYR	259103	422177	220	0,38	0,62	0	681500	0,89	929170	903	588131

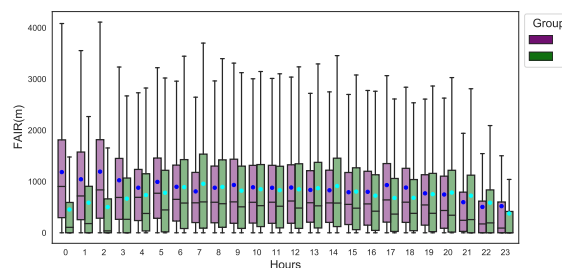
Table B.4: Individual airline efficiency and FAIR values. Both 'flights' columns refer to the total flights in 2017 used in each analysis.

# C

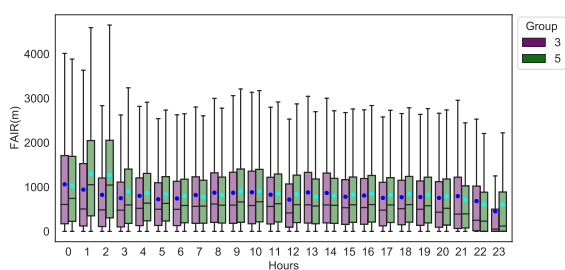
# FAIR



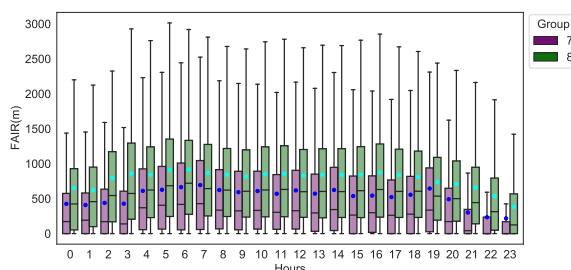
(C.1.a) Group 1-6



(C.1.b) Groups 2-4



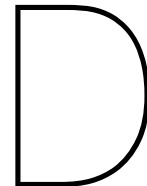
(C.1.c) Group 3-5



(C.1.d) Groups 7-8

Figure C.1: M3 hourly FAIR comparison between groups. Note the slightly different axes.

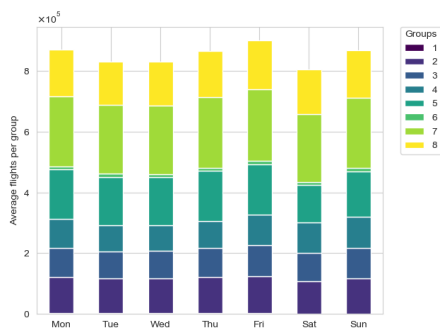




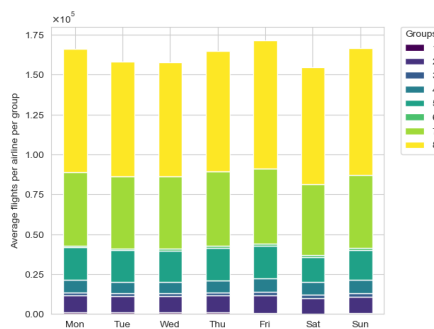
# Additional trajectory analysis results

This annex provides context for the horizontal efficiency and FAIR results. It emphasizes two points: first, that the vertical and horizontal indices are comparable across groups, and second, that the variation of the number of flights between the average airlines within each group is significant.

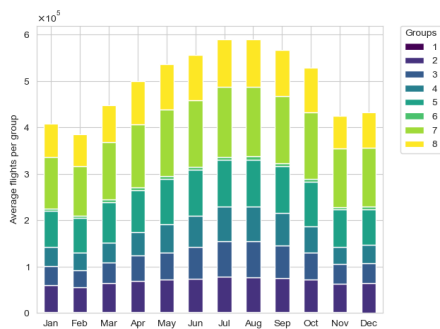
Figure D.1 presents an overview of the total flights in 2017 and used to assess the horizontal efficiency: the total number of flights are fairly equally distributed between groups, except for groups 1 and 6 which had completed a number of flights with an order of magnitude lower than the rest. The average number of flights within each group, i.e. the average of average, unveils a greater disparity between the average airline of each group  $|F0_{m,g}| = \frac{|F_{m,g}|}{n}$ , where  $n$  is the number of airlines in each group, and  $|F_{m,g}|$  is the cardinality of the set of flights of group  $g$  in month  $m$ .



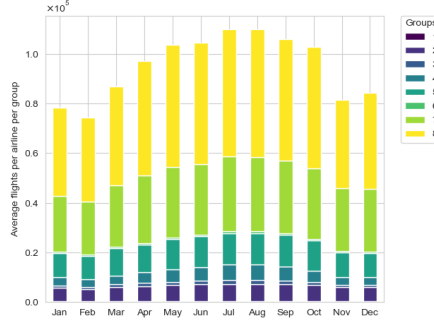
(D.1.a) Daily average flights per group



(D.1.b) Daily average flights per average airline



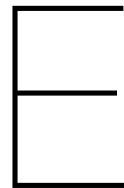
(D.1.c) Monthly average flights per group



(D.1.d) Monthly average flights per average airline

Figure D.1: Daily (first row) and monthly (second row) flights exhibit a peak during Fridays, Sundays and Mondays, and during summer months. Besides showing weekly and monthly trends, the images in the left and right columns show that, although most airline groups (6/8) fly similar number of flights, the average airline within each group behaves differently.





## Mutual Information

This appendix provides more background on Mutual Information and Entropy  $H$ . The equations below correspond to: entropy, joint entropy, conditional entropy, and mutual information.

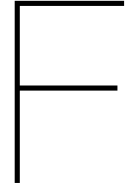
$$\begin{aligned} H(\mathbf{U}) &= - \sum_{i=1}^R \frac{a_i}{N} \log \frac{a_i}{N} \\ H(\mathbf{U}, \mathbf{V}) &= - \sum_{i=1}^R \sum_{j=1}^C \frac{n_{ij}}{N} \log \frac{n_{ij}}{N} \\ H(\mathbf{U}|\mathbf{V}) &= - \sum_{i=1}^R \sum_{j=1}^C \frac{n_{ij}}{N} \log \frac{n_{ij}/N}{b_j/N} \\ MI(\mathbf{U}, \mathbf{V}) &= \sum_{i=1}^R \sum_{j=1}^C \frac{n_{ij}}{N} \log \frac{n_{ij}/N}{a_i b_j / N^2} \end{aligned} \tag{E.1}$$

From a communication theory point of view, the above quantities can be defined as follows:  $H(\mathbf{U})$  is the average rate at which  $\mathbf{U}$  produces information and can be imagined as a bit or 'chunk'. In this case, the information is the labels in cluster  $\mathbf{U}$ . Then  $H(\mathbf{U}|\mathbf{V})$  denotes the average size of information 'chunk' needed to transmit each label in  $\mathbf{U}$  if  $\mathbf{V}$  is already known. This naturally leads to the definition of  $MI(\mathbf{U}, \mathbf{V}) = H(\mathbf{U}) - H(\mathbf{U}|\mathbf{V})$ . MI indicates how much the knowledge of  $\mathbf{V}$  helps us to reduce the number of bits needed to encode labels in  $\mathbf{U}$ . Clearly, the higher the MI, the more useful the information in  $\mathbf{V}$ . The reverse also holds true  $MI(\mathbf{U}, \mathbf{V}) = H(\mathbf{V}) - H(\mathbf{V}|\mathbf{U})$ . [49]

In addition, the Adjusted Mutual Information (Eq. 16) has all three desirable properties of clustering comparison metrics:

- Metric property - the metric property conforms to our intuition of distance [66];
- Normalization property - the values of the index should lie either in  $[-1, 1]$  or  $[0, 1]$ ;
- Constant baseline property - for a similarity index to be relevant, its expected value between randomly sampled clusterings should always be constant, irrespective of the number of clusters.





# Metric Altitude Reference

True track from 000° to 179°						True track from 180° to 359°					
IFR Flights			VFR Flights			IFR Flights			VFR Flights		
FL	m	ft	FL	m	ft	FL	m	ft	FL	m	ft
010	300	1000				020	600	2000			
030	900	3000	035	1050	3500	040	1200	4000	045	1350	4500
050	1500	5000	055	1700	5500	060	1850	6000	065	2000	6500
070	2150	7000	075	2300	7500	080	2450	8000	085	2600	8500
090	2750	9000	095	2900	9500	100	3050	10000	105	3200	10500
110	3350	11000	115	3500	11500	120	3650	12000	125	3800	12500
130	3950	13000	135	4100	13500	140	4250	14000	145	4400	14500
150	4550	15000	155	4700	15500	160	4900	16000	165	5050	16500
170	5200	17000	175	5350	17500	180	5500	18000	185	5650	18500
190	5800	19000	195	5950	19500	200	6100	20000	205	6250	20500
210	6400	21000	215	6550	21500	220	6700	22000	225	6850	22500
230	7000	23000	235	7150	23500	240	7300	24000	245	7450	24500
250	7600	25000	255	7750	25500	260	7900	26000	265	8100	26500
270	8250	27000	-	-	-	280	8550	28000	-	-	-
290	8850	29000	-	-	-	300	9150	30000	-	-	-
310	9450	31000	-	-	-	320	9750	32000	-	-	-
330	10050	33000	-	-	-	340	10350	34000	-	-	-
350	10650	35000	-	-	-	360	10950	36000	-	-	-
370	11300	37000	-	-	-	380	11600	38000	-	-	-
390	11900	39000	-	-	-	400	12200	40000	-	-	-
410	12500	41000	-	-	-	430	13100	43000	-	-	-
450	13700	45000	-	-	-	470	14350	47000	-	-	-
490	14950	49000	-	-	-	510	15550	51000	-	-	-

Table F.1: Metric Altitude Reference table. Source: Skybrary. This table shows the function by which the unit transformation of vertical deviation has been transformed from Flight Levels (FL) which are measured in feet, to meters.